

## WIDE COOL AND ULTRACOOL COMPANIONS TO NEARBY STARS FROM Pan-STARRS 1

NIALL R. DEACON<sup>1,2</sup>, MICHAEL C. LIU<sup>2,10</sup>, EUGENE A. MAGNIER<sup>2</sup>, KIMBERLY M. ALLER<sup>2</sup>, WILLIAM M. J. BEST<sup>2</sup>, TRENT DUPUY<sup>3,11</sup>, BRENDAN P. BOWLER<sup>2,4,12,13</sup>, ANDREW W. MANN<sup>5</sup>, JOSHUA A. REDSTONE<sup>6</sup>, WILLIAM S. BURGETT<sup>2</sup>, KENNETH C. CHAMBERS<sup>2</sup>, PETER W. DRAPER<sup>7</sup>, H. FLEWELLING<sup>2</sup>, KLAUS W. HODAPP<sup>8</sup>, NICK KAISER<sup>2</sup>, ROLF-PETER KUDRITZKI<sup>2</sup>, JEFF S. MORGAN<sup>2</sup>, NIGEL METCALFE<sup>7</sup>, PAUL A. PRICE<sup>9</sup>, JOHN L. TONRY<sup>2</sup>, AND RICHARD J. WAINSCOAT<sup>2</sup>

<sup>1</sup> Max Planck Institute for Astronomy, Koenigstuhl 17, D-69117 Heidelberg, Germany; deacon@mpia.de

<sup>2</sup> Institute for Astronomy, University of Hawai'i, 2680 Woodlawn Drive, Honolulu, HI 96822, USA

<sup>3</sup> Harvard-Smithsonian Center for Astrophysics, 60 Garden Street, Cambridge, MA 02138, USA

<sup>4</sup> California Institute of Technology, Division of Geological and Planetary Sciences, 1200 East California Boulevard, Pasadena, CA 91125, USA

<sup>5</sup> Harlan J. Smith Fellow, Department of Astronomy, The University of Texas at Austin, Austin, TX 78712, USA

<sup>6</sup> Equinox Labs, 89 Antrim Street, #2, Cambridge, MA 02139, USA

<sup>7</sup> Department of Physics, University of Durham, South Road, Durham DH1 3LE, UK

<sup>8</sup> Institute for Astronomy, University of Hawai'i, 640 North Aohoku Place, Hilo, HI 96720, USA

<sup>9</sup> Princeton University Observatory, 4 Ivy Lane, Peyton Hall, Princeton University, Princeton, NJ 08544, USA

Received 2013 November 8; accepted 2014 July 8; published 2014 August 22

### ABSTRACT

We present the discovery of 57 wide ( $>5''$ ) separation, low-mass (stellar and substellar) companions to stars in the solar neighborhood identified from Pan-STARRS 1 (PS1) data and the spectral classification of 31 previously known companions. Our companions represent a selective subsample of promising candidates and span a range in spectral type of K7–L9 with the addition of one DA white dwarf. These were identified primarily from a dedicated common proper motion search around nearby stars, along with a few as serendipitous discoveries from our Pan-STARRS 1 brown dwarf search. Our discoveries include 23 new L dwarf companions and one known L dwarf not previously identified as a companion. The primary stars around which we searched for companions come from a list of bright stars with well-measured parallaxes and large proper motions from the *Hipparcos* catalog (8583 stars, mostly A–K dwarfs) and fainter stars from other proper motion catalogs (79170 stars, mostly M dwarfs). We examine the likelihood that our companions are chance alignments between unrelated stars and conclude that this is unlikely for the majority of the objects that we have followed-up spectroscopically. We also examine the entire population of ultracool ( $>M7$ ) dwarf companions and conclude that while some are loosely bound, most are unlikely to be disrupted over the course of  $\sim 10$  Gyr. Our search increases the number of ultracool M dwarf companions wider than 300 AU by 88% and increases the number of L dwarf companions in the same separation range by 82%. Finally, we resolve our new L dwarf companion to HIP 6407 into a tight ( $0''.13$ , 7.4 AU) L1+T3 binary, making the system a hierarchical triple. Our search for these key benchmarks against which brown dwarf and exoplanet atmosphere models are tested has yielded the largest number of discoveries to date.

**Key words:** binaries: general – brown dwarfs – stars: low-mass – surveys

**Online-only material:** color figures

### 1. INTRODUCTION

Wide ( $\gtrsim 100$  AU) binary companions have long been used as a tool for identifying and studying faint stellar and substellar objects. Such systems are relatively common, with at least 4.4% of solar-type stars having a companion wider than 2000 AU (Tokovinin & Lépine 2012) and  $\sim 25\%$  having companions wider than 100 AU (Raghavan et al. 2010). Indeed, the Sun’s closest stellar neighbor, Proxima Centauri, is a  $\sim 15,000$  AU common proper motion companion to Alpha Centauri (Innes 1915). These objects are an important population for understanding models of binary star formation. The widest systems may have been formed by capture within a young cluster

(Kouwenhoven et al. 2010), a mechanism that has been used to explain the apparent increase in the number of companions per log separation bin at separations over 20,000 AU (Dhital et al. 2010). Another possibility is that these objects formed closer in and were pushed out to wider orbits by three-body interactions (Delgado-Donate et al. 2004; Umbreit et al. 2005; Reipurth & Mikkola 2012). In this scenario the wide companion fraction should be higher for close binary systems. Indeed Law et al. (2010) have found that  $45^{+18}_{-16}\%$  of wide M dwarf systems were resolved as hierarchical triples with high-resolution imaging.

Wide binaries also provide test cases for characterizing stellar and substellar properties. As these systems likely formed from the same birth cluster, the companions will have the same metallicity and age as their host stars. Hence if one component has these parameters determined, the values can be applied to the other component. For example, wide M dwarf companions to FGK stars have been used as calibrators for spectroscopic determinations of M dwarf metallicity relations (Rojas-Ayala et al. 2010; Mann et al. 2013a, 2014). This “benchmarking” process is even more important for substellar objects as brown dwarfs lack a stable internal energy source and hence exhibit a degeneracy between their mass, luminosity, and age.

<sup>10</sup> Visiting Astronomer at the Infrared Telescope Facility, which is operated by the University of Hawaii under Cooperative Agreement No. NNX-08AE38A with the National Aeronautics and Space Administration, Science Mission Directorate, Planetary Astronomy Program.

<sup>11</sup> Hubble Fellow.

<sup>12</sup> Visiting Astronomer, Kitt Peak National Observatory, National Optical Astronomy Observatory, which is operated by the Association of Universities for Research in Astronomy (AURA) under cooperative agreement with the National Science Foundation.

<sup>13</sup> Caltech Joint Center for Planetary Astronomy Fellow.

For substellar companions this degeneracy can be broken using the age of the primary (in combination with the bolometric luminosity derived from their absolute magnitude and spectrum of the secondary) to estimate the radius, mass, and effective temperature of the secondary from evolutionary models. This effective temperature can then be compared to that derived from model fits to the secondary's spectrum, testing the agreement between atmospheric and evolutionary models (e.g., Saumon et al. 2007; Deacon et al. 2012b). There are also a handful of systems where the ultracool<sup>14</sup> secondary itself is a binary. Such very rare systems are not simply “age benchmarks” (Liu et al. 2008); since the mass of the secondary is measured dynamically, they provide the opportunity for even more stringent tests of theoretical models (Dupuy et al. 2009).

As a result of their importance, wide substellar companions have been an active area of study in recent years. Many substellar companions have been identified as byproducts of larger searches for brown dwarfs (e.g., Burningham et al. 2009) or by matching known brown dwarfs with catalogs of known stars (e.g., Faherty et al. 2010; Dupuy & Liu 2012). Dedicated large-scale companion searches such as Pinfield et al. (2006) are more rare. A summary of discoveries prior to 2010 is presented in Faherty et al. (2010). Since then wide-field surveys such as Sloan Digital Sky Survey (SDSS; Ahn et al. 2012; see studies by Zhang et al. 2010; Dhital et al. 2010) and WISE (Wright et al. 2010; see work by Luhman et al. 2012; Wright et al. 2013) have been used to identify wide companions to stars. As these surveys are either single epoch or taken over a short period of time, they often require additional data sets, such as Two Micron All Sky Survey (2MASS; Skrutskie et al. 2006), to allow the identification of companions from their common proper motion with the primary. Hence the ideal tool for identifying wide, low-mass companions to stars is a red-sensitive, wide-field, multi-epoch survey.

Pan-STARRS 1 is a wide-field 1.8 m telescope situated on Haleakala on Maui in the Hawaiian Islands. Run by a consortium of astronomical research institutions, it has been surveying the sky north of  $\delta = -30^\circ$  since 2010 May. Just over half of the telescope's operating time is reserved for the  $3\pi$  Survey, a multi-filter, multi-epoch survey of three-fourths of the sky ( $\sim 30,000 \text{ deg}^2$ ). The Pan-STARRS 1 photometric system is defined in Tonry et al. (2012) and consists of five filters used for the  $3\pi$  Survey ( $g_{P1}, r_{P1}, i_{P1}, z_{P1}$ , and  $y_{P1}$ ) as well as an extra-wide  $w_{P1}$  filter specially designed for asteroid searches. It is the  $y_{P1}$  filter, centered on 0.99 microns ( $\delta\lambda = 70 \text{ nm}$ ), which makes Pan-STARRS 1 ideal for surveying the local population of brown dwarfs. So far over 100 T dwarfs have been identified (Deacon et al. 2011; Liu et al. 2011; M. C. Liu et al., in preparation), many in the early-T regime (Best et al. 2013). Such objects were often missed by previous surveys due to their indistinct colors in the near-infrared compared to background M dwarfs. However, the addition of Pan-STARRS 1 astrometry and far-red optical photometry disentangles them from the much larger number of M dwarfs with similar near-infrared colors.

As a wide-field multi-epoch survey, Pan-STARRS 1 also provides an ideal data set for identifying wide, common proper motion companions to nearby stars. This is a natural extension of our search for nearby field brown dwarfs and involves searching the Pan-STARRS 1 proper motion database for objects moving with a common proper motion to known stars. This approach

<sup>14</sup> A term typically used to mean objects of spectral type M7 or later. These may be free-floating planetary mass objects, brown dwarfs, or very low-mass stars, depending on the spectral type and age of the object.

**Table 1**  
Summary Information on the Sources for Our Input Primary List

Survey	Reference	$n_{\text{total}}$	$n_{\text{passed}}^{\text{a}}$
Hipparcos	van Leeuwen (2007)	117955	9466
Lepine & Gaidos bright M dwarfs	Lépine & Gaidos (2011)	8889	5432
LSPM North	Lépine & Shara (2005)	61977	60793
rNLTT	Salim & Gould (2003)	36085	31696
Total <sup>b</sup>			79593

#### Notes.

<sup>a</sup> The number of objects that passed our Galactic latitude, total proper motion, and declination cuts and (for *Hipparcos* stars) our parallax.

<sup>b</sup> Total number excluding duplicate appearances of the same object in different catalogs.

has already led to the discovery of a wide T4.5 companion to the nearby K dwarf HIP 38939 (Deacon et al. 2012b). Additionally, objects discovered in our field brown dwarf search can be cross-matched with catalogs of nearby stars to serendipitously identify wide multiple systems. In Deacon et al. (2012a), we used this method to identify a wide T5 companion to the M dwarf LHS 2803 (simultaneously found by Mužić et al. 2012). We present here the results of our full search for wide cool and ultracool companions identified using PS1 proper motions.

## 2. IDENTIFICATION IN PAN-STARRS1 DATA

### 2.1. Primary Star Selection

To identify objects with proper motion in common with nearby stars, we first began by collating lists of stars to search in. We started with stars from the *Hipparcos* catalog (van Leeuwen 2007). To limit the contamination by distant background stars in our sample, we included only *Hipparcos* stars with proper motions above  $0.^f1 \text{ yr}^{-1}$  and parallaxes more significant than  $5\sigma$  ( $d \lesssim 200 \text{ pc}$ ). This provided us with a relatively complete sample of stars in the solar neighborhood with spectral types A–K. We supplemented this catalog with lower-mass primaries drawn from the LSPM (Lépine & Shara 2005;  $\mu > 0.^f15 \text{ yr}^{-1}$ ,  $\delta > 0^\circ$ ) and rNLTT (Salim & Gould 2003;  $\mu > 0.^f2 \text{ yr}^{-1}$ ) proper motion catalogs and with the bright M dwarf catalog of Lépine & Gaidos (2011) to which we applied a proper motion cut of  $\mu > 0.^f1 \text{ yr}^{-1}$ . See Table 1 for details on the number of primary stars from each input catalog.

### 2.2. Selection of Companions from Pan-STARRS 1 Data

Pan-STARRS 1 is an ongoing survey and as such the available data products are constantly evolving. We conducted our search over several iterations of the Pan-STARRS 1  $3\pi$  database. In all our searches we queried the most up-to-date Pan-STARRS 1  $3\pi$  database using the *Desktop Virtual Observatory* software (Magnier et al. 2008). Initially, our search involved combining 2MASS and Pan-STARRS 1 data to calculate proper motions in a similar process to that used by Deacon et al. (2011). For this PS1 + 2MASS search, we required that objects had more than one detection in the  $y_{P1}$  band. PS1 detections were required to have a significance greater than  $5\sigma$  to be included in the astrometric and photometric solutions of their parent object. We also required that the objects be classified as good quality, point-source detections in both Pan-STARRS 1 and 2MASS.

Since 2012 June, we have used proper motions calculated using Pan-STARRS 1 only data (although 2MASS data is included if a detection is within  $1''$  of the mean Pan-STARRS 1

position). In these cases, we required that the proper motion measurement of the candidate companion was more significant than  $5\sigma$ , be calculated from more than seven position measurements, and that the time baseline over which it was calculated be greater than 400 days. Note that the Pan-STARRS 1 survey strategy consists of pairs of observations in the same filter taken  $\sim 25$  minutes apart and often two filters will be taken in the same night. Hence our requirement of seven position measurements does not imply seven independent epochs evenly spread across the time baseline of the proper motion calculation.

In the case of the *Hipparcos* and Lépine & Gaidos (2011) catalogs, distance estimates were available for all our target stars. Hence we searched for companions out to projected separations of 10,000 AU. For the LSPM and rNLTT catalogs, where distance estimates are not available for all the stars, we used a maximum search radius of 20 arcmin. In all cases we made an initial cut on our candidates, requiring that candidates have proper motions that agree with their supposed primaries' proper motions to within  $0''.1 \text{ yr}^{-1}$  in both R.A. and declination. This initial cut uses a tolerance that is much larger than our typical Pan-STARRS 1 proper motion errors of  $\sim 5 \text{ mas yr}^{-1}$ . Next, we made much more stringent cuts on proper motion to select only likely companions.

We restricted our search to objects which had proper motion differences compared to their primaries that were less significant than  $5\sigma$ ; here  $\sigma$  is the quadrature sum of the proper motion difference in each axis divided by the total proper motion error in that axis.

$$\sigma^2 = \frac{(\mu_{\alpha,1} - \mu_{\alpha,2})^2}{\sigma_{\mu_{\alpha,1}}^2 + \sigma_{\mu_{\alpha,2}}^2} + \frac{(\mu_{\delta,1} - \mu_{\delta,2})^2}{\sigma_{\mu_{\delta,1}}^2 + \sigma_{\mu_{\delta,2}}^2} \quad (1)$$

Our typical proper motion errors in Pan-STARRS 1 + 2MASS data are  $\sim 5 \text{ mas yr}^{-1}$ . We selected two samples for follow-up observations. In all cases we set a zone of exclusion around the Galactic center  $|b| < 5^\circ$  and  $l < 90$  or  $l > 270$ .

**1. Ultracool companions.** Objects with red Pan-STARRS 1 colors ( $z_{P1} - y_{P1} > 0.8 \text{ mag}$ ) or ( $y_{P1} - J_{2\text{MASS}} > 1.8 \text{ mag}$ ) were selected as candidate ultracool companions. These cuts should only select objects of spectral types M7 or later (Deacon et al. 2011). These targets also had their Pan-STARRS 1 and 2MASS colors inspected to ensure they truly were red objects and had not entered our sample due to erroneous  $z_{P1}$  or  $y_{P1}$  photometry. This involved removing objects with more than one  $g_{P1}$  detection or with blue  $i_{P1} - y_{P1}$  colors.

Note that two objects (the companions to LSPM J2153+1157 and NLTT 39312) are both close companions that did not meet our  $z_{P1} - y_{P1}$  color cut but were selected due to their red  $y_{P1} - J_{2\text{MASS}}$  colors ( $> 1.6$ ) and close proximity ( $< 12''$ ) to their primaries. These were subsequently spectrally typed as ultracool dwarfs. These two objects may have had their photometry affected by the proximity of their primary.

This sample yielded a total of 38 new discoveries, one of which (HIP 13589B) was simultaneously discovered by Allen et al. (2012). We have also re-identified and typed the NLTT 22073 system originally identified by Deacon & Hambly (2007) and HIP 78184 B originally proposed as a candidate companion by Pinfield et al. (2006).

**2. Bright companions.** We selected the brightest of our common proper motion candidates ( $J_{2\text{MASS}} < 15.5 \text{ mag}$ ) for a poor-weather back-up program for our NASA IRTF SpeX

observations regardless of their color. These objects were mostly within an arcminute of the primary, with all having separations smaller than  $3'$ . This resulted in the discovery of 16 new, bright companions and the typing of 26 previously known companions.

### 2.3. Serendipitous Discoveries

As part of our ongoing search for T dwarfs in Pan-STARRS 1 data (see Deacon et al. 2011 and Liu et al. 2011 for more details), we have been obtaining follow-up near-infrared photometry of Pan-STARRS 1 selected candidates. UKIDSS (Lawrence et al. 2007) or VISTA (Emerson & Sutherland 2010) data were used where available; otherwise our candidate T dwarfs were observed using WFCAM (Casali et al. 2007) on the United Kingdom Infrared Telescope (UKIRT). We then cross-matched all our observed candidates with our combined proper motion catalog from Lépine & Shara (2005), Salim & Gould (2003), and Lépine & Gaidos (2011) with a pairing radius of  $20''$ . Objects that had  $y_{P1} - J_{2\text{MASS}} > 2.2 \text{ mag}$  were initially selected to be T dwarf candidates. However, if the additional near-IR photometry did not match our  $y_{P1} - J_{\text{MKO}} > 2.4 \text{ mag}$  and  $J_{\text{MKO}} - H_{\text{MKO}} < 0.7 \text{ mag}$  high priority T dwarf cut, but still met our  $y_{P1} - J_{\text{MKO}} > 2.0 \text{ mag}$  criterion, those objects were considered to be candidate L dwarfs. Any of these  $\sim 500$  candidates that then had proper motions which did not deviate by more than  $5\sigma$  from their supposed primary stars were selected as candidate L companions for this search.

One of the serendipitous candidates we selected was a possible companion to the late-type high proper motion star NLTT 730. After searching the SIMBAD database, we identified our candidate object as 2MASS J00150206+2959323, a blue L7.5 dwarf found by Kirkpatrick et al. (2010) as a field object. As a blue L benchmark, this is similar to the G 203–50AB system identified by Radigan et al. (2008) although it is substantially wider (5070 AU versus 135 AU). This object is included in our subsequent analysis. In total we selected five serendipitous candidate companions.

Our proper motion companions are reported in Tables 2 and 3. A comparison between their proper motions and photometric distances (see Section 4.1.1) and the proper motions and distances of their primaries are shown in Table 4 for the *Hipparcos* companions and Table 5 for the companions to M dwarfs. In all our tables, the proper motions from the secondaries come from Pan-STARRS 1 + 2MASS proper motions. Where the object's 2MASS position was not included in the initial astrometric analysis we recalculated the proper motion solution including the 2MASS data. The proper motions and distances for all of our *Hipparcos* primaries come from van Leeuwen (2007).

## 3. FOLLOW-UP OBSERVATIONS AND ARCHIVAL DATA

### 3.1. Infrared Photometry

Where companions have confused or noisy photometry, we have used UKIRT/WFCAM (Casali et al. 2007) to acquire additional near-infrared photometry. These data were reduced at the Cambridge Astronomical Survey Unit using the WFCAM survey pipeline (Irwin et al. 2004; Hodgkin et al. 2009). See Table 6 for the near-infrared photometry of our companions from our UKIRT observations, 2MASS (Skrutskie et al. 2006), UKIDSS (Lawrence et al. 2007), VISTA; (Emerson & Sutherland 2010), pre-release photometry from the UKIRT Hemisphere Survey (UHS; S. Dye et al., in preparation, accessed through the

**Table 2**  
Summary Information on Our Wide Companions

Object	WDS Designation	Position (Eq. = J2000 Ep. = 2010.0)	SpT Primary	SpT Secondary	$y_{P1}$ (mag)	$J_{2MASS}$ (mag)	$d_{\text{primary}}$ (pc)	Separation (")	Separation (AU)	Metallicity <sup>k</sup> (dex)	Age (Gyr)	
HIP search companions												
HIP 2397 B	...	00 30 24.94 +22 44 47.1	K5	L0.5	$16.606 \pm 0.008$	$14.586 \pm 0.038$	[ $33.9^{+1.4}_{-1.3}$ ]	117.1	3970	...	$0.5 \sim 10^y$	
HIP 6217 C	...	01 19 44.74 +00 06 18.5	K0	M9.5	$16.859 \pm 0.009$	$15.441 \pm 0.060$	[ $70.9^{+14.0}_{-11.0}$ ]	27.4	2767	...	$0.4 \sim 10^y$	
HIP 6407 B	...	01 22 16.99 +03 31 22.0	G5	L1+T3 <sup>l</sup>	$17.527 \pm 0.027$	$15.471 \pm 0.046$	[ $57.2^{+3.3}_{-3.0}$ ]	44.9	2570	...	$0.5 \sim 10^y$	
HIP 9269 B <sup>‡</sup>	...	01 59 10.98 +33 12 27.8	G5	L6	$18.266 \pm 0.031$	$15.956 \pm 0.088$	[ $25.0^{+0.3}_{-0.4}$ ]	52.1	1300	0.15	$2.2 \sim 10.2^i$	
HIP 10033 B	...	02 09 10.58 -02 19 19.0	F8	M5	$15.14 \pm 0.003$	$13.761 \pm 0.027$	[ $69.7^{+3.4}_{-3.1}$ ]	42.9	2990	-0.08	$2.7 \sim 3.7^j$	
HIP 11161 B	...	02 23 36.59 +52 40 05.9	F5	L1.5	$18.785 \pm 0.067$	$16.636 \pm 0.161$	[ $69.3^{+4.1}_{-3.6}$ ]	47.7	3300	-0.23	$0.5 \sim 2.4^j$	
HIP 13589 B*	...	02 55 07.10 +21 36 21.1	G0	M7.5	$17.098 \pm 0.009$	$14.928 \pm 0.034$	[ $72.8^{+4.6}_{-4.0}$ ]	49.2	3580	...	$0.4 \sim 10^y$	
HIP 26653 B	...	05 39 49.51 +52 53 58.3	G5	L5	$16.905 \pm 0.012$	$14.756 \pm 0.044$	[ $18.8^{+3.7}_{-3.1}$ ]	27.0	753	-0.07	$1.1 \sim 9.3^i$	
										-0.1	$1.6 \sim 13.8^i$	
HIP 32728 B	...	06 49 30.59 +36 26 26.0	G0	M6.5	$16.060 \pm 0.006$	$14.508 \pm 0.031$	[ $46.6^{+2.9}_{-2.6}$ ]	94.3	4400	...	$0.3 \sim 10^y$	
HIP 37283 B <sup>†</sup>	07394+5032 B	07 39 32.03 +50 31 07.3	F5	M6	$14.214 \pm 0.002$	$12.797 \pm 0.027$	[ $45.3^{+1.2}_{-1.2}$ ]	106.1	4830	-0.1	$0.4 \sim 2.1^j$	
HIP 46984 B	...	09 34 33.18 +03 34 07.0	F8	M4	$14.521 \pm 0.002$	$13.285 \pm 0.027$	[ $74.7^{+8.6}_{-6.9}$ ]	37.5	2800	...	$0.4 \sim 10^y$	
HIP 49046 B <sup>†</sup>	10004+2716 B	10 00 35.71 +27 17 06.7	M0	M6.5	$14.482 \pm 0.002$	$13.022 \pm 0.022$	[ $34.7^{+2.6}_{-2.3}$ ]	136.1	4720	...	$0.3 \sim 10^z$	
HIP 51877 B	...	10 35 54.72 +36 55 41.0	G5	M9.5	$16.935 \pm 0.008$	$15.205 \pm 0.063$	[ $57.4^{+11.5}_{-9.6}$ ]	17.6	954	0.22 <sup>u</sup>	$2.4 \sim 7.5^i$	
HIP 52463 B <sup>†</sup>	10435-1852 B	10 43 26.65 -18 52 18.2	G4	M5	$15.043 \pm 0.003$	$13.703 \pm 0.024$	[ $74.2^{+5.2}_{-4.5}$ ]	43.5	3230	0.14	$1.0 \sim 4.9^j$	
HIP 55666 B <sup>‡</sup>	...	11 24 23.43 -05 54 09.8	F5	M5.5	$14.533 \pm 0.037$	$12.674 \pm 0.024$	[ $49.8^{+1.5}_{-1.5}$ ]	37.2	1850	0.14	$3.6 \sim 5.1^j$	
+	HIP 58918 B <sup>†</sup>	12049+3437 B	12 04 52.15 +34 37 23.2	K1	M7	$15.849 \pm 0.004$	$14.471 \pm 0.03$	[ $55.8^{+6.2}_{-5.1}$ ]	20.0	1110	...	$0.1 \sim 10^y$
	HIP 59310 B <sup>†</sup>	12101+1859 B	12 10 09.79 +18 58 07.9	K5	M7	$15.252 \pm 0.002$	$13.691 \pm 0.027$	[ $44.4^{+3.2}_{-2.8}$ ]	82.1	3650	...	$0.2 \sim 10^y$
	HIP 59933 B	...	12 17 36.41 +14 27 11.7	F8	L1	$18.111 \pm 0.032$	$16.101 \pm 0.088$	[ $57.0^{+2.7}_{-2.4}$ ]	38.1	2170	0.03	$0.3 \sim 2.5^j$
	HIP 60501 B <sup>†</sup>	12241+0357 B	12 24 09.68 +03 56 03.3	M0	M5	$12.876 \pm 0.022$	$11.378 \pm 0.027$	[ $56.6^{+7.6}_{-6.0}$ ]	37.1	2100	...	$0.3 \sim 10^z$
	HIP 60987 B <sup>‡c</sup>	12300-0601 B	12 30 01.60 -06 01 23.7	F2	K7	...	...	[ $61.9^{+2.4}_{-2.3}$ ]	~5	~300	-0.12	$1.3 \sim 2.4^j$
	HIP 60987 C <sup>†</sup>	12300-0601 C	12 30 00.68 -06 01 17.9	F2	M3	$12.553 \pm 0.001$	$11.402 \pm 0.028$	[ $61.9^{+2.4}_{-2.3}$ ]	19.0	1170	-0.12	2.0 <sup>j</sup>
	HIP 63506 Cf	13008+4213 C	13 00 50.27 +42 14 47.6	M0	L1	$16.999 \pm 0.008$	$15.15 \pm 0.042$	[ $42.5^{+4.7}_{-3.9}$ ]	132.8	5640	...	$0.3 \sim 10^z$
	HIP 65706 B <sup>†</sup>	13284+3005 B	13 28 20.77 +30 03 17.0	K7	M7	$15.016 \pm 0.003$	$13.315 \pm 0.022$	[ $51.1^{+4.8}_{-4.0}$ ]	52.6	2690	...	$0.3 \sim 10^z$
	HIP 65780 Cf	13291+1128 C	13 29 06.09 +11 27 52.2	K0	M5	$14.327 \pm 0.001$	$13.580 \pm 0.002^h$	[ $58.0^{+3.7}_{-3.3}$ ]	16.0	928	...	$0.5 \sim 10^y$
	HIP 70623 B <sup>†</sup>	14268-0511 B	14 26 45.74 -05 10 20.9	K0	M5.5	$13.619 \pm 0.003$	$12.191 \pm 0.026$	[ $72.6^{+5.5}_{-4.7}$ ]	41.9	3040	0.46	$3.3 \sim 6.0^i$
	HIP 75310 B	...	15 23 10.01 -10 28 58.4	G5	M5	$14.668 \pm 0.003$	$13.291 \pm 0.032$	[ $66.9^{+6.0}_{-5.1}$ ]	22.9	1530	-0.22	$6.3 \sim 9.3^j$
	HIP 76456 B	...	15 36 56.27 +29 59 31.1	F5	M6.5	$14.753 \pm 0.002$	$13.300 \pm 0.031$	[ $36.8^{+0.6}_{-0.6}$ ]	36.1	1330	-0.25	$0.4 \sim 2.2^j$
	HIP 76641 B	...	15 38 59.53 +43 52 17.2	G5	M3.5	$12.158 \pm 0.001$	$10.817 \pm 0.018$	[ $82.1^{+5.3}_{-4.7}$ ]	42.1	3460	...	$0.4 \sim 10^y$
	HIP 78184 B <sup>m</sup>	15578+5916 B	15 57 55.32 +59 14 25.3	M0	M9	$16.219 \pm 0.024$	$14.32 \pm 0.031$	[ $31.4^{+1.4}_{-1.3}$ ]	121.8	3820	...	$0.3 \sim 10^z$
	HIP 78859 B <sup>†</sup>	16059+3500 B	16 05 49.62 +34 59 53.9	G0	M5	$13.57 \pm 0.009$	$12.258 \pm 0.021$	[ $57.2^{+2.3}_{-2.1}$ ]	42.6	2440	...	$0.7 \sim 10^y$
	HIP 78916 B	...	16 06 32.22 +22 53 34.5	G0	M8	$16.694 \pm 0.008$	$15.227 \pm 0.043$	[ $92.9^{+11.5}_{-9.2}$ ]	35.5	3294	...	$0.4 \sim 10^y$
	HIP 78923 B	...	16 06 38.65 +34 06 19.3	G5	M8	$15.565 \pm 0.004$	$14.052 \pm 0.048$	[ $46.1^{+1.8}_{-1.7}$ ]	15.5	714	-0.1 <sup>j</sup>	$0.4 \sim 4.0^j$
	HIP 79180 B <sup>†</sup>	16097+6550 B	16 09 42.06 +65 49 18.1	K7	M5	$15.315 \pm 0.003$	$13.941 \pm 0.022$	[ $74.7^{+3.7}_{-3.4}$ ]	29.0	2170	...	$0.3 \sim 10^z$
	HIP 80258 B <sup>†</sup>	16231+3650 B	16 23 09.09 +36 50 50.2	K3	M4	$14.487 \pm 0.004$	$13.113 \pm 0.021$	[ $63.7^{+9.6}_{-7.5}$ ]	54.9	3500	...	$0.1 \sim 10^y$
	HIP 81910 B	...	16 43 49.50 -26 48 40.2	G2	M6	$13.852 \pm 0.025$	$12.44 \pm 0.024$	[ $46.4^{+0.9}_{-0.8}$ ]	26.7	1240	0.19	$4.0 \sim 5.8^j$
	HIP 82233 B	...	16 48 03.98 -15 57 56.7	G2	M5.5	$13.198 \pm 0.009$	$11.889 \pm 0.024$	[ $42.1^{+1.3}_{-1.2}$ ]	30.4	1280	-0.05	$0.7 \sim 4.7^j$
	HIP 83651 B <sup>†</sup>	17058+0458 B	17 05 49.00 +04 57 24.8	K5	M3	$12.529 \pm 0.052$	$10.599 \pm 0.024$	[ $50.9^{+4.9}_{-4.2}$ ]	28.9	1470	...	$0.1 \sim 10^y$

**Table 2**  
(Continued)

Object	WDS Designation	Position (Eq. = J2000 Ep. = 2010.0)	SpT Primary	SpT Secondary	$y_{P1}$ (mag)	$J_{2MASS}$ (mag)	$d_{\text{primary}}$ (pc)	Separation ( $\text{''}$ )	Separation (AU)	Metallicity <sup>k</sup> (dex)	Age (Gyr)	
HIP 84840 B <sup>2</sup>	...	17 20 22.02 +20 17 01.1	G1.5	M4	$13.852 \pm 0.007$	$12.508 \pm 0.024$	[ $112^{+19}_{-15}$ ]	16.9	1890	...	$0.1 \sim 10^y$	
HIP 85365 B	...	17 26 22.29 -05 02 11.2	F3	L5.5	$18.55 \pm 0.045$	$16.693 \pm 0.168$	[ $30.1^{+0.2}_{-0.2}$ ]	294.1	8850	-0.09	$1.6 \sim 1.9^j$	
HIP 86722 B <sup>jb</sup>	17433+2137 B	17 43 15.32 +21 36 04.2	K0	M5.5	$12.971 \pm 0.018$	$11.511 \pm 0.025$	[ $22.7^{+0.4}_{-0.5}$ ]	22.8	520	-0.33	$3.0 \sim 11.8^i$	
HIP 88728 B	...	18 06 50.92 +08 52 24.0	F5	DA	$12.571 \pm 0.019$	$10.269 \pm 0.097$	[ $40.4^{+1.2}_{-1.1}$ ]	9.6	316	-0.1 <sup>o</sup>	$1.5 \sim 10^y$	
HIP 90273 B <sup>j</sup>	18251+3016 B	18 25 11.57 +30 16 43.2	K7	M3.5	$12.891 \pm 0.054$	$11.56 \pm 0.022$	[ $55.4^{+10.0}_{-7.3}$ ]	26.9	1490	...	$0.3 \sim 10^z$	
HIP 90869 B	...	18 32 11.05 -26 29 45.1	G2	M2	$12.428 \pm 0.042$	$11.101 \pm 0.029$	[ $56.4^{+3.4}_{-3.0}$ ]	17.5	990	-0.46	$5.3 \sim 10.8^i$	
											$1.9 \sim 5.7^k$	
HIP 93967 B	...	19 07 56.43 -15 14 16.3	F9	M3.5	$14.529 \pm 0.007$	$13.357 \pm 0.03$	[ $122.1^{+29.0}_{-19.6}$ ]	22.2	2710	...	$0.2 \sim 10^y$	
HIP 97168 B <sup>j</sup>	19450+5136 B	19 44 59.38 +51 35 31.3	G4	M5.5	$14.997 \pm 0.004$	$13.679 \pm 0.027$	[ $97.5^{+13.1}_{-10.4}$ ]	12.6	1230	...	$0.1 \sim 10^y$	
HIP 98535 C <sup>tf</sup>	20011+4816 E	20 01 02.17 +48 16 27.8	F5	M5.5	$14.763 \pm 0.065$	$13.252 \pm 0.031$	[ $60.0^{+3.8}_{-3.3}$ ]	61.7	3700	-0.02	$0.6 \sim 13.2^j$	
HIP 102582 B <sup>j</sup>	20473+1052 B	20 47 16.75 +10 51 45.1	K2	M5	$13.256 \pm 0.001$	$11.963 \pm 0.033$	[ $31.3^{+1.4}_{-1.3}$ ]	14.7	459	...	$0.2 \sim 10^y$	
HIP 103199 B <sup>j</sup>	20547+3046 B	20 54 33.60 +30 45 40.6	G5	M3.5	$13.161 \pm 0.01$	$11.817 \pm 0.027$	[ $59.5^{+5.1}_{-4.3}$ ]	10.9	650	...	$0.2 \sim 10^y$	
HIP 105202 B <sup>j</sup>	21187+0857 B	21 18 42.31 +08 56 45.0	F5	M4	$13.456 \pm 0.019$	$12.124 \pm 0.024$	[ $41.8^{+1.4}_{-1.3}$ ]	89.4	3740	-0.29	$0.6 \sim 2.9^j$	
HIP 106551 B	...	21 34 45.17 +38 31 00.1	K3III	M5	$14.597 \pm 0.01$	$13.224 \pm 0.025$	[ $71.0^{+2.2}_{-2.1}$ ]	66.1	4690	...	$\leq 10^{aa}$	
HIP 108822 B <sup>j</sup>	22028+1207 B	22 02 48.15 +12 07 05.0	K7	M3	$12.079 \pm 0.002$	$10.622 \pm 0.022$	[ $44.4^{+8.5}_{-6.1}$ ]	31.8	1410	...	$0.3 \sim 10^y$	
HIP 109454 B	...	22 10 27.58 +30 48 28.1	F5	M3	$13.729 \pm 0.116$	$12.422 \pm 0.026$	[ $100.9^{+6.5}_{-5.8}$ ]	18.2	1840	-0.19	$1.4 \sim 2.1^j$	
HIP 111657 B <sup>j</sup>	22371+1159 B	22 37 08.65 +11 58 53.0	K7	M4	$11.978 \pm 0.041$	$10.587 \pm 0.032$	[ $41.9^{+3.3}_{-3.0}$ ]	7.8	330	...	$0.3 \sim 10^z$	
HIP 112422 B <sup>jb</sup>	22463+3319 C	22 46 18.57 +33 19 30.5	K2	L1.5	$17.776 \pm 0.021$	$16.023 \pm 0.113$	[ $65.4^{+8.3}_{-6.6}$ ]	16.0	1040	...	$0.1 \sim 10^{*y}$	
5	HIP 114424 B	...	23 10 22.08 -07 48 54.7	G0	M5.5	$13.089 \pm 0.001$	$11.595 \pm 0.026$	[ $35.1^{+1.1}_{-0.9}$ ]	42.0	1480	0.08	$0.6 \sim 4.5^j$
										0.06	$3.7 \sim 11.7^i$	
HIP 114456 B <sup>††a</sup>	23108+4531 C	23 10 54.78 +45 30 43.8	K0	M5	$12.371 \pm 0.003$	$10.844 \pm 0.021$	[ $24.3^{+0.3}_{-0.3}$ ]	50.4	1220	0.19	$2.1 \sim 9.6^k$	
HIP 115819 B	...	23 27 49.76 +04 51 00.1	K5	M8	$16.865 \pm 0.022$	$15.095 \pm 0.034$	[ $65.7^{+11.0}_{-8.2}$ ]	30.4	2000	...	$0.2 \sim 10^y$	
HIP 116052 B <sup>j</sup>	23309+2747 B	23 30 52.38 +27 46 32.3	G5	M3.5	$13.718 \pm 0.002$	$12.361 \pm 0.019$	[ $49.6^{+2.5}_{-2.3}$ ] <sup>l</sup>	26.8	1330	...	$0.3 \sim 10^y$	
Companions to faint non-HIP primaries												
NLTT 1011 B	...	00 19 32.68 +40 18 55.4	K7	L2	$17.615 \pm 0.015$	$15.544 \pm 0.059$	[ $68.2^{+6.6}_{-6.5}$ ]	58.5	3990	...	$0.3 \sim 10^y$	
GD 280 B	...	01 54 58.13 +48 19 59.1	DA	M9	$17.624 \pm 0.013$	$16.034 \pm 0.082$	[ $77^{+35}_{-26}$ ]	63.4	4882	...	$< 10^{aa}$	
NLTT 8245 B	...	02 33 23.52 +65 45 47.6	M0	M7	$16.465 \pm 0.007$	$14.922 \pm 0.052$	[ $53.0^{+8.7}_{-7.5}$ ]	10.6	562	...	$0.3 \sim 10^y$	
LSPM J0241+2553 B	...	02 41 51.51 +25 53 43.4	WD	L1	$19.074 \pm 0.05$	$17.027 \pm 0.180$	[ $69^{+35}_{-23}$ ]	31.2	2153	...	$< 10^{aa}$	
HD 253662 B	...	06 13 53.35 +15 14 04.4	G8IV	L0.5	$17.691 \pm 0.02$	$15.961 \pm 0.0082$	[ $> 62.3$ ]	20.1	>1252	...	$< 10^{aa}$	
LSPM J0632+5053 B	...	06 32 48.55 +50 53 33.6	G2	L1.5	$18.86 \pm 0.04$	$16.383 \pm 0.108$	[ $95.0^{+16.3}_{-13.9}$ ]	47.4	4499	...	$0.2 \sim 10^y$	
NLTT 18587 B	...	07 54 13.38 +37 21 42.6	M2	M7.5	$18.03 \pm 0.026$	$16.894 \pm 0.199$	[ $132^{+40}_{-31}$ ]	92.4	12200	...	$0.3 \sim 1^z$	
NLTT 19109 B	...	08 11 59.00 -08 58 01.6	M4	M8.5	$18.36 \pm 0.044$	$16.933 \pm 0.170$	[ $132^{+49}_{-36}$ ]	7.5	362	...	$0.3 \sim 10^y$	
NLTT 22073 B <sup>g</sup>	...	09 33 37.11 -27 52 45.4	M2	M7.5	$16.303 \pm 0.007$	$14.671 \pm 0.037$	[ $29.9^{+12.7}_{-6.9}$ ]	26	776	...	$0.4 \sim 10^x$	
NLTT 23716 B	...	10 13 17.05 -06 01 22.9	K7	M8	$15.884 \pm 0.006$	$14.300 \pm 0.036$	[ $48.2^{+7.9}_{-6.8}$ ]	15.0	723	...	$0.3 \sim 10^y$	
NLTT 26746 B	...	11 15 01.22 +16 07 00.8	M4	L4	$18.36 \pm 0.06$	$16.403 \pm 0.118$	[ $41.0^{+12.2}_{-10.3}$ ]	18.0	661	...	$0.3 \sim 10^y$	
NLTT 29395 B	...	12 03 02.61 +58 06 02.4	M3	M8	$17.397 \pm 0.013$	$15.810 \pm 0.080$	[ $56.4^{+16.9}_{-13.0}$ ]	11.9	671	...	$0.3 \sim 10^y$	
NLTT 30510 B	...	12 22 18.59 +36 43 48.1	M2	M9.5	$17.716 \pm 0.016$	$15.971 \pm 0.080$	[ $49.1^{+14.8}_{-11.3}$ ]	19.6	962	...	$0.3 \sim 10^y$	
NLTT 31450 B	...	12 39 49.19 +32 09 03.1	M4	L6	$18.34 \pm 0.03$	$16.135 \pm 0.105$	[ $34.6^{+10.3}_{-8.7}$ ]	12.3	487	...	$0.3 \sim 10^y$	
PMI 13410+0542 B	...	13 41 02.39 +05 42 48.8	M1	L4	$18.00 \pm 0.02$	$16.187 \pm 0.143$	[ $51.3^{+21.7}_{-11.8}$ ]	9.4	484	...	$0.3 \sim 10^y$	
PMI 13518+4157 B	...	13 51 47.41 +41 57 47.4	M2.5	L1.5	$17.17 \pm 0.01$	$15.081 \pm 0.032$	[ $43.1^{+9.9}_{-8.8}$ ]	21.6	613	...	$0.3 \sim 10^y$	

**Table 2**  
(Continued)

Object	WDS Designation	Position (Eq. = J2000 Ep. = 2010.0)	SpT Primary	SpT Secondary	$y_{P1}$ (mag)	$J_{2MASS}$ (mag)	$d_{\text{primary}}$ (pc)	Separation ( $\text{''}$ )	Separation (AU)	Metallicity <sup>k</sup> (dex)	Age (Gyr)
NLTT 38489 B	...	14 48 46.28 +56 10 57.8	M4	M9	$18.62 \pm 0.04$	$16.64 \pm 0.143$	$62.3^{+23.3}_{-17.0}$	6.7	418	...	$1.2 \sim 10^8$
NLTT 39312 B	...	15 05 59.27 +33 39 30.2	M2	M8	$17.768 \pm 0.018$	$16.09 \pm 0.096$	$140.9^{+42.6}_{-32.7}$	5.1	713	...	$0.3 \sim 10^2$
LSPM J1627+3328 B	...	16 27 01.44 +33 28 21.4	K7	M9	$16.386 \pm 0.018$	$14.362 \pm 0.083$	$38.0^{+6.3}_{-5.4}$	9.0	341	...	$0.3 \sim 10^2$
NLTT 44368 B	...	17 11 57.29 +54 30 43.8	M3	L1.5	$16.754 \pm 0.016$	$14.736 \pm 0.058$	$55.0^{+12.7}_{-11.3}$	90.2	7760	...	$0.3 \sim 10^2$
LSPM J1717+5925 B	...	17 17 30.94 +59 25 30.2	G6	M9	$18.043 \pm 0.015$	$16.580 \pm 0.168$	$108.0^{+34.8}_{-26.4}$	14.4	1555	...	$0.2 \sim 10^9$
NLTT 52268 B	...	21 51 07.23 +30 45 54.7	M3	M9	$16.67 \pm 0.03$	$14.945 \pm 0.052$	$37.3^{+11.3}_{-8.7}$	14.7	549	...	$0.3 \sim 10^2$
LSPM J2153+1157 B	...	21 53 46.92 +11 57 46.4	M3	M7	$16.005 \pm 0.004$	$14.403 \pm 0.038$	$36.2^{+10.9}_{-8.4}$	11.3	408	...	$0.3 \sim 10^2$
PM I22118–1005 B	...	22 11 41.25 –10 08 20.8	M2	L1.5	$17.412 \pm 0.010$	$15.246 \pm 0.049$	$37.4^{+8.6}_{-7.7}$	204.5	8892	...	$0.3 \sim 10^2$
NLTT 55219 B	...	22 54 28.58 +22 02 56.1	M2	L5.5	$18.791 \pm 0.039$	$16.313 \pm 0.122$	$44.7^{+13.5}_{-10.4}$	9.7	432	...	$0.3 \sim 10^2$
Serendipitous Companion Discoveries											
NLTT 730 B	...	00 15 02.40 +29 59 29.8	M4	L7.5 <sup>d</sup>	$18.37 \pm 0.06$	$16.16 \pm 0.08$	$21.7^{+8.1}_{-5.3}$	233.6	5070	...	$3 \sim 10^2$
NLTT 27966 B	...	11 36 39.44 +48 52 43.0	M5	L4	$18.48 \pm 0.05$	$16.155 \pm 0.103$	$39.6^{+13.3}_{-10.2}$	15.9	630	...	$0.3 \sim 10^2$
LSPMJ1336+2541 B	...	13 36 24.89 +25 40 37.2	M3	L4	$19.45 \pm 0.09$	$16.863 \pm 0.16$	$60.7^{+15.7}_{-13.9}$	121.7	8793	...	$0.3 \sim 10^2$
HIP 73169 B <sup>e</sup>	...	14 57 11.35 –06 19 27.4	M0	L2.5	$18.42 \pm 0.09$	$16.007 \pm 0.09$	[ $27.3^{+8.3}_{-6.3}$ ]	29.1	796	...	$0.3 \sim 10^2$
PM I23492+3458 B	...	23 49 15.11 +34 58 55.3	M2	L9	$18.80 \pm 0.04$	$16.298 \pm 0.105$	$30.7^{+7.1}_{-6.3}$	34.9	949	...	$0.3 \sim 10^2$
Unlikely Companions											
NLTT 35593 B	...	13 54 34.92 –06 07 34.3	M2	L2	$18.56 \pm 0.03$	$16.299 \pm 0.114$	$63.0^{+19.1}_{-14.6}$	1105.8	69706	...	$0.3 \sim 10^{12}$

**Notes.**

<sup>a</sup> Denotes distance from trigonometric parallax; all other distances are photometric.

<sup>†</sup> Previously known in the Washington Double Star Catalog.

<sup>‡</sup> Additional possibly spurious companion in the system in the Washington Double Star Catalog.

<sup>\*</sup> Simultaneously discovered by Allen et al. (2012).

<sup>a</sup> Our object appears in the Washington Double Star Catalog as component C due to a spurious companion listed as B.

<sup>b</sup> Primary is itself a close double listed as Aa and Ab in the Washington Double Star Catalog.

<sup>c</sup> The companion was identified as a visual double during IRTF acquisition; due to saturation, it does not appear in our PS1 catalog. Position is taken from VISTA image.

<sup>d</sup> Spectral type from Kirkpatrick et al. (2010). We identify this object as a companion to NLTT 730.

<sup>e</sup> While HIP 73169 appears in the *Hipparcos* catalog, its parallax measurement was too low significance for it to be included in our input *Hipparcos* sample. Hence it appears in our sample of other primaries due to it being a nearby M dwarf in the proper motion catalog of Salim & Gould (2003).

<sup>f</sup> Primary is itself binary with a listing in the Washington Double Star Catalog. Our companion is component C.

<sup>g</sup> Previously identified by Deacon & Hamby (2007) as a binary pair. The secondary is also known as SIPS 0933–2752

<sup>h</sup> The 2MASS photometry is only an upper limit; photometry taken from UKIDSS Lawrence et al. (2007).

<sup>i</sup> Valenti & Fischer (2005).

<sup>j</sup> Casagrande et al. (2011).

<sup>k</sup> Metallicity definition depends on source; metallicities from <sup>i</sup> are [M/H] while those from <sup>j</sup> are [Fe/H].

<sup>l</sup> Estimated spectral types from spectral deblending. See Section 5.2.1.

<sup>m</sup> Previously identified as a candidate companion by Pinfield et al. (2006).

<sup>o</sup> Metallicity from Lee et al. (2011).

<sup>w</sup> Robinson et al. (2007).

<sup>x</sup> This work, minimum age calculated from lack of activity and the activity lifetimes of West et al. (2008), approximate maximum age from disk-like kinematics.

<sup>y</sup> This work, minimum age calculated from limiting X-ray flux and the relations of Mamajek & Hillenbrand (2008), approximate maximum age from disk-like kinematics.

<sup>z</sup> This work, minimum age is that from Shkolnik et al. (2009) for objects with no X-ray emission, approximate maximum age from disk-like kinematics.

<sup>aa</sup> This work, approximate maximum age from disk-like kinematics.

<sup>1</sup> Object primary is a spectroscopic binary.

<sup>2</sup> Previously identified in Lépine & Bongiorno (2007).

**Table 3**  
PS1 Data of Our Wide Companions

Object	Position (Eq. = J2000 Ep. = 2010.0)	SpT	$g_{P1}$ (mag)	$r_{P1}$ (mag)	$i_{P1}$ (mag)	$z_{P1}$ (mag)	$y_{P1}$ (mag)
HIP search companions							
HIP 2397 B	00 30 24.94 +22 44 47.1	L0.5	...	...	19.085 ± 0.013	17.49 ± 0.022	16.606 ± 0.008
HIP 6217 C	01 19 44.74 +00 06 18.5	M9.5	21.656 ± 0.11	21.076 ± 0.071	18.6 ± 0.019	17.444 ± 0.007	16.859 ± 0.009
HIP 6407 B	01 22 16.99 +03 31 22.0	L1+T3 <sup>d</sup>	...	...	20.094 ± 0.042	18.534 ± 0.015	17.527 ± 0.027
HIP 9269 B <sup>‡</sup>	01 59 10.98 +33 12 27.8	L6	...	...	...	...	18.266 ± 0.031
HIP 10033 B	02 09 10.58 -02 19 19.0	M5	19.709 ± 0.017	18.297 ± 0.007	16.456 ± 0.003	15.54 ± 0.003	15.14 ± 0.003
HIP 11161 B	02 23 36.59 +52 40 05.9	L1.5	...	...	21.24 ± 0.095	19.475 ± 0.051	18.785 ± 0.067
HIP 13589 B*	02 55 07.10 +21 36 21.1	M7.5	...	...	...	18.003 ± 0.012	17.098 ± 0.009
HIP 26653	05 39 49.51 +52 53 58.3	L5	...	20.542 ± 0.043	...	17.719 ± 0.011	16.905 ± 0.012
HIP 32728 B	06 49 30.59 +36 26 26.0	M6.5	...	21.26 ± 0.08	18.057 ± 0.006	16.721 ± 0.007	16.060 ± 0.006
HIP 37283 B <sup>†</sup>	07 39 32.03 +50 31 07.3	M6	18.985 ± 0.01	17.622 ± 0.006	15.593 ± 0.002	14.639 ± 0.001	14.214 ± 0.002
HIP 46984 B	09 34 33.18 +03 34 07.0	M4	18.199 ± 0.006	17.038 ± 0.004	15.444 ± 0.003	14.848 ± 0.002	14.521 ± 0.002
HIP 49046 B <sup>†</sup>	10 00 35.71 +27 17 06.7	M6.5	20.127 ± 0.021	18.7 ± 0.007	16.282 ± 0.002	15.138 ± 0.002	14.482 ± 0.002
HIP 51877 B	10 35 54.72 +36 55 41.0	M9.5	...	20.23 ± 0.039	19.207 ± 0.011	17.801 ± 0.004	16.935 ± 0.008
HIP 52463 B	10 43 26.65 -18 52 18.2	M5	19.576 ± 0.018	18.25 ± 0.02	16.599 ± 0.011	15.479 ± 0.001	15.043 ± 0.003
HIP 55666 B <sup>‡</sup>	11 24 23.43 -05 54 09.8	M5.5	...	...	...	...	14.533 ± 0.037
HIP 58918 B <sup>†</sup>	12 04 52.15 +34 37 23.2	M7	21.445 ± 0.092	20.122 ± 0.026	17.623 ± 0.006	16.491 ± 0.004	15.849 ± 0.004
HIP 59310 B <sup>†</sup>	12 10 09.79 +18 58 07.9	M7	21.021 ± 0.052	19.579 ± 0.012	17.077 ± 0.005	15.88 ± 0.002	15.252 ± 0.002
HIP 59933 B	12 17 36.41 +14 27 11.7	L1	...	...	...	19.079 ± 0.025	18.111 ± 0.032
HIP 60501 B <sup>†</sup>	12 24 09.68 +03 56 03.3	M5	17.074 ± 0.004	15.814 ± 0.002	14.207 ± 0.038	13.313 ± 0.001	12.876 ± 0.022
HIP 60987 B <sup>c</sup>	12 30 01.60 -06 01 23.7	K7	...	...	...	...	...
HIP 60987 C <sup>†</sup>	12 30 00.68 -06 01 17.9	M3	15.395 ± 0.005	14.336 ± 0.001	...	12.825 ± 0.001	12.553 ± 0.001
HIP 63506 C <sup>‡</sup>	13 00 50.27 +42 14 47.6	L1	...	22.019 ± 0.122	19.49 ± 0.014	17.964 ± 0.007	16.999 ± 0.008
HIP 65706 B <sup>†</sup>	13 28 20.77 +30 03 17.0	M7	...	...	...	...	15.016 ± 0.003
HIP 65780 Cf	13 29 06.09 +11 27 52.2	M5	18.523 ± 0.001	17.393 ± 0.001	15.669 ± 0.001	14.724 ± 0.001	14.327 ± 0.001
HIP 70623 C <sup>†</sup>	14 26 45.74 -05 10 20.9	M5.5	17.424 ± 0.008	16.233 ± 0.013	14.762 ± 0.061	13.981 ± 0.001	13.619 ± 0.003
HIP 75310 B	15 23 10.01 -10 28 58.4	M5	20.018 ± 0.062	...	15.647 ± 0.003	15.055 ± 0.003	14.668 ± 0.003
HIP 76456 B <sup>†</sup>	15 36 56.27 +29 59 31.1	M6.5	19.827 ± 0.017	19.027 ± 0.006	16.513 ± 0.002	15.343 ± 0.002	14.753 ± 0.002
HIP 76641 B	15 38 59.53 +43 52 17.2	M3.5	...	...	17.225 ± 0.036	13.026 ± 0.001	12.158 ± 0.001
HIP 78184 B	15 57 55.32 +59 14 25.3	M9	...	21.043 ± 0.054	18.642 ± 0.014	17.167 ± 0.013	16.219 ± 0.024
HIP 78859 B <sup>†</sup>	16 05 49.62 +34 59 53.9	M5	16.9 ± 0.004	15.633 ± 0.024	14.422 ± 0.004	13.832 ± 0.009	13.57 ± 0.009
HIP 78916 B	16 06 32.22 +22 53 34.5	M8	22.05 ± 0.16	19.694 ± 0.021	18.506 ± 0.009	17.354 ± 0.006	16.694 ± 0.008
HIP 78923 B	16 06 38.65 +34 06 19.3	M8	...	...	17.219 ± 0.006	16.187 ± 0.002	15.565 ± 0.004
HIP 79180 B <sup>†</sup>	16 09 42.06 +65 49 18.1	M5	20.008 ± 0.02	18.815 ± 0.013	16.718 ± 0.003	15.985 ± 0.003	15.315 ± 0.003
HIP 80258 B <sup>†</sup>	16 23 09.09 +36 50 50.2	M4	18.321 ± 0.062	16.993 ± 0.023	15.497 ± 0.002	14.782 ± 0.111	14.487 ± 0.004
HIP 81910 B	16 43 49.50 -26 48 40.2	M6	...	17.478 ± 0.068	15.494 ± 0.012	14.678 ± 0.344	13.852 ± 0.025
HIP 82233 B	16 48 03.98 -15 57 56.7	M5.5	...	15.693 ± 0.003	14.218 ± 0.001	...	13.198 ± 0.009
HIP 83651 B <sup>†</sup>	17 05 49.00 +04 57 24.8	M3	14.977 ± 0.001	13.978 ± 0.035	12.809 ± 0.07	12.018 ± 0.001	12.529 ± 0.052
HIP 84840 B	17 20 22.02 +20 17 01.1	M4	17.489 ± 0.019	16.272 ± 0.008	14.869 ± 0.002	14.126 ± 0.014	13.852 ± 0.007
HIP 85365 B	17 26 22.29 -05 02 11.2	L5.5	...	...	21.606 ± 0.13	19.547 ± 0.05	18.55 ± 0.045
HIP 86722 B <sup>†</sup>	17 43 15.32 +21 36 04.2	M5.5	...	...	...	14.184 ± 0.003	12.971 ± 0.018
HIP 88728 B	18 06 50.92 +08 52 24.0	DA	...	14.377 ± 0.203	...	13.66 ± 0.002	12.571 ± 0.019
HIP 90273 B	18 25 11.57 +30 16 43.2	M3.5	16.348 ± 0.003	15.307 ± 0.294	13.905 ± 0.066	13.117 ± 0.004	12.891 ± 0.054
HIP 90869 B	18 32 11.05 -26 29 45.1	M2	15.375 ± 0.024	14.156 ± 0.026	...	12.443 ± 0.001	12.428 ± 0.042
HIP 93967 B	19 07 56.43 -15 14 16.3	M3.5	17.723 ± 0.023	...	15.433 ± 0.028	14.75 ± 0.027	14.529 ± 0.007
HIP 97168 B	19 44 59.38 +51 35 31.3	M5.5	18.5 ± 0.014	17.241 ± 0.009	16.081 ± 0.007	15.38 ± 0.007	14.997 ± 0.004
HIP 98535 Cf	20 01 02.17 +48 16 27.8	M5.5	19.513 ± 0.046	...	16.077 ± 0.031	15.183 ± 0.057	14.763 ± 0.065
HIP 102582 B <sup>†</sup>	20 47 16.75 +10 51 45.1	M5	17.437 ± 0.003	16.140 ± 0.003	14.408 ± 0.001	13.601 ± 0.002	13.256 ± 0.001
HIP 103199 B <sup>†</sup>	20 54 33.60 +30 45 40.6	M3.5	16.513 ± 0.004	...	15.03 ± 0.912	13.415 ± 0.005	13.161 ± 0.01
HIP 105202 B <sup>†</sup>	21 18 42.31 +08 56 45.0	M4	17.221 ± 0.097	15.867 ± 0.031	14.41 ± 0.01	13.718 ± 0.002	13.456 ± 0.019
HIP 106551 B	21 34 45.17 +38 31 00.1	M5	19.019 ± 0.056	17.677 ± 0.034	15.958 ± 0.01	14.979 ± 0.01	14.597 ± 0.01
HIP 108822 B <sup>†</sup>	22 02 48.15 +12 07 05.0	M3	15.019 ± 0.007	13.995 ± 0.185	13.459 ± 0.451	12.478 ± 0.092	12.079 ± 0.002
HIP 109454 B	22 10 27.58 +30 48 28.1	M3	16.605 ± 0.004	...	...	13.895 ± 0.002	13.729 ± 0.116
HIP 111657 B <sup>†</sup>	22 37 08.65 +11 58 53.0	M4	15.678 ± 0.011	14.389 ± 0.015	14.477 ± 0.337	...	11.978 ± 0.041
HIP 112422 B <sup>jb</sup>	22 46 18.57 +33 19 30.5	L1.5	...	...	19.899 ± 0.041	18.907 ± 0.016	17.776 ± 0.021
HIP 114424 B <sup>††</sup>	23 10 22.08 -07 48 54.7	M5.5	...	16.296 ± 0.004	14.444 ± 0.004	13.548 ± 0.076	13.089 ± 0.001
HIP 114456 B <sup>††a</sup>	23 10 54.78 +45 30 43.8	M5	17.26 ± 0.054	...	14.055 ± 0.001	13.063 ± 0.001	12.371 ± 0.003
HIP 115819 B	23 27 49.76 +04 51 00.1	M8	...	...	19.272 ± 0.023	...	16.865 ± 0.022
HIP 116052 B <sup>†</sup>	23 30 52.38 +27 46 32.3	M3.5	...	...	...	14.013 ± 0.02	13.718 ± 0.002
Companions to faint non-HIP primaries							
NLTT 1011 B	00 19 32.68 +40 18 55.4	L2	...	...	20.203 ± 0.034	18.651 ± 0.013	17.615 ± 0.015
GD 280	01 54 58.13 +48 19 59.1	M9	...	...	19.915 ± 0.017	18.524 ± 0.017	17.624 ± 0.013
NLTT 8245	02 33 23.52 +65 45 47.6	M7	...	...	18.689 ± 0.015	17.362 ± 0.005	16.465 ± 0.007
LSPM J0241+2553	02 41 51.51 +25 53 43.4	L1	...	...	21.357 ± 0.132	19.986 ± 0.065	19.074 ± 0.05

**Table 3**  
(Continued)

Object	Position (Eq. = J2000 Ep. = 2010.0)	SpT	$g_{P1}$ (mag)	$r_{P1}$ (mag)	$i_{P1}$ (mag)	$z_{P1}$ (mag)	$y_{P1}$ (mag)
HD 253662	06 13 53.35 +15 14 04.4	L0.5	...	21.39 ± 0.109	20.306 ± 0.073	18.692 ± 0.022	17.691 ± 0.02
LSPMJ0632+5053 B	06 32 48.55 +50 53 33.6	L1.5	...	...	...	19.86 ± 0.12	18.86 ± 0.04
NLTT 18587	07 54 13.38 +37 21 42.6	M7.5	...	...	20.507 ± 0.057	18.879 ± 0.019	18.03 ± 0.026
NLTT 19109	08 11 59.00 –08 58 01.6	M8.5	...	...	20.679 ± 0.042	19.193 ± 0.023	18.36 ± 0.044
NLTT 22073 B	09 33 37.11 –27 52 45.4	M7.5	...	21.185 ± 0.047	18.619 ± 0.007	17.115 ± 0.006	16.303 ± 0.007
NLTT 23716	10 13 17.05 –06 01 22.9	M8	22.289 ± 0.221	...	17.995 ± 0.006	16.703 ± 0.005	15.884 ± 0.006
NLTT 26746 B	11 15 01.22 +16 07 00.8	L4	...	...	21.23 ± 0.07	19.43 ± 0.05	18.36 ± 0.06
NLTT 29395	12 03 02.61 +58 06 02.4	M8	...	...	19.605 ± 0.018	18.181 ± 0.008	17.397 ± 0.013
NLTT 30510	12 22 18.59 +36 43 48.1	M9.5	...	...	20.371 ± 0.064	18.657 ± 0.014	17.716 ± 0.016
NLTT 31450 B	12 39 49.19 +32 09 03.1	L6	...	...	20.8 ± 0.09	19.29 ± 0.02	18.34 ± 0.03
PMI 13410+0542 B	13 41 02.39 +05 42 48.8	L4	...	21.5 ± 0.2	20.10 ± 0.05	18.92 ± 0.03	18.00 ± 0.02
PMI 13518+4157 B	13 51 47.41 +41 57 47.4	L1.5	...	21.64 ± 0.13	19.636 ± 0.018	18.190 ± 0.009	17.17 ± 0.01
NLTT 38489 B	14 48 46.28 +56 10 57.8	M9	...	...	20.88 ± 0.05	19.52 ± 0.04	18.62 ± 0.04
NLTT 39312 B	15 05 59.27 +33 39 30.2	M8	...	...	19.588 ± 0.018	18.476 ± 0.017	17.768 ± 0.018
LSPM J1627+3328 B	16 27 01.44 +33 28 21.4	M9	...	...	18.94 ± 0.16	17.32 ± 0.03	16.386 ± 0.018
NLTT 44368 B	17 11 57.29 +54 30 43.8	L1.5	...	21.28 ± 0.07	...	17.688 ± 0.011	16.754 ± 0.016
LSPM J1717+5925 B	17 17 30.94 +59 25 30.2	M9	...	...	20.232 ± 0.053	18.890 ± 0.013	18.043 ± 0.015
NLTT 52268 B	21 51 07.23 +30 45 54.7	M9	...	...	19.08 ± 0.01	17.63 ± 0.01	16.67 ± 0.03
LSPM J2153+1157 B	21 53 46.92 +11 57 46.4	M7	22.28 ± 0.08	20.90 ± 0.03	18.149 ± 0.005	16.787 ± 0.003	16.005 ± 0.004
PM I22118–1005 B	22 11 41.25 –10 08 20.8	L1.5	...	22.28 ± 0.14	19.77 ± 0.02	18.347 ± 0.010	17.412 ± 0.010
NLTT 55219 B	22 54 28.58 +22 02 56.1	L5.5	...	...	...	19.665 ± 0.04	18.791 ± 0.039
Serendipitous Companion Discoveries							
NLTT 730 B	00 15 02.40 +29 59 29.8	L7.5p <sup>d</sup>	...	...	21.63 ± 0.11	19.49 ± 0.04	18.37 ± 0.06
NLTT 27966 B	11 36 39.44 +48 52 43.0	L4	...	...	21.06 ± 0.13	19.52 ± 0.03	18.48 ± 0.05
LSPMJ1336+2541 B	13 36 24.89 +25 40 37.2	L4	...	...	22.19 ± 0.16	20.21 ± 0.07	19.45 ± 0.09
HIP 73169 Be <sup>e</sup>	14 57 11.35 –06 19 27.4	L2.5	...	...	20.55 ± 0.18	19.06 ± 0.02	18.42 ± 0.09
PM I23492+3458 B	23 49 15.11 +34 58 55.3	L9	...	...	...	19.99 ± 0.04	18.80 ± 0.04
Unlikely Companions							
NLTT 35593 B	13 54 34.92 –06 07 34.3	L2	...	...	20.74 ± 0.12	19.37 ± 0.11	18.56 ± 0.03

**Notes.**<sup>a</sup> Previously known in the Washington Double Star Catalog.<sup>b</sup> Additional possibly spurious companion in the system in the Washington Double Star Catalog.<sup>c</sup> Simultaneously discovered by Allen et al. (2012).<sup>d</sup> Our object appears in the Washington Double Star Catalog as component C due to a spurious companion listed as B.<sup>e</sup> Primary is itself a close double listed as Aa and Ab in the Washington Double Star Catalog.<sup>f</sup> The companion was identified as visual double during IRTF acquisition, due to saturation, it does not appear in our PS1 catalog, position is taken from VISTA image.<sup>g</sup> Spectral type from Kirkpatrick et al. (2010). We identify this object as a companion to NLTT 730.<sup>h</sup> While HIP 73169 appears in the *Hipparcos* catalog, its parallax measurement was too low-significance for it to be included in our input *Hipparcos* sample. Hence it appears in our sample of other primaries due to it being a nearby M dwarf in the proper motion catalog of Salim & Gould (2003).<sup>i</sup> Primary is itself a binary with a listing in the Washington Double Star Catalog. Our companion is component C.<sup>j</sup> Previously identified by Deacon & Hambley (2007) as a binary pair. The secondary is also known as SIPS 0933–2752.

WFCAM Science Archive; Hambley et al. 2008) and Table 7 for mid-infrared photometry from *WISE* (Wright et al. 2010; Cutri et al. 2012).

### 3.2. Near-infrared Spectroscopy

To characterize our companions, we obtained 0.8–2.5  $\mu$ m spectroscopy using the SpeX instrument (Rayner et al. 2003) on the NASA Infrared Telescope (IRTF). To minimize the possibility of observing an unrelated background object due to a non-physical chance alignment with one of our primaries, we preferentially followed-up (i.e., we were more likely to follow-up) companions closer than five arcminutes but did not follow-up all of our candidate companions. In total 115 candidate companions to stars were passed to the IRTF queue, 87 are presented here as true companions, 1 we classify as an unlikely companion, 2 are candidate white dwarf companions

not presented in this work, and the remaining 26 were not observed.

Depending on the brightness of the object and the weather conditions, we used either the low-resolution ( $R \approx 75$ –120) single-order prism mode or the moderate-resolution ( $R \approx 750$ –2000) multiple-order cross-dispersed SXD mode. The slit width was chosen to match the seeing and was oriented along the parallactic angle to minimize atmospheric dispersion. The observations were taken in nodded ABBA patterns. The standards were taken contemporaneously with each science target and at similar airmass and sky position. We reduced all our spectra using version 3.4 of the SpeXtool software package (Cushing et al. 2004; Vacca et al. 2003). See Table 8 for details of the exposure times, weather conditions, and standard stars used for each object.

We spectrally classified our objects by visually comparing with the M and L near-infrared standards from Kirkpatrick

**Table 4**  
Astrometric Data on Our Data of Our Multiple Systems

Object	$d$	$\mu_\alpha \cos \delta$	$\mu_\delta$	$d\mu_\alpha \cos \delta$	$d\mu_\delta$	$d\mu$	Projected Separation ('')	Projected Separation (AU)
	(pc)	('' yr $^{-1}$ )	('' yr $^{-1}$ )	$n_\sigma$	$n_\sigma$	$n_\sigma$		
HIP 2397	[33.9 $^{+1.4}_{-1.3}$ ]	0.186 $\pm$ 0.001	-0.185 $\pm$ 0.001	3.2	2.1	3.8	117.1	3970
HIP 2397B	39.2 $^{+7.6}_{-6.4}$	0.2 $\pm$ 0.004	-0.176 $\pm$ 0.004					
HIP 6217	[101 $^{+18}_{-13}$ ]	0.119 $\pm$ 0.001	0.030 $\pm$ 0.001	1.94	1.94	2.74	27.4	2767
HIP 6217 B	70.9 $^{+14.0}_{-11.7}$	0.111 $\pm$ 0.004	0.022 $\pm$ 0.004					
HIP 6407	[57.2 $^{+3.3}_{-3.0}$ ]	0.046 $\pm$ 0.001	-0.159 $\pm$ 0.001	2.1	2.7	3.4	44.9	2570
HIP 6407B	53.6 $^{+10.5}_{-8.8}$	0.03 $\pm$ 0.008	-0.138 $\pm$ 0.008					
HIP 9269	[25.0 $^{+0.3}_{-0.4}$ ]	0.244 $\pm$ 0.001	-0.352 $\pm$ 0.001	0.1	0.5	0.5	52.1	1300
HIP 9269B	27.8 $^{+5.4}_{-4.5}$	0.243 $\pm$ 0.011	-0.347 $\pm$ 0.011					
HIP 10033	[69.7 $^{+3.4}_{-3.1}$ ]	-0.093 $\pm$ 0.001	-0.046 $\pm$ 0.001	2.9	2.6	3.9	42.9	2990
HIP 10033B	89.5 $^{+17.3}_{-14.5}$	-0.114 $\pm$ 0.007	-0.027 $\pm$ 0.007					
HIP 11161	[69.3 $^{+4.1}_{-3.6}$ ]	-0.081 $\pm$ 0.001	-0.061 $\pm$ 0.001	0.4	0.6	0.7	47.7	3300
HIP 11161B	83.6 $^{+16.3}_{-13.6}$	-0.079 $\pm$ 0.005	-0.058 $\pm$ 0.005					
HIP 13589	[72.8 $^{+4.6}_{-4.0}$ ]	0.148 $\pm$ 0.001	-0.097 $\pm$ 0.001	0.5	1.7	1.8	49.2	3580
HIP 13589B	64.6 $^{+12.5}_{-10.5}$	0.15 $\pm$ 0.005	-0.089 $\pm$ 0.005					
HIP 26653	27.9 $^{+0.8}_{-0.7}$	-0.013 $\pm$ 0.001	-0.142 $\pm$ 0.001	2.91	2.94	4.66	27.0	753
HIP 26653 B	18.8 $^{+3.7}_{-3.1}$	-0.001 $\pm$ 0.004	-0.157 $\pm$ 0.004					
HIP 32728	[46.6 $^{+2.9}_{-2.6}$ ]	0.191 $\pm$ 0.001	-0.14 $\pm$ 0.001	0.2	0.9	1.0	94.3	4400
HIP 32728B	67.1 $^{+13.4}_{-11.2}$	0.188 $\pm$ 0.016	-0.13 $\pm$ 0.011					
HIP 37283	[45.5 $^{+1.2}_{-1.2}$ ]	-0.08 $\pm$ 0.001	-0.061 $\pm$ 0.001	1.4	0.6	1.6	106.1	4830
HIP 37283B	34.6 $^{+7.4}_{-6.1}$	-0.087 $\pm$ 0.005	-0.058 $\pm$ 0.005					
HIP 46984	[74.7 $^{+8.6}_{-6.9}$ ]	0.026 $\pm$ 0.002	0.108 $\pm$ 0.002	1.6	1.8	2.4	37.5	2800
HIP 46984B	111.9 $^{+22.4}_{-18.6}$	0.032 $\pm$ 0.004	0.101 $\pm$ 0.003					
HIP 49046	[34.7 $^{+2.6}_{-2.3}$ ]	-0.015 $\pm$ 0.002	0.119 $\pm$ 0.001	1.5	1.1	1.9	136.1	4720
HIP 49046B	33.3 $^{+6.7}_{-5.6}$	-0.008 $\pm$ 0.005	0.113 $\pm$ 0.005					
HIP 51877	54.2 $^{+2.3}_{-2.1}$	-0.063 $\pm$ 0.001	-0.122 $\pm$ 0.001	0.50	0.33	0.60	17.6	954
HIP 51877 B	57.4 $^{+11.5}_{-9.6}$	-0.066 $\pm$ 0.006	-0.124 $\pm$ 0.006					
HIP 52463	[74.2 $^{+5.2}_{-4.5}$ ]	-0.07 $\pm$ 0.001	0.083 $\pm$ 0.001	1.1	2.2	2.4	43.5	3230
HIP 52463B	84.6 $^{+16.9}_{-14.1}$	-0.064 $\pm$ 0.006	0.096 $\pm$ 0.006					
HIP 55666	[49.8 $^{+1.5}_{-1.5}$ ]	-0.085 $\pm$ 0.001	-0.093 $\pm$ 0.001	0.2	2.3	2.3	37.2	1850
HIP 55666B	42.2 $^{+8.3}_{-6.9}$	-0.087 $\pm$ 0.009	-0.074 $\pm$ 0.009					
HIP 58918	[55.8 $^{+6.2}_{-5.1}$ ]	-0.297 $\pm$ 0.002	0.018 $\pm$ 0.001	1.1	2.9	3.1	20.0	1110
HIP 58918B	61.9 $^{+12.3}_{-10.2}$	-0.289 $\pm$ 0.007	0.038 $\pm$ 0.007					
HIP 59310	[44.4 $^{+3.2}_{-2.8}$ ]	-0.157 $\pm$ 0.002	-0.041 $\pm$ 0.001	2.8	2.7	3.9	82.1	3650
HIP 59310B	42.4 $^{+8.4}_{-7.0}$	-0.144 $\pm$ 0.004	-0.053 $\pm$ 0.004					
HIP 59933	[57.0 $^{+2.7}_{-2.4}$ ]	-0.103 $\pm$ 0.001	-0.036 $\pm$ 0.001	2.0	1.0	2.3	38.1	2170
HIP 59933B	67.8 $^{+13.6}_{-11.3}$	-0.088 $\pm$ 0.007	-0.029 $\pm$ 0.007					
HIP 60501	[56.6 $^{+7.6}_{-6.0}$ ]	-0.012 $\pm$ 0.002	-0.134 $\pm$ 0.001	1.6	0.7	1.8	37.1	2100
HIP 60501B	30.8 $^{+6.0}_{-5.0}$	-0.001 $\pm$ 0.006	-0.13 $\pm$ 0.006					
HIP 60987	[61.9 $^{+2.4}_{-2.3}$ ]	-0.108 $\pm$ 0.001	-0.068 $\pm$ 0.001	1.0	1.5	1.8	19.0	1170
HIP 60987C	64.6 $^{+12.9}_{-10.8}$	-0.104 $\pm$ 0.004	-0.074 $\pm$ 0.004					
HIP 63506	[42.5 $^{+4.7}_{-3.9}$ ]	-0.396 $\pm$ 0.002	0.026 $\pm$ 0.002	0.5	0.0	0.5	132.8	5640
HIP 63506 C	45.0 $^{+9.0}_{-7.5}$	-0.401 $\pm$ 0.009	0.026 $\pm$ 0.009					

**Table 4**  
(Continued)

Object	$d$	$\mu_\alpha \cos \delta$	$\mu_\delta$	$d\mu_\alpha \cos \delta$	$d\mu_\delta$	$d\mu$	Projected Separation ('')	Projected Separation (AU)
	(pc)	('' yr $^{-1}$ )	('' yr $^{-1}$ )	$n_\sigma$	$n_\sigma$	$n_\sigma$		
HIP 65706	[51.1 $^{+4.8}_{-4.0}$ ]	-0.186 $\pm$ 0.002	-0.185 $\pm$ 0.001	2.2	2.3	3.2	52.6	2690
HIP 65706B	34.4 $^{+6.8}_{-5.7}$	-0.176 $\pm$ 0.004	-0.175 $\pm$ 0.004					
HIP 65780	[58.0 $^{+3.7}_{-3.3}$ ]	-0.193 $\pm$ 0.001	-0.218 $\pm$ 0.001	1.56	1.51	2.2	16.0	928
HIP 65780 C	60.8 $^{+11.9}_{-9.9}$	-0.179 $\pm$ 0.009	-0.204 $\pm$ 0.009					
HIP 70623	[72.6 $^{+5.5}_{-4.7}$ ]	-0.152 $\pm$ 0.001	-0.148 $\pm$ 0.001	0.4	1.7	1.8	41.9	3040
HIP 70623 C	33.1 $^{+6.5}_{-5.4}$	-0.154 $\pm$ 0.003	-0.142 $\pm$ 0.003					
HIP 75310	[66.9 $^{+6.0}_{-5.1}$ ]	-0.025 $\pm$ 0.001	-0.154 $\pm$ 0.001	0.3	0.3	0.4	22.9	1530
HIP 75310B	71.8 $^{+14.3}_{-12.0}$	-0.023 $\pm$ 0.004	-0.153 $\pm$ 0.004					
HIP 76456	[36.8 $^{+0.6}_{-0.6}$ ]	0.089 $\pm$ 0.001	-0.057 $\pm$ 0.001	0.3	1.8	1.9	36.1	1330
HIP 76456B	41.6 $^{+8.3}_{-6.9}$	0.09 $\pm$ 0.004	-0.064 $\pm$ 0.004					
HIP 76641	[82.1 $^{+5.3}_{-4.7}$ ]	-0.104 $\pm$ 0.001	0.031 $\pm$ 0.001	1.7	0.7	1.8	42.1	3460
HIP 76641B	41.6 $^{+13.4}_{-9.6}$	-0.11 $\pm$ 0.004	0.028 $\pm$ 0.004					
HIP 78184	[31.4 $^{+1.4}_{-1.3}$ ]	-0.296 $\pm$ 0.001	0.202 $\pm$ 0.002	1.6	1.5	2.2	121.8	3820
HIP 78184B	40.3 $^{+7.9}_{-6.6}$	-0.285 $\pm$ 0.006	0.213 $\pm$ 0.006					
HIP 78859	[57.2 $^{+2.3}_{-2.1}$ ]	-0.06 $\pm$ 0.001	-0.252 $\pm$ 0.001	1.2	0.6	1.4	42.6	2440
HIP 78859B	44.9 $^{+8.7}_{-7.3}$	-0.056 $\pm$ 0.003	-0.254 $\pm$ 0.003					
HIP 78916	[92.9 $^{+11.5}_{-9.2}$ ]	-0.098 $\pm$ 0.0010	0.092 $\pm$ 0.0010	2.9	0.6	3.0	35.5	3294
HIP 78916 B	70.6 $^{+13.8}_{-11.6}$	-0.080 $\pm$ 0.006	0.095 $\pm$ 0.006					
HIP 78923	[46.1 $^{+1.8}_{-1.7}$ ]	-0.301 $\pm$ 0.0010	0.184 $\pm$ 0.0010	1.9	3.2	3.7	15.5	714
HIP 78923 B	44.5 $^{+8.8}_{-7.3}$	-0.315 $\pm$ 0.007	0.206 $\pm$ 0.007					
HIP 79180	[74.7 $^{+3.7}_{-3.4}$ ]	0.092 $\pm$ 0.001	-0.258 $\pm$ 0.001	0.9	1.6	1.9	29.0	2170
HIP 79180B	93.7 $^{+18.7}_{-15.6}$	0.096 $\pm$ 0.005	-0.265 $\pm$ 0.004					
HIP 80258	[63.7 $^{+9.6}_{-7.5}$ ]	-0.181 $\pm$ 0.002	0.144 $\pm$ 0.002	2.2	2.4	3.3	54.9	3500
HIP 80258B	103 $^{+21}_{-17}$	-0.173 $\pm$ 0.003	0.135 $\pm$ 0.003					
HIP 81910	[46.4 $^{+0.9}_{-0.8}$ ]	-0.02 $\pm$ 0.001	-0.103 $\pm$ 0.001	0.6	1.5	1.6	26.7	1240
HIP 81910B	31.3 $^{+6.1}_{-5.1}$	-0.023 $\pm$ 0.007	-0.093 $\pm$ 0.007					
HIP 82233	[42.1 $^{+1.3}_{-1.2}$ ]	0.076 $\pm$ 0.001	-0.092 $\pm$ 0.001	1.4	2.6	3.0	30.4	1280
HIP 82233B	29.7 $^{+5.9}_{-4.9}$	0.085 $\pm$ 0.006	-0.075 $\pm$ 0.006					
HIP 83651	[50.9 $^{+4.9}_{-4.2}$ ]	-0.142 $\pm$ 0.002	0.136 $\pm$ 0.002	1.6	1.7	2.4	28.9	1470
HIP 83651B	53.8 $^{+10.8}_{-9.0}$	-0.149 $\pm$ 0.003	0.13 $\pm$ 0.003					
HIP 84840	[112 $^{+19}_{-15}$ ]	-0.051 $\pm$ 0.001	-0.174 $\pm$ 0.001	0.6	1.9	2.0	16.9	1890
HIP 84840B	77.9 $^{+15.6}_{-13.0}$	-0.049 $\pm$ 0.003	-0.168 $\pm$ 0.003					
HIP 85365	[30.1 $^{+0.2}_{-0.2}$ ]	-0.092 $\pm$ 0.001	-0.043 $\pm$ 0.001	0.8	3.8	3.9	294.1	8850
HIP 85365B	34.7 $^{+6.8}_{-5.7}$	-0.087 $\pm$ 0.006	-0.019 $\pm$ 0.006					
HIP 86722	[22.7 $^{+0.4}_{-0.5}$ ]	-0.123 $\pm$ 0.001	-0.62 $\pm$ 0.001	1.7	1.2	2.1	22.8	520
HIP 86722B	25.7 $^{+5.0}_{-4.2}$	-0.112 $\pm$ 0.007	-0.628 $\pm$ 0.007					
HIP 88728	[40.4 $^{+1.2}_{-1.1}$ ]	0.040 $\pm$ 0.001	-0.150 $\pm$ 0.001	0.6	3.3	3.4	9.6	316
HIP 88728B	...	0.036 $\pm$ 0.005	-0.133 $\pm$ 0.005					
HIP 90273	[55.4 $^{+10.0}_{-7.3}$ ]	0.006 $\pm$ 0.002	0.257 $\pm$ 0.003	2.5	0.8	2.7	26.9	1490
HIP 90273B	59.5 $^{+11.8}_{-9.8}$	0.016 $\pm$ 0.003	0.26 $\pm$ 0.003					
HIP 90869	[56.4 $^{+3.4}_{-3.0}$ ]	-0.144 $\pm$ 0.001	-0.122 $\pm$ 0.001	2.5	0.1	2.5	17.5	990
HIP 90869B	83.6 $^{+16.9}_{-14.1}$	-0.134 $\pm$ 0.004	-0.121 $\pm$ 0.004					

**Table 4**  
(Continued)

Object	$d$	$\mu_\alpha \cos \delta$	$\mu_\delta$	$d\mu_\alpha \cos \delta$	$d\mu_\delta$	$d\mu$	Projected Separation (")	Projected Separation (AU)
	(pc)	( $'' \text{ yr}^{-1}$ )	( $'' \text{ yr}^{-1}$ )	$n_\sigma$	$n_\sigma$	$n_\sigma$		
HIP 93967	[122.1 $^{+29.0}_{-19.6}$ ]	-0.146 $\pm$ 0.002	-0.276 $\pm$ 0.001	0.3	0.1	0.3	22.2	2710
HIP 93967B	135.1 $^{+26.9}_{-22.4}$	-0.145 $\pm$ 0.005	-0.275 $\pm$ 0.005					
HIP 97168	[97.5 $^{+13.1}_{-10.4}$ ]	0.127 $\pm$ 0.001	0.136 $\pm$ 0.001	0.6	3.1	3.2	12.6	1230
HIP 97168B	72.9 $^{+14.3}_{-12.0}$	0.124 $\pm$ 0.004	0.149 $\pm$ 0.004					
HIP 98535	[60.0 $^{+3.8}_{-3.3}$ ]	-0.113 $\pm$ 0.001	-0.095 $\pm$ 0.001	0.2	1.9	1.9	61.7	3700
HIP 98535C	56.0 $^{+11.0}_{-9.2}$	-0.114 $\pm$ 0.005	-0.086 $\pm$ 0.005					
HIP 102582	[31.3 $^{+1.4}_{-1.3}$ ]	0.091 $\pm$ 0.0020	-0.592 $\pm$ 0.0010	0.5	1.8	1.9	14.7	459
HIP 102582 B	40.7 $^{+7.9}_{-6.6}$	0.093 $\pm$ 0.005	-0.583 $\pm$ 0.005					
HIP 103199	[59.5 $^{+5.1}_{-4.3}$ ]	0.15 $\pm$ 0.001	0.057 $\pm$ 0.001	3.1	2.3	3.8	10.9	650
HIP 103199B	73.6 $^{+14.7}_{-12.3}$	0.135 $\pm$ 0.005	0.046 $\pm$ 0.005					
HIP 105202	[41.8 $^{+1.4}_{-1.3}$ ]	0.144 $\pm$ 0.001	-0.041 $\pm$ 0.001	0.9	0.3	1.0	89.4	3740
HIP 105202B	64.1 $^{+12.8}_{-10.7}$	0.147 $\pm$ 0.003	-0.04 $\pm$ 0.003					
HIP 106551	[71.0 $^{+2.2}_{-2.1}$ ]	0.116 $\pm$ 0.001	0.095 $\pm$ 0.001	0.9	0.8	1.2	66.1	4690
HIP 106551B	67.9 $^{+13.2}_{-11.0}$	0.119 $\pm$ 0.004	0.092 $\pm$ 0.004					
HIP 108822	[44.4 $^{+8.5}_{-6.1}$ ]	-0.025 $\pm$ 0.004	-0.354 $\pm$ 0.004	3.6	1.2	3.8	31.8	1410
HIP 108822B	53.1 $^{+10.7}_{-8.9}$	-0.046 $\pm$ 0.004	-0.347 $\pm$ 0.004					
HIP 109454	[100.9 $^{+6.5}_{-5.8}$ ]	-0.069 $\pm$ 0.001	-0.091 $\pm$ 0.001	0.4	1.9	1.9	18.2	1840
HIP 109454B	109.7 $^{+22.0}_{-18.3}$	-0.072 $\pm$ 0.005	-0.081 $\pm$ 0.005					
HIP 111657	[41.9 $^{+3.3}_{-3.0}$ ]	-0.248 $\pm$ 0.002	-0.187 $\pm$ 0.002	2.4	2.5	3.5	7.8	330
HIP 111657B	34.9 $^{+7.0}_{-5.8}$	-0.259 $\pm$ 0.004	-0.176 $\pm$ 0.004					
HIP 112422	[65.4 $^{+8.3}_{-6.6}$ ]	0.148 $\pm$ 0.002	0.031 $\pm$ 0.001	1.6	1.1	1.9	16.0	1040
HIP 112422B	64.7 $^{+12.6}_{-10.5}$	0.168 $\pm$ 0.012	0.044 $\pm$ 0.012					
HIP 114424	[35.1 $^{+1.1}_{-0.9}$ ]	0.138 $\pm$ 0.001	-0.136 $\pm$ 0.001	2.0	0.0	2.0	42.0	1480
HIP 114424B	26.3 $^{+5.2}_{-4.3}$	0.146 $\pm$ 0.004	-0.136 $\pm$ 0.004					
HIP 114456	[24.3 $^{+0.3}_{-0.3}$ ]	-0.087 $\pm$ 0.001	-0.287 $\pm$ 0.001	2.2	2.7	3.5	50.4	1220
HIP 114456B	23.9 $^{+4.6}_{-3.9}$	-0.097 $\pm$ 0.005	-0.3 $\pm$ 0.005					
HIP 115819	[65.7 $^{+11.0}_{-8.2}$ ]	0.441 $\pm$ 0.003	0.181 $\pm$ 0.002	0.9	2.4	2.5	30.4	2000
HIP 115819B	64.0 $^{+12.5}_{-10.5}$	0.435 $\pm$ 0.006	0.196 $\pm$ 0.006					
HIP 116052	[49.6 $^{+2.5}_{-2.3}$ ]	-0.137 $\pm$ 0.001	-0.133 $\pm$ 0.001	0.2	1.0	1.0	26.8	1330
HIP 116052 B	87.2 $^{+17.5}_{-14.6}$	-0.136 $\pm$ 0.004	-0.129 $\pm$ 0.004					

**Notes.**  $n_\sigma$  is the number of standard deviations the proper motions differ by. [...] denotes distance from trigonometric parallax; all other distances are photometric.

et al. (2010). Additionally, for our L dwarf companions we measured three flux indices ( $H_2O-J$ ,  $H_2O-H$ , and  $CH_4-K$ ) from Burgasser et al. (2006) relevant for L dwarfs. We then applied the polynomial relations of Burgasser (2007) to derive spectral types, averaging over the types derived from each index. We note that the  $CH_4-K$  index does not depend strongly on spectral type earlier than mid-L and hence excluded this from the averaging for objects with this visual classification (see Table 9). Figures 1 and 2 show our early to mid-M dwarf companions to *Hipparcos* stars, Figure 3 shows our late-M and L dwarf *Hipparcos* companions, and Figure 4 shows our companions around non-*Hipparcos* primaries and serendipitous discoveries. Additionally, we observed a number of our primary stars that

lacked spectral types in the literature. The spectra for these objects are shown in Figure 5.

For objects with spectral types earlier than M, there are no near-infrared standards so we compared with the spectral library of Cushing et al. (2005) and Rayner et al. (2009), selecting the best comparison spectrum visually. For any of our objects with spectral types earlier than M5, we specifically examined the  $\sim 0.85 \mu\text{m}$  TiO feature in the Z-band and the Y-band  $1 \mu\text{m}$  FeH feature. For two primaries classified as G dwarfs we also examined the strengths of metal and hydrogen lines. We identified one of our companions (HIP 88728 B) as having blue continua and weak Paschen lines. Hence we classify this object as a DA white dwarf (see Figure 6).

**Table 5**  
The Data of Our Non-*Hipparcos* and Serendipitous Pairs

Object	distance	$\mu_\alpha \cos \delta$	$\mu_\delta$	$d\mu_\alpha \cos \delta$	$d\mu_\delta$	$d\mu$	Projected Separation ('')	Projected Separation (AU)
	(pc)	('' yr <sup>-1</sup> )	('' yr <sup>-1</sup> )	$n_\sigma$	$n_\sigma$	$n_\sigma$		
Other Companion Discoveries								
NLTT 1011	68.2 <sup>+6.6</sup> <sub>-6.5</sub> <sup>a</sup>	-0.076 ± 0.008 <sup>f</sup>	-0.192 ± 0.008	0.08	0.43	0.44	58.5	3990
NLTT 1011B	46.1 <sup>+9.3</sup> <sub>-7.7</sub> <sup>b</sup>	-0.077 ± 0.007	-0.197 ± 0.007					
GD 280	77 <sup>+35</sup> <sub>-26</sub>	0.171 ± 0.008	-0.059 ± 0.008 <sup>f</sup>	0.32	0.53	0.62	63.4	4882
GD 280 B	82.3 <sup>+16.7</sup> <sub>-13.9</sub>	0.174 ± 0.005	-0.054 ± 0.005					
NLTT 8245	53.0 <sup>+8.7</sup> <sub>-7.5</sub>	-0.096 ± 0.008	-0.164 ± 0.008 <sup>f</sup>	0.42	0.21	0.47	10.6	562
NLTT 8245 B	72.9 <sup>+14.6</sup> <sub>-12.2</sub>	-0.092 ± 0.005	-0.162 ± 0.005					
LSPM J0241+2553	69 <sup>+35</sup> <sub>-23</sub>	-0.032 ± 0.008	-0.158 ± 0.008 <sup>f</sup>	1.41	0.70	1.58	31.2	2153
LSPM J0241+2553 B	93.1 <sup>+20.2</sup> <sub>-16.62</sub>	-0.048 ± 0.008	-0.150 ± 0.008					
HD 253662	>62.3	0.020 ± 0.001	-0.157 ± 0.001 <sup>i</sup>	0.20	0.50	0.54	20.1	>1252
HD 253662 B	67.2 <sup>+13.7</sup> <sub>-11.4</sub>	-0.022 ± 0.010	-0.162 ± 0.010					
LSPM J0632+5053	95.0 <sup>+16.3</sup> <sub>-13.9</sub> <sup>a</sup>	0.035 ± 0.008 <sup>f</sup>	-0.154 ± 0.008	2.1	1.2	2.4	47.4	4499
LSPM J0632+5053 B	85.3 <sup>+16.7</sup> <sub>-14.0</sub> <sup>b</sup>	0.054 ± 0.004	-0.143 ± 0.004					
NLTT 18587	132 <sup>+40</sup> <sub>-31</sub>	0.167 ± 0.008	-0.089 ± 0.008 <sup>f</sup>	1.06	0.09	2.37	92.4	12200
NLTT 18587 B	158 <sup>+36</sup> <sub>-29</sub>	0.155 ± 0.008	-0.088 ± 0.008					
NLTT 19109	48.2 <sup>+7.9</sup> <sub>-6.8</sub>	0.035 ± 0.008	-0.181 ± 0.008 <sup>g</sup>	1.59	1.9	2.48	7.5	362
NLTT 19109 B	127 <sup>+25</sup> <sub>-21</sub>	0.050 ± 0.005	-0.163 ± 0.005					
NLTT 22073	29.9 <sup>+12.7</sup> <sub>-6.9</sub> <sup>c</sup>	-0.315 ± 0.008	0.16 ± 0.008 <sup>g</sup>	1.1	1.5	1.8	26	776
NLTT 22073 B	62.2 <sup>+12.4</sup> <sub>-10.4</sub>	-0.301 ± 0.014	0.141 ± 0.014					
NLTT 23716	48.2 <sup>+7.9</sup> <sub>-6.8</sub>	0.054 ± 0.005	-0.286 ± 0.005 <sup>h</sup>	1.41	1.41	1.99	15.0	723
NLTT 23716 B	47.5 <sup>+9.3</sup> <sub>-7.8</sub>	0.063 ± .004	-0.277 ± 0.004					
NLTT 26746	41.0 <sup>+12.2</sup> <sub>-10.3</sub> <sup>d</sup>	-0.251 ± 0.008 <sup>f</sup>	-0.147 ± 0.008	1.22	0.87	1.5	18.0	661
NLTT 26746 B	42.5 <sup>+8.3</sup> <sub>-6.9</sub> <sup>b</sup>	-0.235 ± 0.01	-0.136 ± 0.01					
NLTT 29395	56.4 <sup>+16.9</sup> <sub>-13.0</sub>	-0.182 ± 0.008	-0.115 ± 0.008 <sup>f</sup>	2.01	0.78	2.16	11.9	671
NLTT 29395 B	96.0 <sup>+19.5</sup> <sub>-16.2</sub>	-0.164 ± 0.004	-0.108 ± 0.004					
NLTT 30510	49.1 <sup>+14.8</sup> <sub>-11.3</sub>	0.215 ± 0.008	-0.067 ± 0.008	<sup>f</sup> 0.4	0.2.5	2.53	19.6	962
NLTT 30510 B	88.8 <sup>+18.1</sup> <sub>-15.0</sub>	0.219 ± 0.006	-0.042 ± 0.006					
NLTT 31450	34.6 <sup>+10.3</sup> <sub>-8.7</sub> <sup>d</sup>	-0.034 ± 0.008 <sup>f</sup>	-0.202 ± 0.008	-0.03	1.75	1.75	12.3	487
NLTT 31450 B	27.2 <sup>+5.3</sup> <sub>-4.4</sub> <sup>b</sup>	-0.034 ± 0.01	-0.18 ± 0.01					
PMI 13410+0542	51.3 <sup>+21.7</sup> <sub>-11.8</sub> <sup>c</sup>	0.047 ± 0.008 <sup>g</sup>	-0.014 ± 0.008	1.7	1.8	2.5	9.4	484
PMI 13410+0542 B	44.3 <sup>+8.7</sup> <sub>-7.2</sub>	0.062 ± 0.004	-0.030 ± 0.004					
PMI 13518+4157	43.1 <sup>+9.9</sup> <sub>-8.8</sub> <sup>d</sup>	-0.059 ± 0.008 <sup>g</sup>	-0.058 ± 0.008	0.7	0.6	1.0	21.6	613
PMI 13518+4157 B	39.6 <sup>+7.9</sup> <sub>-6.6</sub>	-0.05 ± 0.009	-0.065 ± 0.009					
NLTT 38489	62.3 <sup>+23.3</sup> <sub>-17.0</sub> <sup>a</sup>	-0.147 ± 0.008 <sup>f</sup>	0.183 ± 0.008	0.7	1.4	1.6	6.7	418
NLTT 38489 B	128 <sup>+25</sup> <sub>-21</sub> <sup>b</sup>	-0.141 ± 0.004	0.170 ± 0.004					
NLTT 39312	141 <sup>+43</sup> <sub>-33</sub> <sup>a</sup>	-0.025 ± 0.008 <sup>f</sup>	-0.347 ± 0.008	4.3	1.2	4.4	5.1	713
NLTT 39312 B	124 <sup>+24</sup> <sub>-20</sub>	0.09 ± 0.02	-0.32 ± 0.02					
LSPM J1627+3328	38.0 <sup>+6.3</sup> <sub>-5.4</sub> <sup>c</sup>	-0.171 ± 0.008 <sup>f</sup>	-0.014 ± 0.008	3.29	-1.64	3.67	9.0	341
LSPM J1627+3328	49.9 <sup>+9.7</sup> <sub>-8.1</sub>	-0.140 ± 0.005	-0.030 ± 0.005					
NLTT 44368	55.0 <sup>+12.7</sup> <sub>-11.3</sub> <sup>d</sup>	-0.056 ± 0.008 <sup>f</sup>	0.215 ± 0.008	0.33	-0.37	0.49	90.2	7760
NLTT 44368 B	35.3 <sup>+6.9</sup> <sub>-5.8</sub> <sup>b</sup>	-0.053 ± 0.006	0.211 ± 0.006					
LSPM J1717+5925	108 <sup>+35</sup> <sub>-26</sub> <sup>d</sup>	-0.085 ± 0.008 <sup>i</sup>	-0.143 ± 0.008	1.8	1.6	2.4	14.4	1555
LSPM J1717+5925 B	119 <sup>+27</sup> <sub>-22</sub>	-0.101 ± 0.004	-0.157 ± 0.004					

**Table 5**  
(Continued)

Object	distance	$\mu_\alpha \cos \delta$	$\mu_\delta$	$d\mu_\alpha \cos \delta$	$d\mu_\delta$	$d\mu$	Projected Separation ('')	Projected Separation (AU)
	(pc)	('' yr <sup>-1</sup> )	('' yr <sup>-1</sup> )	$n_\sigma$	$n_\sigma$	$n_\sigma$		
NLTT 52268	37.3 <sup>+11.3<sup>a</sup></sup> <sub>-8.7</sub>	0.16 ± 0.008	-0.089 ± 0.008 <sup>f</sup>	0.5	0.2	0.6	14.7	549
NLTT 52268 B	55.6 <sup>+10.8</sup> <sub>-9.1</sub>	0.155 ± 0.006	-0.087 ± 0.006					
LSPM J2153+1157	36.2 <sup>+10.9<sup>a</sup></sup> <sub>-8.4</sub>	-0.093 ± 0.008 <sup>f</sup>	-0.128 ± 0.008	0.8	0.8	1.2	11.3	408
LSPM J2153+1157 B	58.1 <sup>+11.4</sup> <sub>-9.5</sub>	-0.085 ± 0.006	-0.136 ± 0.006					
PM I22118–1005	37.4 <sup>+8.6<sup>d</sup></sup> <sub>-7.7</sub>	0.028 ± 0.008 <sup>g</sup>	-0.25 ± 0.008	1.6	0.9	1.9	204.5	8892
PM I22118–1005 B	43.9 <sup>+8.8</sup> <sub>-7.3</sub>	0.05 ± 0.011	-0.262 ± 0.010					
NLTT 55219	44.7 <sup>+13.5<sup>a</sup></sup> <sub>-10.4</sub>	0.324 ± 0.008 <sup>f</sup>	0.16 ± 0.008	0.9	3.1	3.2	9.7	432
NLTT 55219 B	40.0 <sup>+7.8</sup> <sub>-6.5</sub>	0.35 ± 0.03	0.26 ± 0.03					
Serendipitous Companion Discoveries								
NLTT 730	21.7 <sup>+8.1<sup>d</sup></sup> <sub>-5.3</sub>	0.375 ± 0.008 <sup>f</sup>	-0.234 ± 0.008	0.5	1.58	1.66	233.6	5070
NLTT 730 B	23.7 <sup>+4.6<sup>b</sup></sup> <sub>-3.9</sub>	0.381 ± 0.009	-0.215 ± 0.009					
NLTT 27966	39.6 <sup>+13.3<sup>a</sup></sup> <sub>-10.2</sub>	-0.153 ± 0.008 <sup>f</sup>	0.182 ± 0.008	-0.79	0.42	0.89	15.9	630
NLTT 27966 B	42.3 <sup>+8.2<sup>b</sup></sup> <sub>-6.9</sub>	-0.164 ± 0.011	0.188 ± 0.011					
LSPMJ1336+2541	60.7 <sup>+15.7<sup>d</sup></sup> <sub>-13.9</sub>	-0.157 ± 0.008 <sup>f</sup>	0.057 ± 0.008	2.1	2.8	3.5	121.7	8793
LSPM J1336+2541 B	63.2 <sup>+12.4<sup>b</sup></sup> <sub>-10.3</sub>	-0.177 ± 0.005	0.031 ± 0.005					
HIP 73169	[27.3 <sup>+8.3<sup>e</sup></sup> <sub>-6.3</sub> ]	-0.267 ± 0.007	-0.076 ± 0.007	0.5	0.42	0.65	29.1	796
HIP 73169 B	50.7 <sup>+9.9<sup>b</sup></sup> <sub>-8.3</sub>	-0.261 ± 0.009	-0.081 ± 0.009					
PM I23492+3458	30.7 <sup>+7.1<sup>d</sup></sup> <sub>-6.3</sub>	-0.011 ± 0.008 <sup>f</sup>	-0.108 ± 0.008	1.0	1.0	1.4	34.9	949
PM I23492+3458 B	23.3 <sup>+4.5<sup>b</sup></sup> <sub>-3.8</sub>	-0.002 ± 0.005	-0.099 ± 0.005					
Unlikely companions								
NLTT 35593	63.0 <sup>+19.1<sup>a</sup></sup> <sub>-14.6</sub>	-0.184 ± 0.005 <sup>h</sup>	-0.055 ± 0.005	1.76	-0.34	1.79	1105.8	69706
NLTT 35593 B	65.5 <sup>+12.8<sup>b</sup></sup> <sub>-10.7</sub>	-0.162 ± 0.011	-0.059 ± 0.011					

**Notes.**  $n_\sigma$  is the number of standard deviations the proper motions differ by. [...] Denotes distance from trigonometric parallax; all other distances are photometric.

<sup>a</sup> Photometric distance from Lépine (2005).

<sup>b</sup> Photometric distance from 2MASS magnitudes and Dupuy & Liu (2012).

<sup>c</sup> Photometric distance from Lépine & Gaidos (2011).

<sup>d</sup> Photometric distance from spectral type and spectrophotometric relations of Kraus & Hillenbrand (2007).

<sup>e</sup> Trigonometric parallax from van Leeuwen (2007).

<sup>f</sup> Proper motion from Lépine & Shara (2005).

<sup>g</sup> Proper motion from Lépine & Gaidos (2011).

<sup>h</sup> Proper motion from Salim & Gould (2003).

<sup>i</sup> Proper motion from Hog et al. (2000).

### 3.3. Optical Spectroscopy

As a number of our primaries were poorly characterized, we obtained optical spectroscopy from both the Kitt Peak Mayall 4 m telescope and the University of Hawaii 2.2 m telescope.

#### 3.3.1. Kitt Peak Mayall 4 m Spectroscopy

On 2013 December 31 UT we obtained optical spectra of NLTT 38389 and NLTT 1011 with the Ritchey–Chretien Spectrograph equipped with the T2KA CCD on the Kitt Peak National Observatory 4 m Mayall telescope. The BL 420 grating was blazed at 7800 Å (first order) with the GG495 order blocking filter. The slit was set at 1''.5 by 98'', resulting in spectra spanning 6300–8500 Å at a resolving power of ∼3 Å. NLTT 38389 and NLTT 1011 were targeted at airmasses of 1.25 and 1.01 with exposures of 600 s and 240 s, respectively. We also acquired optical spectroscopy for one of our companions (HIP 84840 B)

on 2014 May 22 UT with the same set-up at airmass 1.03.. The slit was oriented in the N–S direction for all observations, so slit losses from chromatic dispersion may be non-negligible for NLTT 38389. The spectrophotometric standards HR 3454 (Hamuy et al. 1992) (2013 December 31 UT) and HZ 44 (2014 May 22 UT) were observed at airmasses of 1.15 and 1.0, respectively, for flux calibration. Each 2D image was corrected for bad pixels and cosmic rays, bias subtracted, and flat fielded. After sky subtraction, each spectrum was corrected for throughput losses using our standard star measurements.

#### 3.3.2. University of Hawaii 2.2 m Telescope/SNIFS Spectroscopy

To aid in characterizing the primary stars, we took spectra of GD 280, NLTT 730, LSPM J2153+1157, and NLTT 22073 with the SuperNova Integral Field Spectrograph (Aldering et al. 2002; Lantz 2004) on the University of Hawaii 2.2 m telescope on Mauna Kea on UT 2013 October 19 and December 13–14.

**Table 6**  
The IR Data of Our Secondaries

Object	<i>Y</i> (mag)	<i>J</i> (mag)	<i>H</i> (mag)	<i>K</i> / <i>K<sub>s</sub></i> (mag)	Source
HIP search companions					
HIP 2397 B	...	14.586 ± 0.038*	13.975 ± 0.048*	>13.181*	2MASS
	...	14.552 ± 0.012	13.912 ± 0.011	...	UKIRT
HIP 6217 B		15.441 ± 0.060*	14.731 ± 0.081*	14.423 ± 0.079*	2MASS
	...	...	...	14.461 ± 0.009	UKIDSS
HIP 6407 B	...	15.471 ± 0.046	14.651 ± 0.061	14.402 ± 0.08	2MASS
	16.442 ± 0.008	15.345 ± 0.005	14.738 ± 0.006	14.203 ± 0.006	UKIDSS
HIP 9269 B	...	15.956 ± 0.088*	14.99 ± 0.096*	14.317 ± 0.085*	2MASS
	...	16.126 ± 0.017	15.082 ± 0.014	14.298 ± 0.019	UKIRT
HIP 10033 B	...	13.761 ± 0.027	13.185 ± 0.031	12.929 ± 0.033	2MASS
	...	13.746 ± 0.013	13.245 ± 0.011	...	UKIRT
HIP 11161 B	...	16.636 ± 0.161*	15.77 ± 0.173	15.392 ± 0.195*	2MASS
	...	16.512 ± 0.019	15.862 ± 0.017	15.25 ± 0.028	UKIRT
HIP 13589 B	...	14.928 ± 0.034	14.275 ± 0.037	13.838 ± 0.046	2MASS
	...	14.794 ± 0.034	14.226 ± 0.012	...	UKIRT
HIP 26653 B		14.756 ± 0.044*	13.91 ± 0.042*	13.322 ± 0.029*	2MASS
HIP 32728 B	...	14.508 ± 0.031	13.933 ± 0.038	13.509 ± 0.035	2MASS
HIP 37283 B	...	12.797 ± 0.027	12.234 ± 0.03	11.943 ± 0.024	2MASS
HIP 46984 B	...	13.285 ± 0.027*	12.745 ± 0.024	12.483 ± 0.027*	2MASS
	13.794 ± 0.002	13.215 ± 0.002	12.767 ± 0.002	12.463 ± 0.002	UKIDSS
HIP 49046 B	...	13.022 ± 0.022	12.418 ± 0.024	12.038 ± 0.021	2MASS
	...	12.930 ± 0.092	...	...	UKIRT
HIP 51877 B		15.205 ± 0.063*	14.510 ± 0.062*	13.988 ± 0.052*	2MASS
HIP 52463 B	...	13.703 ± 0.024	13.117 ± 0.027	12.801 ± 0.031	2MASS
HIP 55666 B	...	12.674 ± 0.024	12.108 ± 0.024	11.746 ± 0.019	2MASS
	13.322 ± 0.002	12.581 ± 0.001	12.103 ± 0.003	11.762 ± 0.002	VISTA
HIP 58918 B	...	14.471 ± 0.03*	13.899 ± 0.044	13.524 ± 0.023	2MASS
HIP 59310 B	...	13.691 ± 0.027	13.052 ± 0.033	12.692 ± 0.024	2MASS
HIP 59933 B	...	16.101 ± 0.088*	15.162 ± 0.075*	14.616 ± 0.084	2MASS
	17.126 ± 0.015	15.995 ± 0.008	15.218 ± 0.009	14.62 ± 0.01	UKIDSS
HIP 60501 B	...	11.378 ± 0.027	10.792 ± 0.024	10.453 ± 0.023	2MASS
	11.916 ± 0.001	11.309 ± 0.001	10.979 ± 0.001	10.554 ± 0.001	UKIDSS
HIP 60987 B	...	...	...	10.869 ± 0.001	VISTA <sup>†</sup>
HIP 60987 C	...	11.402 ± 0.028*	10.81 ± 0.029	10.592 ± 0.024	2MASS
	11.782 ± 0.001	11.267 ± 0.001	10.7497 ± 0.001	10.488 ± 0.001	VISTA
HIP 63506 C	...	15.15 ± 0.042	14.426 ± 0.045	14.006 ± 0.047	2MASS
HIP 65706 B	...	13.315 ± 0.022	12.642 ± 0.026	12.297 ± 0.024	2MASS
	14.011 ± 0.002	13.246 ± 0.001	12.693 ± 0.001	12.258 ± 0.002	UKIDSS
HIP 65780 C	...	>12.717	>12.197	12.007 ± 0.034*	2MASS
	13.580 ± 0.002	12.937 ± 0.001	12.404 ± 0.002	12.044 ± 0.002	UKIDSS
HIP 70623 C	...	12.191 ± 0.026	11.506 ± 0.023	11.224 ± 0.019	2MASS
	...	12.039 ± 0.001	11.541 ± 0.001	11.233 ± 0.001	VISTA
HIP 75310 B	...	13.291 ± 0.032*	12.724 ± 0.03	12.51 ± 0.027	2MASS
HIP 76456 B	...	13.300 ± 0.031*	12.762 ± 0.028*	12.43 ± 0.029*	2MASS
	13.973 ± 0.002	13.240 ± 0.002	12.809 ± 0.002	12.397 ± 0.002	UKIDSS
HIP 76641 B	...	10.817 ± 0.018	10.176 ± 0.016	9.919 ± 0.014	2MASS
HIP 78184 B	...	14.32 ± 0.031	13.607 ± 0.035	13.122 ± 0.03	2MASS
	...	14.252 ± 0.022	13.615 ± 0.037	13.091 ± 0.028	UKIRT
HIP 78859 B	...	12.258 ± 0.021	11.694 ± 0.02	11.496 ± 0.02	2MASS
	...	12.214 ± 0.010	11.734 ± 0.010	...	UKIRT
HIP 78916 B	...	15.227 ± 0.043*	14.542 ± 0.045	14.193 ± 0.053	2MASS
	...	15.148 ± 0.0179	14.603 ± 0.028	...	UKIRT
HIP 78923 B	...	14.052 ± 0.048*	13.566 ± 0.051*	13.28 ± 0.041*	2MASS
	...	14.136 ± 0.011	13.621 ± 0.11	...	UKIRT
HIP 79180 B	...	13.941 ± 0.022	13.361 ± 0.027	12.965 ± 0.033	2MASS
HIP 80258 B	...	13.113 ± 0.021	12.556 ± 0.023	12.28 ± 0.021	2MASS
	...	13.101 ± 0.016	12.562 ± 0.010	...	UKIRT
HIP 81910 B	...	12.44 ± 0.024*	11.887 ± 0.026	11.526 ± 0.025	2MASS
	...	12.400 ± 0.010	11.858 ± 0.010	...	UKIRT
HIP 82233 B	...	11.889 ± 0.024	11.288 ± 0.021	11.043 ± 0.023	2MASS
	...	11.874 ± 0.011	11.366 ± 0.010	...	UKIRT
HIP 83651 B	...	10.599 ± 0.024	10.057 ± 0.024	9.771 ± 0.021	2MASS
	...	10.734 ± 0.010	10.877 ± 0.011	...	UKIRT
HIP 84840 B	...	12.508 ± 0.022	11.901 ± 0.023	11.685 ± 0.018	2MASS
	...	12.491 ± 0.019	11.950 ± 0.010	...	UKIRT

**Table 6**  
(Continued)

Object	<i>Y</i> (mag)	<i>J</i> (mag)	<i>H</i> (mag)	<i>K</i> / <i>K<sub>s</sub></i> (mag)	Source
HIP 85365 B	...	16.693 ± 0.168*	15.471 ± 0.118	>14.664	2MASS
	...	16.184 ± 0.010	...	14.718 ± 0.010	VISTA
HIP 86722 B	...	11.511 ± 0.025	11.016 ± 0.021	10.7 ± 0.019	2MASS
	...	11.506 ± 0.015	11.089 ± 0.01	...	UKIRT
HIP 88728 B	...	10.269 ± 0.097*	10.043 ± 0.047*	9.876 ± 0.057*	2MASS
	...	11.103 ± 0.019	10.965 ± 0.018	10.953 ± 0.027	UKIRT
HIP 90273 B	...	11.56 ± 0.022	11.019 ± 0.022	10.731 ± 0.018	2MASS
	...	11.495 ± 0.010	11.012 ± 0.018	...	UKIRT
HIP 90869 B	...	11.101 ± 0.029*	10.569 ± 0.027	10.358 ± 0.023	2MASS
	...	11.071 ± 0.10	10.818 ± 0.010	...	UKIRT
HIP 93967 B	...	13.357 ± 0.03	12.74 ± 0.025	12.525 ± 0.019	2MASS
	...	13.24 ± 0.02	12.751 ± 0.02	...	UKIRT
HIP 97168 B	...	13.679 ± 0.027*	13.212 ± 0.026*	13.012 ± 0.033*	2MASS
	...	13.784 ± 0.014	13.332 ± 0.014	...	UKIRT
HIP 98535 C	...	13.252 ± 0.031	12.724 ± 0.031	12.445 ± 0.032	2MASS
	...	13.223 ± 0.010	12.752 ± 0.010	...	UKIRT
HIP 102582 B	...	11.963 ± 0.033*	11.494 ± 0.034	11.232 ± 0.032*	2MASS
	...	11.972 ± 0.015	11.551 ± 0.010	...	UKIRT
HIP 103199 B	...	11.817 ± 0.027*	11.229 ± 0.024*	10.997 ± 0.019*	2MASS
	12.378 ± 0.014	11.850 ± 0.18	11.307 ± 0.010	11.250 ± 0.010	UKIRT
HIP 105202 B	...	12.124 ± 0.024	11.53 ± 0.022	11.246 ± 0.023	2MASS
	...	12.0337 ± 0.010	11.571 ± 0.014	...	UKIRT
HIP 106551 B	...	13.224 ± 0.025*	12.606 ± 0.03	12.287 ± 0.022	2MASS
	...	13.211 ± 0.010	12.630 ± 0.010	...	UKIRT
HIP 108822 B	...	10.622 ± 0.022	10.051 ± 0.021	9.821 ± 0.02	2MASS
	...	10.805 ± 0.020	10.650 ± 0.010	...	UKIRT
HIP 109454 B	...	12.422 ± 0.026*	11.863 ± 0.032	11.62 ± 0.02	2MASS
	...	12.452 ± 0.01	11.904 ± 0.017	...	UKIRT
HIP 111657 B	...	10.587 ± 0.032*	10.028 ± 0.034*	9.73 ± 0.027*	2MASS
	...	10.583 ± 0.010	10.545 ± 0.016	...	UKIRT
HIP 112422 B	...	16.023 ± 0.113*	15.111 ± 0.103*	14.651 ± 0.093*	2MASS
	17.171 ± 0.022	16.016 ± 0.017	15.251 ± 0.015	...	UKIRT
HIP 114424 B	...	11.595 ± 0.026	10.976 ± 0.022	10.663 ± 0.022	2MASS
	...	11.483 ± 0.010	11.185 ± 0.010	...	UKIRT
HIP 114456 B	...	10.844 ± 0.021*	10.227 ± 0.028*	9.896 ± 0.024*	2MASS
	...	10.840 ± 0.014	10.446 ± 0.010	...	UKIRT
HIP 115819 B	...	15.095 ± 0.034	14.357 ± 0.029	13.974 ± 0.045	2MASS
	15.844 ± 0.007	14.965 ± 0.005	14.370 ± 0.004	13.907 ± 0.005	UKIDSS
HIP 116052 B	...	12.361 ± 0.019	11.79 ± 0.024	11.512 ± 0.025	2MASS
	...	12.332 ± 0.019	11.793 ± 0.010	...	UKIRT

## Companions to faint non-HIP primaries

NLTT 1011	...	15.544 ± 0.059	14.928 ± 0.069	14.318 ± 0.066	2MASS
GD 280 B		16.034 ± 0.082	14.993 ± 0.09	14.547 ± 0.08	2MASS
NLTT 8245 B		14.922 ± 0.052*	14.221 ± 0.068*	13.812 ± 0.056*	2MASS
LSPM J0241+2553 B		17.027 ± 0.180	16.028 ± 0.180	15.331 ± 0.149	2MASS
HD 253662 B		15.961 ± 0.082*	15.182 ± 0.087*	14.506 ± 0.095*	2MASS
	16.511 ± 0.009	15.653 ± 0.007	...	...	UKIDSS
LSPM J0632+5053 B	...	16.383 ± 0.108	15.421 ± 0.133	15.171 ± 0.122	2MASS
	...	16.612 ± 0.027	15.864 ± 0.022	...	UKIRT
NLTT 18587 B		16.894 ± 0.199	15.921 ± 0.215	>15.221	2MASS <sup>‡</sup>
NLTT 19109 B		16.933 ± 0.17*	15.89 ± 0.169*	15.463 ± 0.21*	2MASS
	...	16.512 ± 0.017	...	15.679 ± 0.026	VISTA
NLTT 22073 B	...	14.671 ± 0.037	14.070 ± 0.044	13.696 ± 0.049	2MASS
NLTT 23716 B		14.300 ± 0.036*	13.716 ± 0.035*	13.348 ± 0.028*	2MASS
	15.085 ± 0.005	14.225 ± 0.003	13.713 ± 0.004	13.309 ± 0.005	VISTA
NLTT 26746 B	...	16.403 ± 0.118*	15.224 ± 0.092	14.555 ± 0.105	2MASS
	17.377 ± 0.015	16.056 ± 0.008	15.295 ± 0.0090	14.61 ± 0.008	UKIDSS
NLTT 29395 B		15.81 ± 0.08*	15.133 ± 0.076*	14.781 ± 0.091*	2MASS
NLTT 30510 B		15.971 ± 0.08*	15.267 ± 0.095	14.854 ± 0.09	2MASS
NLTT 31450 B	...	16.135 ± 0.105*	15.048 ± 0.095*	14.331 ± 0.092*	2MASS
	...	16.004 ± 0.21	15.081 ± 0.023	...	UKIRT
PMI 13410+0542 B	...	16.187 ± 0.143*	15.128 ± 0.131*	14.799 ± 0.138*	2MASS
	17.349 ± 0.017	16.125 ± 0.009	15.358 ± 0.008	14.727 ± 0.008	UKIDSS
PMI 13518+4157 B	...	15.081 ± 0.032	14.352 ± 0.049	13.851 ± 0.04	2MASS

**Table 6**  
(Continued)

Object	<i>Y</i> (mag)	<i>J</i> (mag)	<i>H</i> (mag)	<i>K</i> / <i>K<sub>s</sub></i> (mag)	Source
NLTT 38489 B	...	16.64 ± 0.143*	15.789 ± 0.176*	15.481 ± 0.154*	2MASS
	...	16.717 ± 0.031	16.147 ± 0.037	...	UKIRT
NLTT 39312 B	...	16.09 ± 0.096*	15.573 ± 0.118*	>13.601	2MASS
	...	16.277 ± 0.035	16.006 ± 0.045	...	UKIRT
LSPM J1627+3328 B	...	14.362 ± 0.083*	13.742 ± 0.066*	13.417 ± 0.055*	2MASS
	...	14.730 ± 0.012	14.052 ± 0.011	...	UKIRT
NLTT 44368 B	...	14.736 ± 0.058	13.907 ± 0.064	13.467 ± 0.049*	2MASS
	...	14.637 ± 0.013	13.993 ± 0.012	...	UKIRT
LSPM J1717+5925 B	...	16.580 ± 0.168*	15.934 ± 0.174*	15.581 ± 0.255*	2MASS
	...	16.509 ± 0.018	...	...	UHS
NLTT 52268 B	...	14.945 ± 0.052*	14.29 ± 0.05	13.839 ± 0.05	2MASS
	...	14.950 ± 0.02	14.295 ± 0.015	...	UKIRT
LSPM J2153+1157 B	...	14.403 ± 0.038*	13.785 ± 0.044*	13.427 ± 0.045*	2MASS
	...	14.450 ± 0.011	13.834 ± 0.011	13.368 ± 0.011	UKIRT
PM I22118–1005 B	...	15.246 ± 0.049	14.69 ± 0.063	14.051 ± 0.052	2MASS
NLTT 55219 B	...	16.313 ± 0.122*	15.469 ± 0.137*	14.778 ± 0.145*	2MASS
	...	16.612 ± 0.028	15.769 ± 0.024	...	UKIRT
Serendipitous Companion Discoveries					
NLTT 730 B	...	16.16 ± 0.08	15.23 ± 0.08	14.48 ± 0.07	2MASS
	...	16.16 ± 0.03	15.22 ± 0.03	...	UKIRT
NLTT 27966 B	...	16.155 ± 0.103	15.27 ± 0.11	14.58 ± 0.082	2MASS
	17.308 ± 0.044	16.106 ± 0.019	15.283 ± 0.018	...	UKIRT
LSPM J1336+2541 B	...	16.863 ± 0.16	16.017 ± 0.172	15.713 ± 0.2	2MASS
	18.228 ± 0.033	16.935 ± 0.017	16.122 ± 0.018	15.478 ± 0.016	UKIDSS
HIP 73169 B	...	16.007 ± 0.09*	15.047 ± 0.083	14.36 ± 0.081	2MASS
	17.223 ± 0.033	15.929 ± 0.02	15.054 ± 0.015	14.446 ± 0.016	VISTA
PM I23492+3458 B	...	16.298 ± 0.105	15.45 ± 0.112	15.008 ± 0.127	2MASS
	...	16.387 ± 0.029	15.472 ± 0.021	...	UKIRT
Unlikely companions					
NLTT 35593 B	...	16.299 ± 0.114	15.408 ± 0.117	14.737 ± 0.098	2MASS
	17.468 ± 0.02	16.227 ± 0.01	15.469 ± 0.011	14.876 ± 0.011	VISTA

**Notes.**

† Object saturated in VISTA data.

\* Object has a confusion flag (ccflag) set in this filter.

‡ Photometry from the 2MASS reject table.

SNIFS provides simultaneous coverage from 3200 Å to 9700 Å at a resolution of  $R \sim 1000$ . Integration times varied from 65 to 500 s, depending on the  $R$  magnitude. This was sufficient to get reasonable S/N ( $>70$  at 6000 Å) on all targets except GD 280, which had particularly low S/N ( $\sim 15$ ) due to patchy cloud cover and a fainter magnitude. The SNIFS pipeline (Bacon et al. 2001) performed basic reduction, including dark, bias, and flat-field corrections, wavelength calibration, sky subtraction, and extraction of the 1D spectrum. We took spectra of the spectrophotometric standards EG 131, Feige 110, GD 71, Feige 66, and HR 7596 during the night, which were then used to flux calibrate the data and remove telluric lines. Additional information on SNIFS data processing can be found in Lépine et al. (2013) and Mann et al. (2013b).

#### 4. NEW COMMON PROPER MOTION COMPANIONS

In total we have spectrally typed 87 companions to nearby stars of which 56 are new discoveries. Of these, 24 of our new discoveries are L dwarf companions, 1 is a late K, 2 are DA white dwarfs, 23 M7–M9.5 dwarfs, with the remaining 39 being M0–M6.5 dwarfs. Finder charts for our new companions are shown in Figure 7. In addition, we identified one previously

known blue L dwarf (2MASS J00150206+2959323, Kirkpatrick et al. 2010) as a companion to an M dwarf (NLTT 730), and a candidate L dwarf companion to an M dwarf (NLTT 35593), which we consider an unlikely companion to its M dwarf primary.

#### 4.1. Companionship Checks

In order to assess whether our candidate companions are merely alignments of unassociated stars, we undertook a test similar to Lépine & Bongiorno (2007). This consisted of taking all the objects in our input lists (*Hipparcos*, LSPM/rNLTT, and Lépine & Gaidos 2011) and offsetting their positions by two degrees in right ascension. We then searched for common proper motion companions to this list of modified positions. This test should only yield non-physical (coincident) pairings. To accurately reflect the probability of our objects being coincident contaminants, we applied the same cuts that were applied to our initial target sample. As an additional cut to exclude spuriously red objects (which we have excluded from our candidate sample by checking the objects'  $g_{P1}$ ,  $r_{P1}$ , and  $i_{P1}$  magnitudes) we excluded objects with more than one  $g_{P1}$  detection.

In Figure 8, we compare the separation and proper motion differences for our HIP samples and the coincident population.

**Table 7**  
The WISE Data of Our Companions

Object	W1 (mag)	W2 (mag)	W3 (mag)	W4 (mag)	Note
HIP search companions					
HIP 2397 B	13.077 ± 0.026	12.818 ± 0.027	12.167	8.924 ± 0.409	
HIP 6217 B	14.154 ± 0.03*	13.836 ± 0.042*	>12.790	>8.943	
HIP 6407 B	13.91 ± 0.027*	13.584 ± 0.035*	>12.375	>9.305	
HIP 9269 B	13.486 ± 0.026*	13.265 ± 0.033*	>12.573*	9.119 ± 0.473	
HIP 10033 B	12.597 ± 0.023*	12.33 ± 0.023*	12.578 ± 0.337*	>9.229	
HIP 11161 B	15.173 ± 0.043*	15.274 ± 0.111*	>12.738*	>9.179	
HIP 13589 B	13.572 ± 0.026*	13.295 ± 0.035*	>12.558*	>9.002	
HIP 26653 B	...	...	...	...	
HIP 32728 B	13.326 ± 0.027	13.133 ± 0.033	>12.04	>9.08	
HIP 37283 B	11.631 ± 0.024*	11.425 ± 0.021*	11.101 ± 0.105	9.329	
HIP 46984 B	12.313 ± 0.025*	12.129 ± 0.024*	12.3 ± 0.4	>8.6	
HIP 49046 B	11.777 ± 0.025	11.582 ± 0.023	11.424 ± 0.145	8.916	
HIP 51877 B	...	...	...	...	
HIP 52463 B	12.595 ± 0.025*	12.44 ± 0.025*	12.1 ± 0.3	>8.9	
HIP 55666 B	11.525 ± 0.023*	11.289 ± 0.023*	11.463 ± 0.176	9.097	
HIP 58918 B	13.252 ± 0.025*	12.954 ± 0.029*	>12.284	>9.101	
HIP 59310 B	12.400 ± 0.024	12.198 ± 0.024*	12.232 ± 0.310	>8.855	
HIP 59933 B	14.271 ± 0.031*	13.939 ± 0.048*	>12.707	>8.876	
HIP 60501 B	10.281 ± 0.023	10.12 ± 0.022*	10.038 ± 0.067	8.39 ± 0.325	
HIP 60987 B	...	...	...	...	†
HIP 60987 C	10.434 ± 0.022*	10.279 ± 0.019*	10.167 ± 0.066	>8.887	
HIP 63506 C	13.696 ± 0.027	13.405 ± 0.031	>12.498	>9.324	
HIP 65706 B	12.007 ± 0.024*	11.799 ± 0.023*	11.697 ± 0.162	>9.243	
HIP 65780 C	...	...	...	...	†
HIP 70623 C	11.06 ± 0.022*	10.921 ± 0.021*	10.851 ± 0.084	>8.628	
HIP 75310 B	12.181 ± 0.025*	11.984 ± 0.024*	11.342 ± 0.178	>8.493	
HIP 76456 B	12.139 ± 0.023*	11.867 ± 0.022*	11.525 ± 0.100*	>8.974	
HIP 76641 B	9.776 ± 0.023*	9.676 ± 0.021*	9.5590 ± 0.024	9.362 ± 0.360	
HIP 78184 B	12.8 ± 0.023	12.516 ± 0.022	12.403 ± 0.153	>9.755	
HIP 78859 B	11.285 ± 0.022*	11.086 ± 0.021*	11.038 ± 0.059	>9.703	
HIP 78916 B	...	...	...	...	†
HIP 78923 B	...	...	...	...	†
HIP 79180 B	12.746 ± 0.023*	12.558 ± 0.022*	12.241 ± 0.157	>9.305	
HIP 80258 B	12.078 ± 0.024	11.884 ± 0.024*	12.218 ± 0.248	>9.435	
HIP 81910 B	11.143 ± 0.025*	11.011 ± 0.025*	10.793 ± 0.147*	>8.691	
HIP 82233 B	10.855 ± 0.023*	10.661 ± 0.02*	10.588 ± 0.092	>8.774	
HIP 83651 B	9.631 ± 0.024*	9.495 ± 0.021*	9.387 ± 0.033	9.004 ± 0.428	
HIP 84840 B	11.45 ± 0.023*	11.294 ± 0.021*	11.376 ± 0.105*	>9.348	
HIP 85365 B	13.875 ± 0.03	13.643 ± 0.044	>12.394	>9.059	
HIP 86722 B	10.517 ± 0.024*	10.253 ± 0.022*	9.908 ± 0.041*	9.376 ± 0.54	
HIP 88728 B	...	...	...	...	
HIP 90273 B	10.523 ± 0.023*	10.361 ± 0.021*	10.208 ± 0.048	9.386 ± 0.513	
HIP 90869 B	10.148 ± 0.022*	10.012 ± 0.020*	10.089 ± 0.064	8.217 ± 0.288	
HIP 93967 B	12.331 ± 0.023*	12.137 ± 0.026	>11.605	>8.52	
HIP 97168 B	...	...	...	...	†
HIP 98535 C	12.14 ± 0.023*	11.917 ± 0.021*	12.603 ± 0.321	>9.516	
HIP 102582 B	11.059 ± 0.025*	10.795 ± 0.026*	10.771 ± 0.096	>9.105	
HIP 103199 B	10.855 ± 0.056*	10.644 ± 0.041*	10.61 ± 0.107	>9.209	
HIP 105202 B	11.046 ± 0.024*	10.865 ± 0.021*	10.583 ± 0.08	>9.01	
HIP 106551 B	...	...	...	...	†
HIP 108822 B	9.708 ± 0.024*	9.564 ± 0.020*	9.461 ± 0.032	8.63 ± 0.276	
HIP 109454 B	11.5 ± 0.025*	11.233 ± 0.022*	11.171 ± 0.111	>9.279	
HIP 111657 B	9.566 ± 0.050*	9.371 ± 0.038*	9.259 ± 0.05	8.819 ± 0.517	
HIP 112422 B	...	...	...	...	†
HIP 114424 B	10.418 ± 0.023*	10.213 ± 0.020*	10.154 ± 0.062	>8.394	
HIP 114456 B	9.685 ± 0.023*	9.511 ± 0.020*	9.299 ± 0.025*	8.744 ± 0.242	
HIP 115819 B	13.511 ± 0.026*	13.184 ± 0.033*	12.42 ± 0.467	8.425 ± 0.313	
HIP 116052 B	11.324 ± 0.025*	11.135 ± 0.023*	10.925 ± 0.091	>9.236	
Companions to faint non-HIP primaries					
NLTT 1011	13.762 ± 0.026	13.414 ± 0.032*	>12.3	>8.7	
GD 280 B	14.396 ± 0.032	14.149 ± 0.052	>12.794	>9.206	
NLTT 8245 B	...	...	...	...	†
LSPM J0241+2553 B	14.994 ± 0.044	14.826 ± 0.093	12.301 ± 0.396	>8.97	

**Table 7**  
(Continued)

Object	W1 (mag)	W2 (mag)	W3 (mag)	W4 (mag)	Note
HD 253662 B	...	...	...	...	
LSPM J0632+5053 B	14.94 ± 0.038*	14.757 ± 0.078	>12.814	>9.183	
NLTT 18587 B	15.096 ± 0.043	14.828 ± 0.085	>12.008	>9.129	
NLTT 19109 B	...	...	...	...	†
NLTT 22073 B	13.295 ± 0.027*	13.000 ± 0.030*	>12.224	>8.756	
NLTT 23716 B	...	...	...	...	†
NLTT 26746 B	14.058 ± 0.029*	13.871 ± 0.045	>12.715	>8.755	
NLTT 29395 B	...	...	...	...	†
NLTT 30510 B	14.546 ± 0.032*	14.247 ± 0.051*	>12.617	>8.982	
NLTT 31450 B	...	...	...	...	†
PM I13410+0542	...	...	...	...	†
PM I13518+4157	13.556 ± 0.026*	13.222 ± 0.029	12.46 ± 0.31	>9.328	
NLTT 38489 B	...	...	...	...	†
NLTT 39312 B	...	...	...	...	†
LSPM J1627+3328 B	...	...	...	...	†
NLTT 44368 B	12.951 ± 0.026	12.692 ± 0.025	12.054 ± 0.15	>8.934	
LSPM J1717+5925 B	...	...	...	...	†
NLTT 52268 B	...	...	...	...	†
LSPM J2153+1157 B	...	...	...	...	†
PM I22118–1005 B	13.571 ± 0.027	13.335 ± 0.036	>11.969	>8.984	
NLTT 55219 B	...	...	...	...	†
Serendipitous Companion Discoveries					
NLTT 730 B	13.69 ± 0.03	13.38 ± 0.04	11.7 ± 0.2	>9.011	
NLTT 27966 B	14.204 ± 0.028	13.853 ± 0.042	>12.773	>9.18	
LSPM J1336+2541 B	14.844 ± 0.034	14.553 ± 0.06	>12.869	>8.916	
HIP 73169 B	13.988 ± 0.027*	13.678 ± 0.035*	12.692 ± 0.409	>9.423	
PM I23492+3458 B	14.036 ± 0.028*	13.396 ± 0.032*	12.311 ± 0.305	>8.985	
Unlikely companions					
NLTT 35593 B	14.44 ± 0.03	14.287 ± 0.052	>12.517	>9.277	

#### Notes.

\* Has contaminated photometry in at least one *WISE* band.

† Too close to their primary to have an independent photometry measurement in *WISE*.

All objects in both our bright and ultracool companion samples that were followed up spectroscopically lie in portions of the plot sparsely populated by coincident pairings. This is likely due to our approach of preferentially following-up closer companions. Figure 9 shows the results for companions to non-*Hipparcos* primaries and our serendipitous discoveries. Most of our discoveries lie in a completely different area of the plot from the coincident pairings. However, one object, the apparent companion to NLTT 35593, is in a region of the diagram populated by many coincident pairings, and therefore we do not consider it to be a bona-fide companion. Excluding this object, we consider it likely that less than five of our companions to *Hipparcos* stars will be chance alignments with background stars. For our faint non-*Hipparcos* primaries, at most, two could be chance alignments. All of these coincident pairs would lie in the lowest proper motion bin of our sample.

#### 4.1.1. Photometric Distance

To further check the companionship of the objects, we derived photometric distances for all of our companions based on their spectral type. For objects of spectral types M6 and later, we derived the absolute magnitudes for our objects using the relations of Dupuy & Liu (2012) in *J*, *H*, and *K*/*K<sub>S</sub>*. For earlier-type objects, we used the spectral energy distribution

(SED) templates of Kraus & Hillenbrand (2007), who do not quote an rms for their relations. To estimate this we calculated the standard deviation of non-saturated 2MASS photometry of the FGK stars in Valenti & Fischer (2005) about the main sequence. These were found to be 0.25, 0.22, and 0.22 mag in *J*, *H* and *K<sub>S</sub>*, respectively. Cruz & Reid (2002) calculated fits to the *J*-band absolute magnitude as a function of temperature-sensitive spectral features for M dwarfs. They found that the M dwarf population was well-fitted by two relations, one covering early M with an rms of ∼0.2 mag and the other covering late M with an rms of ∼0.35 mag. This latter number is comparable with the 0.39 mag rms on the 2MASS *J*-band relation of Dupuy & Liu (2012). Hence we use the rms of Dupuy & Liu (2012) for objects of spectral type M5 and later and our calculated rms for earlier-type objects.

Next, we calculated absolutes magnitude from the Kraus & Hillenbrand (2007) or Dupuy & Liu (2012) relations and compared these with the object’s 2MASS photometry, or if available VISTA, UKIDSS, or UKIRT photometry, producing a distance estimate for each filter. Where non-2MASS near-infrared photometry was available for an object in a particular filter, we used this instead of 2MASS, making use of the Dupuy & Liu (2012) MKO relations for ultracool dwarfs and converting to the 2MASS system using the transformations of Carpenter (2001) for comparisons to the Kraus & Hillenbrand

**Table 8**  
Log of Spectroscopic Observations

Object	Date (UT)	$t_{\text{int}}$ (s)	Conditions	Seeing (")	Slit (")	Mode	Resolution $\lambda/\Delta\lambda$	Airmass	Standard
HIP search companions									
HIP 2397 B	2012 Jul 5	360	cloudy	1.5	$0.8 \times 15$	prism	75	1.12	HD 222749
HIP 6217 B	2013 Dec 11	360	cloudy	1.3	$0.5 \times 15$	prism	120	1.30	HD 13936
HIP 6407 B	2012 Jul 6	480	clear	1.3	$0.3 \times 15$	prism	200	1.37	HD 219545
HIP 9269 B	2011 Dec 2	1440	thin clouds	0.4	$0.8 \times 15$	prism	75	1.156	HD 23452
HIP 10033 B	2012 Oct 25	720	cloudy	0.5	$0.8 \times 15$	prism	75	1.14	HD 13936
HIP 11161 B	2012 Oct 28	720	thin clouds	0.8	$0.8 \times 15$	prism	75	1.202	HD 21038
HIP 13589 B	2012 Jul 8	480	clear	>1	$0.8 \times 15$	prism	75	1.44	HD 19600
HIP 26653 B	2014 Jan 18	120	clear	0.6	$0.8 \times 15$	prism	75	1.34	HD 32090
HIP 32728 B	2013 Apr 3	360	clear	0.7	$0.8 \times 15$	prism	75	1.05	HD 56386
HIP 37283 B	2012 Nov 16	240	thin clouds	0.4	$0.8 \times 15$	SXD	750	1.18	HD 63586
HIP 46984 B	2013 Apr 5	480	clouds	0.5	$0.8 \times 15$	prism	75	1.21	HD 101369
HIP 49046 B	2012 Nov 16	360	thin clouds	0.6	$0.8 \times 15$	SXD	750	1.04	HD 89239
HIP 51877 B	2014 Jan 17	180	clear	0.5	$0.8 \times 15$	prism	75	1.10	HD 71906
HIP 52463 B	2013 Apr 3	360	clear	0.7	$0.8 \times 15$	prism	75	1.28	HD 90606
HIP 55666 B	2011 Apr 20	80	clear	0.5	$0.5 \times 15$	prism	120	1.509	HD 97585
HIP 58918 B	2013 Apr 16	360	clouds	0.5	$0.8 \times 15$	prism	75	1.14	HD 105388
HIP 59310 B	2013 Apr 16	360	clouds	0.5	$0.8 \times 15$	prism	75	1.04	HD 105388
HIP 59933 B	2011 Mar 31	480	clear	0.3	$0.5 \times 15$	prism	120	1.08	HD 10538
HIP 60501 B	2011 Apr 20	80	clear	0.5	$0.5 \times 15$	prism	120	1.208	HD 109309
HIP 60987 B	2013 Apr 16	360	cloudy	0.4	$0.8 \times 15$	prism	75	1.14	HD 101060
HIP 60987 C	2013 Apr 16	360	cloudy	0.4	$0.8 \times 15$	prism	75	1.16	HD 101060
HIP 63506 C	2013 Jan 26	360	clear	0.7	$0.8 \times 15$	prism	75	1.083	HD 109615
HIP 65706 B	2012 Apr 30	180	fog	1.5	$0.8 \times 15$	prism	75	1.4	HD 116960
HIP 65780 C	2013 Jul 14	180	clear	0.9	$0.8 \times 15$	prism	75	1.73	HD 116960
HIP 70623 C	2012 Jul 7	720	clear	0.5	$0.5 \times 15$	SXD	1200	1.11	HD 132072
HIP 75310 B	2013 Apr 17	720	clear	0.7	$0.8 \times 15$	SXD	750	1.30	HD 144425
HIP 76456 B	2013 Apr 5	120	cloudy	0.8	$0.8 \times 15$	prism	75	1.26	HD 40739
HIP 76641 B	2013 Apr 3	90	clear	0.9	$0.8 \times 15$	prism	75	1.3	HD 136831
HIP 78184 B	2011 Mar 31	160	clear	0.3	$0.5 \times 15$	prism	120	1.37	HD 145127
HIP 78859 B	2012 Aug 10	180	clear	0.5	$0.5 \times 15$	SXD	1200	1.40	q Her
HIP 78916 B	2013 Jul 13	180	clear	0.5	$0.8 \times 15$	prism	75	1.07	HD 165029
HIP 78923 B	2013 Jul 13	180	clear	0.5	$0.8 \times 15$	prism	75	1.14	HD 145647
HIP 79180 B	2013 Apr 3	360	clear	0.9	$0.8 \times 15$	prism	75	1.44	HD 172728
HIP 80258 B	2012 Aug 10	50	thin clouds	0.4	$0.8 \times 15$	prism	75	1.2	26 Ser
HIP 81910 B	2011 Apr 20	80	clear	0.5	$0.5 \times 15$	prism	120	1.485	HD 145127
HIP 82233 B	2011 Apr 20	80	clear	0.5	$0.5 \times 15$	prism	120	1.276	HD 148968
HIP 83651 B	2012 Jul 11	100	thin clouds	0.9	$0.8 \times 15$	prism	75	1.1	HD 159008
HIP 85365 B	2012 Jul 7	600	clear	0.5	$0.8 \times 15$	SXD	750	1.25	HD 159415
HIP 86722 B	2011 Apr 20	80	clear	0.5	$0.5 \times 15$	prism	120	1.006	HD 165029
HIP 88728 B	2012 Jul 6	20	clear	1.3	$0.3 \times 15$	prism	200	1.23	HD 165029
HIP 90273 B	2013 Nov 8	200	cloudy	1.3	$0.3 \times 15$	prism	200	1.17	HD 174567
HIP 90869 B	2012 Aug 10	80	clear	0.3	$0.5 \times 15$	SXD	1200	1.51	HD 184533
HIP 93967 B	2011 Oct 14	300	cloudy	1.0	$0.8 \times 15$	prism	75	1.28	HD 182678
HIP 97168 B	2012 Jul 6	40	clear	1.3	$0.3 \times 15$	prism	200	1.15	HD 199217
HIP 98535 C	2012 Jul 6	120	clear	1.3	$0.3 \times 15$	prism	200	1.14	HD 199217
HIP 102582 B	2013 Jul 13	60	clear	0.5	$0.8 \times 15$	prism	75	1.08	HD 192538
HIP 103199 B	2012 Jul 6	120	clear	1.3	$0.3 \times 15$	prism	200	1.046	HD 210501
HIP 105202 B	2012 Jul 6	150	clear	1.3	$0.3 \times 15$	prism	200	1.043	HD 210501
HIP 106551 B	2012 Aug 11	240	clear	0.7	$0.5 \times 15$	prism	120	1.245	HD 199312
HIP 108822 B	2012 Aug 11	80	clear	0.7	$0.5 \times 15$	prism	120	1.247	HD 210501
HIP 109454 B	2011 Oct 15	1440	clear	0.6	$0.8 \times 15$	prism	75	1.04	HD 210501
HIP 111657 B	2012 Oct 2	240	cloudy	0.8	$0.8 \times 15$	SXD	750	1.19	HD 210501
HIP 112422 B	2012 Oct 7	540	thin cloud	0.9	$0.8 \times 15$	prism	75	1.03	HD 210501
HIP 114424 B	2012 Jul 7	140	clear	0.5	$0.5 \times 15$	prism	120	1.163	HD 218639
HIP 114456 B	2012 Oct 2	90	cloudy	0.7	$0.8 \times 15$	SXD	750	1.24	HD 219290
HIP 115819 B	2012 Jul 6	240	clear	1.3	$0.8 \times 15$	prism	75	1.198	HD 203769
HIP 116052 B	2012 Oct 25	420	cloudy	0.6	$0.8 \times 15$	SXD	750	1.01	HD 210501
Non-Hipparcos Companions									
NLTT 1011 B	2013 Sep 23	720	clear	0.6	$0.8 \times 15$	prism	75	1.04	HD 210501
GD 280 B	2013 Dec 11	720	cloudy	1.2	$0.8 \times 15$	prism	75	1.30	HD 15090
NLTT 8245 B	2014 Jan 19	180	clear	0.7	$0.8 \times 15$	prism	75	1.51	HD 10897
LSPM J0241+2553 B	2014 Jan 18	960	clear	0.6	$0.8 \times 15$	prism	75	1.22	HD 22401
HD 253662 B	2014 Jan 18	360	clear	0.6	$0.8 \times 15$	prism	75	1.13	HD 43583

**Table 8**  
(Continued)

Object	Date (UT)	$t_{\text{int}}$ (s)	Conditions	Seeing ( $\text{''}$ )	Slit ( $\text{''}$ )	Mode	Resolution $\lambda/\Delta\lambda$	Airmass	Standard
LSPM J0632+5053 B	2013 Apr 4	480	clear	0.7	$0.8 \times 15$	prism	75	1.30	HD 248790
NLTT 18587 B	2014 Jan 19	960	clear	0.7	$0.8 \times 15$	prism	75	1.07	HD 58296
NLTT 19109 B	2014 Jan 18	240	clear	0.6	$0.8 \times 15$	prism	75	1.35	HD 73687
NLTT 22073 B	2013 Nov 23	160	clear	1.1	$0.8 \times 15$	prism	75	1.49	HD 87727
NLTT 23716 B	2014 Jan 19	80	clear	0.7	$0.8 \times 15$	prism	75	1.12	HD 79108
NLTT 26746 B	2011 Mar 31	480	clear	0.3	$0.5 \times 15$	prism	120	1.05	HD 105388
NLTT 29395 B	2014 Jan 19	360	clear	0.7	$0.8 \times 15$	prism	75	1.28	HD 128039
NLTT 30510 B	2014 Jan 19	240	clear	0.7	$0.8 \times 15$	prism	75	1.05	HD 109615
NLTT 31450 B	2011 Mar 31	480	clear	0.3	$0.5 \times 15$	prism	120	1.03	HD 105388
PMI 13410+0542 B	2013 Jul 13	360	clear	0.9	$0.8 \times 15$	prism	75	1.12	HD 116960
PMI 13518+4157 B	2013 Jul 13	360	clear	0.9	$0.8 \times 15$	prism	75	1.14	HD 116960
NLTT 38489 B	2013 Apr 18	720	clear	0.5	$0.8 \times 15$	prism	75	1.45	HD 143187
NLTT 39312 B	2013 Jul 13	360	clear	0.9	$0.8 \times 15$	prism	75	1.18	HD 136831
LSPM J1627+3328 B	2013 Apr 17	360	cloudy	0.7	$0.8 \times 15$	prism	75	1.12	HD 145647
NLTT 44368 B	2013 Apr 16	360	thin clouds	0.7	$0.8 \times 15$	prism	75	1.27	HD 199217
LSPM J1717+5925 B	2013 Jul 12	1200		1.0	$0.8 \times 15$	prism	75	1.45	HD 179933
NLTT 52268 B	2013 Jul 12	120	clear	0.8	$0.8 \times 15$	prism	75	1.08	HD 210501
LSPM J2153+1157 B	2013 Jul 12	180	clear	0.8	$0.8 \times 15$	prism	75	1.10	HD 210501
PM I22118–1005 B	2013 Jul 12	720	clear	0.8	$0.8 \times 15$	prism	75	1.18	HD 203769
NLTT 55219 B	2013 Jul 12	720	clear	0.8	$0.8 \times 15$	prism	75	1.04	HD 210501
Serendipitous Companion Discoveries									
NLTT 27966 B	2012 Jun 7	360	clear	1.0	$0.8 \times 15$	prism	75	1.16	HD 99966
LSPM J1336+2541 B	2012 Jul 8	960	clear	0.9	$0.8 \times 15$	prism	75	1.06	HD 116960
HIP 73169 B	2012 Jul 6	960	clear	1.0	$0.8 \times 15$	prism	75	1.30	HD 116960
PM 23492+3458 B	2012 Jul 7	720	clear	0.6	$0.8 \times 15$	prism	75	1.31	HD 203030
Unlikely companions									
NLTT 35593 B	2013 Apr 18	360	clear	0.5	$0.8 \times 15$	prism	75	1.40	HD 116960
Primary Stars									
NLTT 730	2013 Sep 23	180	clear	0.7	$0.8 \times 15$	SXD	750	1.03	HD 210501
LSPMJ0632+5053	2013 Apr 17	90	patchy cloud	0.7	$0.3 \times 15$	SXD	2000	1.24	HD 39250
NLTT 26746	2012 Jul 5	280		1.2	$0.3 \times 15$	SXD	2000	1.30	HD 99966
NLTT 27966	2012 Jul 5	720	clear	1.2	$0.3 \times 15$	SXD	2000	1.56	HD 101060
NLTT 31450	2012 Jul 5	240	clear	0.8	$0.3 \times 15$	SXD	2000	1.30	HD 118214
LSPMJ1336+2541	2013 Jul 12	90	clear	1.0	$0.3 \times 15$	SXD	2000	1.10	HD 109691
PM I13518+4157	2013 Jul 12	90	clear	1.0	$0.3 \times 15$	SXD	2000	1.06	HD 123233
HIP 83651	2013 Apr 17	90	cloudy	0.7	$0.8 \times 15$	SXD	750	1.11	HD 167163
HIP 84840	2013 Apr 16	180	cloudy	0.8	$0.3 \times 15$	SXD	2000	1.07	HD 165029
NLTT 44368	2013 Jul 12	90	clear	0.8	$0.3 \times 15$	SXD	2000	1.32	HD 199217
HIP 97168	2013 Apr 17	90	cloudy	0.7	$0.8 \times 15$	SXD	750	1.20	HD 197291
HIP 108822	2013 Jul 12	90	clear	1.0	$0.3 \times 15$	SXD	2000	1.08	HD 210501
PM I22118–1005	2013 Jul 12	90	clear	1.0	$0.3 \times 15$	SXD	2000	1.25	HD 203893
PM I23492+3458	2013 Jul 12	90	clear	1.0	$0.3 \times 15$	SXD	2000	1.31	HD 219290

(2007) SEDs. We calculated the errors in distance caused by an uncertainty in spectral type, by the rms of the fits, and by the error on the 2MASS photometry. We then calculated the weighted mean of these distance estimates, weighting only by our measurement errors, i.e., the quadrature sum of the error in the photometric measurements and the propagated error in spectral typing. We then calculated a final error on this distance based on the quadrature sum of the photometric error, intrinsic scatter, and propagated error in spectral type for each band. Hence the final quoted error includes both the effects of measurement errors and the rms intrinsic scatter about the photometric relations. The calculated photometric distances are shown in Tables 4 and 5. Note that our white dwarf companion (HIP 88728 B), which was saturated in Pan-STARRS 1, is not resolved in plate images.

We also calculated photometric distances for our primaries that lacked trigonometric parallaxes. For primaries with measured spectral types, we applied a similar process as for our secondaries. Where there were no literature spectral distances we used relations from Lépine (2005) and the errors in those distances were calculated in the same way as for the secondaries. For our two white dwarf primaries we used the photometric distance relations of Limoges et al. (2013). For this we assumed a DA spectral type and a mass of  $0.6 M_{\odot}$ . Limoges et al. (2013) quote a photometric distance error of 15 pc for their sample with approximate distances of 30 pc. Hence we assume errors of 50% for our white dwarf photometric distances. It appears that most of our companions have photometric distances that are in good agreement with the distances to their primaries. This is shown in Figure 10.

**Table 9**  
Spectroscopic Classification of Our L Dwarf Companions

Object	SpT(Visual)	H <sub>2</sub> O_J	SpT(H <sub>2</sub> O_J)	H <sub>2</sub> O_H	SpT(H <sub>2</sub> O_H)	CH <sub>4</sub> _K	SpT(CH <sub>4</sub> _K)	SpT(Final) Type
HIP search companions								
HIP 6407B	L0	0.831	L3.3	0.776	L3.6	1.002	L4.3	L1+T5 <sup>c</sup>
HIP 2397B	L0	0.935	L0.6	0.846	L0.8	1.053	L2.3	L0.5
HIP 59933B	L1.5	0.922	L0.9	0.838	L1.1	1.042	L2.8	L1
HIP 63506 C	L1 <sup>a</sup>	0.909	L1.2	0.82	L1.8	1.025	L3.5	L1
HIP 85365B	L5	0.752	L5.7	0.701	L6.5	0.965	L5.6	L5.5
HIP 9269B	L6	0.752	L5.7	0.781	L3.3	0.978	L5.2	L6
HIP 11161B	L1.5	0.900	L1.4	0.834	L1.2	1.01	L4.0	L1.5
HIP 112422B	L2	0.809	L4.0	0.837	L1.1	1.028	L3.3	L1.5
Companions to faint non-HIP primaries								
NLTT 1011B	L1.5	0.843	L2.9	0.763	L4.0	1.01	L4.2	L2
NLTT 55219B <sup>b</sup>	L2	0.793	L4.5	0.707	L6.3	0.943	L6.3	L5.5
PM I22118–1005 B	L1.5	0.906	L1.3	0.806	L2.3	1.03	L3.1	L1.5
PM I13410+0542B	L4	0.852	L2.7	0.734	L5.2	1.115	M9.3	L4
PM I13518+4157B	L1.5	0.882	L1.8	0.829	L1.4	0.985	L4.9	L1.5
LSPM J0241+2553 B	L1.5	0.922	L0.9	0.841	L0.9	1.064	L1.8	L1
HD 253662 B	L1.5	0.942	L0.5	0.0866	L0.0	1.060	L2.0	L0.5
LSPM J0632+5053B	L2	0.919	L1.0	0.846	L0.7	0.999	L4.4	L1.5
NLTT 26746B	L4	0.786	L4.7	0.721	L5.7	1.031	L3.2	L4
NLTT 31450B	L6	0.829	L3.4	0.784	L3.2	1.057	L2.1	L6
NLTT 44368B	L1.5	0.899	L1.4	0.834	L1.2	1.038	L2.9	L1.5
LSPM J1717+5925 B	L1.5	0.953	L0.3	0.850	L0.6	1.042	L2.8	L1
Serendipitous companion discoveries								
NLTT 27966B	L4	0.771	L5.1	0.718	L5.9	1.011	L4.0	L4
LSPM J1336+2541B	L4	0.848	L2.8	0.718	L5.9	0.964	L5.6	L4
HIP 73169B	L2.5	0.87	L2.2	0.787	L3.1	1.059	L2.0	L2.5
PM 23492+3458B	L9	0.615	L9.7	0.63	L9.0	0.79	L9.7	L9
Unlikely discoveries								
NLTT 35593B	L2	0.878	L2.0	0.796	L2.8	1.049	L2.5	L2

**Notes.**

<sup>a</sup> No good standard comparison was found; the best match in the SpeX prism library was the L1 2MASSWJ143928.4+192915 (Burgasser et al. 2004).

<sup>b</sup> No good standard comparison was found; the best match in the SpeX prism library was the L5.5 2MASS J17502484–0016151 (Kendall et al. 2007).

<sup>c</sup> Using spectral decomposition we determined that HIP 6407B is likely itself a double consisting of an L1 and a T5. We later resolved this companion as a tight binary itself. See Section 5.2.1 for more details.

## 4.2. Spectral Types and Ages of the Primaries

### 4.2.1. Spectral Types

We searched the literature for information on our primary stars. While many had spectral types either from previous measurements, 32 were unclassified. For primaries with no published spectral type we have obtained where possible near-infrared or optical spectroscopic observations (see Sections 3.2 and 3.3). These objects are shown in Figures 5 and 11. For objects with no spectral type from the literature or that were not observed as part of our follow-up program, we used the  $V - J$  to spectral type relation of Lépine & Gaidos (2011). For our non-*Hipparcos* primaries, we use the  $M_V$  magnitudes listed in Lépine & Shara (2005) and Salim & Gould (2003) along with  $J$  magnitudes from 2MASS. For the single object that was too blue for this relation to be valid (HIP 111657), we used the primary’s 2MASS photometry and the SED of Kraus & Hillenbrand (2007) to estimate spectral type. Tables 10 and 11 show details of our primary stars.

For objects observed with SNIFS, spectral types for NLTT 730, LSPM J2153+1157, and NLTT 22073 were determined following the methods outlined in Lépine et al. (2013). Specifically, we measured the strengths of the TiO and CaH features and then compared to stars from Reid et al. (1995). We also matched each spectrum by eye to templates from Bochanski et al. (2007) using the IDL spectral typing suite of Covey et al. (2007). Metallicities were determined following the methods of Mann et al. (2013a), which provide empirical relations between visible-wavelength features and metallicities for late-K to mid-M dwarfs. Errors in metallicities were calculated considering both errors in the Mann et al. (2013a) calibration and measurement errors. We classified NLTT 1011 using our Mayall Telescope data and the Covey et al. (2007) HAMMER indices, resulting in a type of K5. Our other Kitt Peak targets, NLTT 38489 and HIP 84840 B, were visually compared to the spectral templates of Bochanski et al. (2007) with best matches of M3 and M4, respectively; these subtypes were confirmed by index measurements using the method of Lépine et al. (2013) for NLTT 38489, while HIP

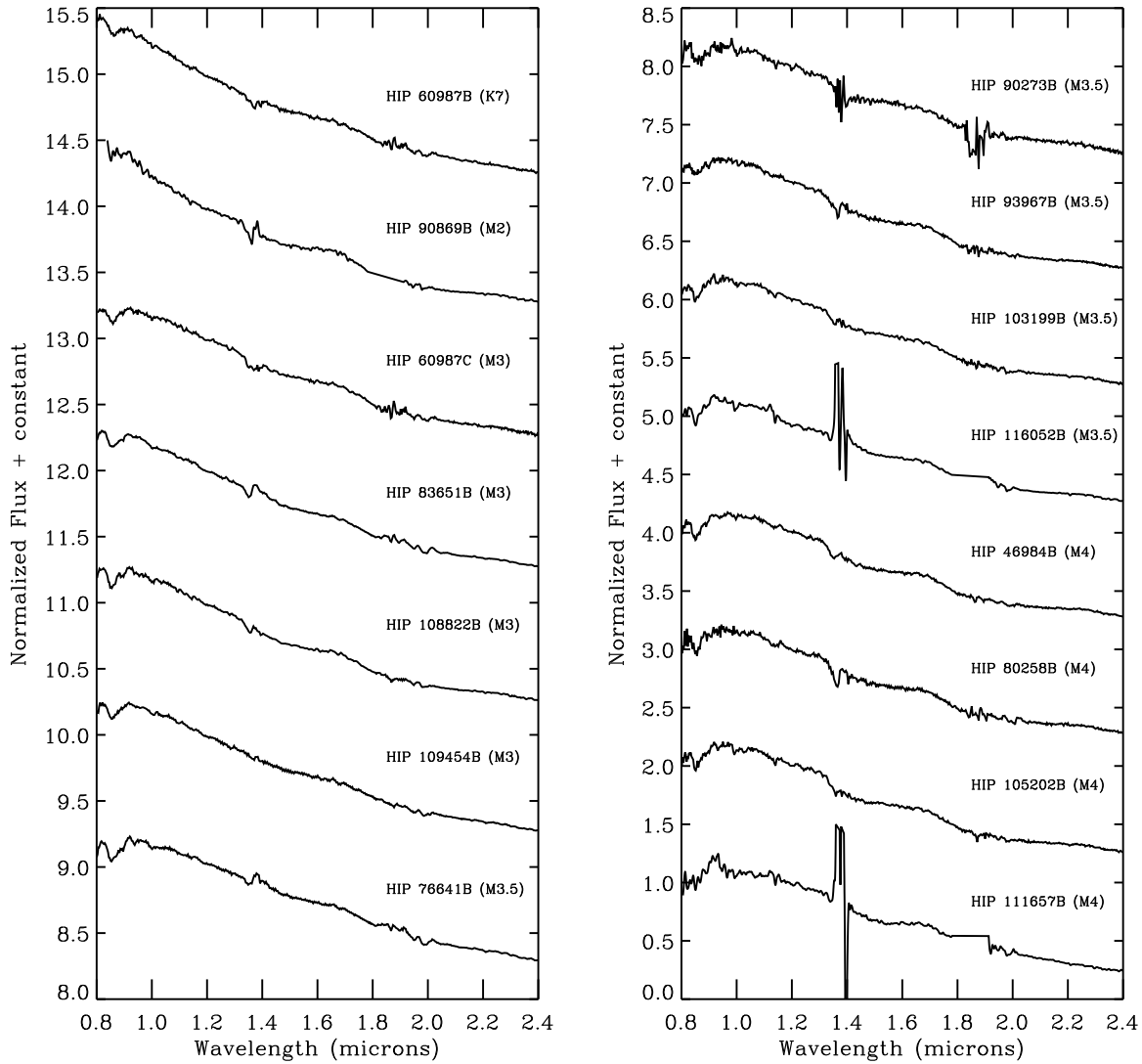


**Figure 1.** IRTF/SpeX spectra for our *Hipparcos* companions with spectral types from M0.5 to M4. Spectra taken with SpeX SXD mode have been Gaussian smoothed to  $R = 200$ . For the SXD spectra note that the noisy gaps at  $1.4 \mu\text{m}$  and  $1.8 \mu\text{m}$  are caused by the order boundaries.

84840 B was classified as an M3.5. We adopt our visual comparisons along with a spectral typing error of half a subclass for these two objects. None of our observed objects showed emission in H $\alpha$ . One of our SNIFS targets, GD 280, was listed as a candidate white dwarf by Giclas et al. (1967). Our spectrum shows clear Balmer line absorption; hence we classify it as a DA white dwarf. We do not have a spectrum for LSPM J0241+2553. The resulting spectral types and metallicities for the objects observed with SNIFS are listed in Table 11 and the spectra are shown in Figure 11.

#### 4.2.2. Age Estimates

Twenty-three of our primary stars have age estimates listed in the literature. For remaining objects with no published ages, we used archival Ca H and K emission and where this was found, applied the age–activity relation of Mamajek & Hillenbrand (2008). The majority of our primaries had no such data, and the only object that did had no age derived from such emission in the literature. For the remaining 54 objects with no Ca H and K measurements, we set an approximate upper age limit of  $\sim 10$  Gyr based on their disk-like kinematics.

To set a lower limit for the handful of M-dwarf primaries where we had an optical spectrum, we used the object’s lack of H $\alpha$  and the activity lifetime of West et al. (2008). Here we used the  $1\sigma$  lower limit for the activity age, taking into account that our spectral types have an uncertainty of 0.5 spectral types. For all our objects without H $\alpha$  or Ca H and K data, we searched the ROSAT Faint Source catalog (Voges et al. 2000) with a matching radius of  $30''$ . We identified four objects as having weak X-ray emission; the rest we assumed that the flux was below the limiting flux quoted by Schmitt et al. (1995). We then used the distances to these objects along with the counts to flux conversion of Schmitt et al. (1995) to estimate the X-ray luminosity. We converted this to the X-ray to bolometric luminosity ratio ( $R_x$ ) using an  $L_{\text{bol}}$  calculated from Tycho photometry (Hog et al. 2000), the color relations of Mamajek et al. (2002), and the bolometric corrections of Pecaut & Mamajek (2013). This was then applied to the age-to-X-ray activity relation of Mamajek & Hillenbrand (2008) to obtain lower age limits. Note that this X-ray relation has not been calibrated beyond mid-K spectral types, hence we used the objects’ lack of X-ray emission to set a lower age limit of 300 Myr for objects of this spectral type. This is the age below

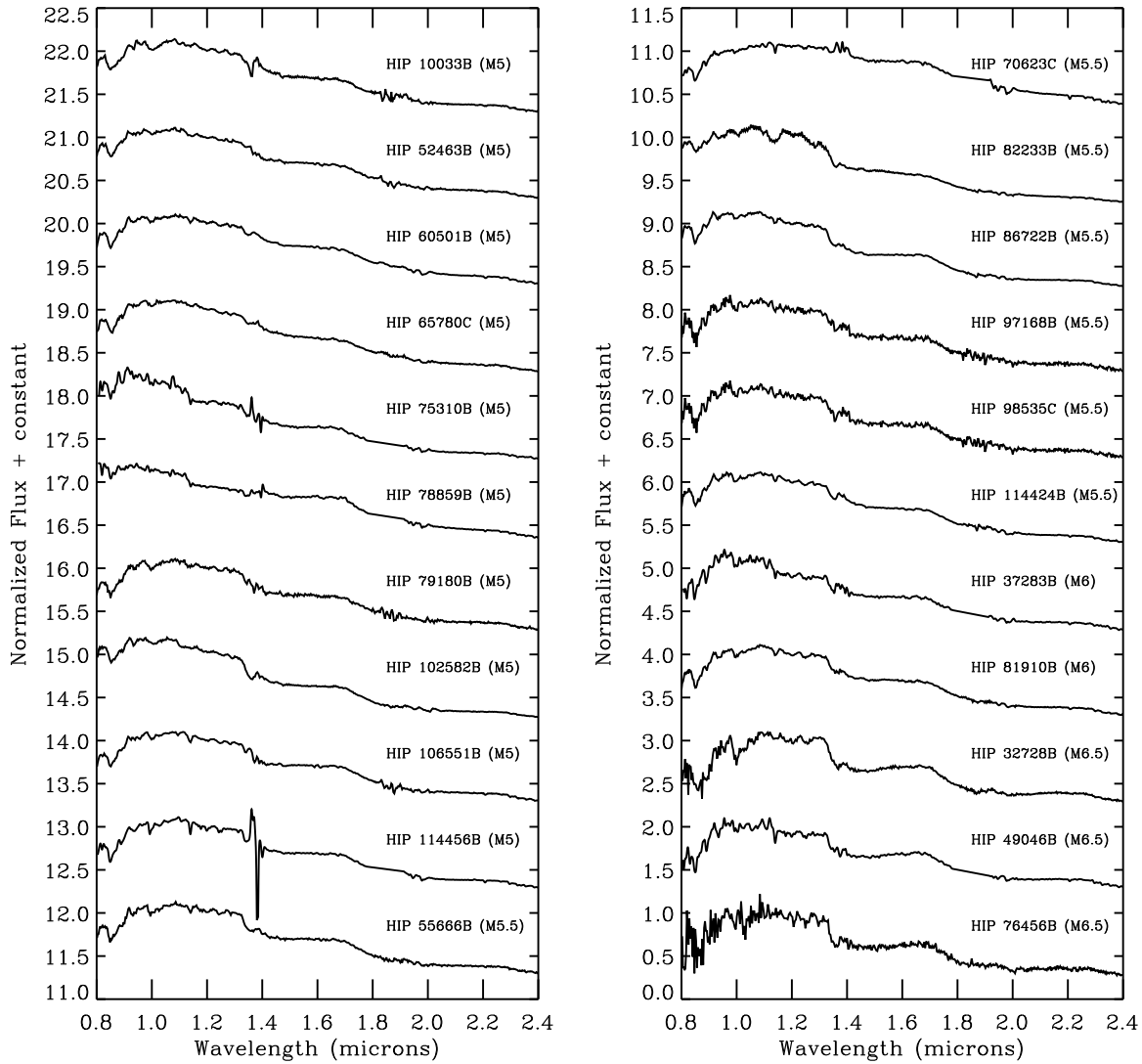


**Figure 2.** IRTF/SpeX spectra for our *Hipparcos* companions with spectral types from M5 to M6.5. Spectra taken with SpeX SXD mode have been Gaussian smoothed to  $R = 200$ .

which low mass stars show significant X-ray emission (Shkolnik et al. 2009).

## 5. DISCUSSION

### 5.1. Comparison with the Field Ultracool Wide Binary Population

Our sample contains 24 new L-dwarf companions to main sequence stars (including the previously typed but unrecognized L7 companion to NLTT 730 but not the unlikely L2 companion to NLTT 35593). Additionally we identified 21 new wide M-dwarf companions with spectral types of M7 or later and typed two previously proposed companions.

In order to study the wide ultracool (spectral type  $\geq M7$ ) binary population, we compiled a list of wide ultracool companions to stars (see Table 12). We began with the compilation of Faherty et al. (2010; excluding the companion to NLTT 20346 that Dupuy & Liu 2012 concluded was not physically related due to its high proper motion difference from its primary) and added spectroscopically confirmed objects from the literature discovered since then. We do not include objects that have been identified as candidate binaries but that lack spectral types such as from the studies of Deacon et al. (2009), Dhital et al. (2010),

and Smith et al. (2014). Figure 12 shows the spectral type of the secondary plotted against the projected separation ( $r_{\text{AU}}$ ). At first glance, there is an apparent scarcity of T dwarf companions wider than 3000 AU. In fact, this is due to previous efforts focusing on identifying close companions and from the known population being drawn from a series of heterogeneous surveys. Figure 13 shows a histogram comparing the combined contribution of this work, Deacon et al. (2012b) and Deacon et al. (2012a) to the total number of companions. This paper's contribution is most significant beyond  $\log_{10} r_{\text{AU}} = 3.5$  where we have doubled the population of L dwarf companions. In total we have increased the wide ( $> 300$  AU) L dwarf companion population by 82% and doubled the number of ultracool M dwarf companions in the same range. While the L dwarf population exhibits an approximately flat distribution in  $\log_{10} r_{\text{AU}}$ , the T dwarf companion population peaks between  $\log_{10} r_{\text{AU}} = 3.0$  and 3.5. However, any claim of a preferred separation for T dwarf companions (or of a log-flat distribution for L dwarfs) should be treated with caution as the sample is drawn from a disparate set of surveys. Similarly the apparent cut-off above 10,000 AU is likely due to incompleteness in surveys (including our own) and the difficulty of disentangling the widest binaries from coincident alignments from field stars. In a future paper

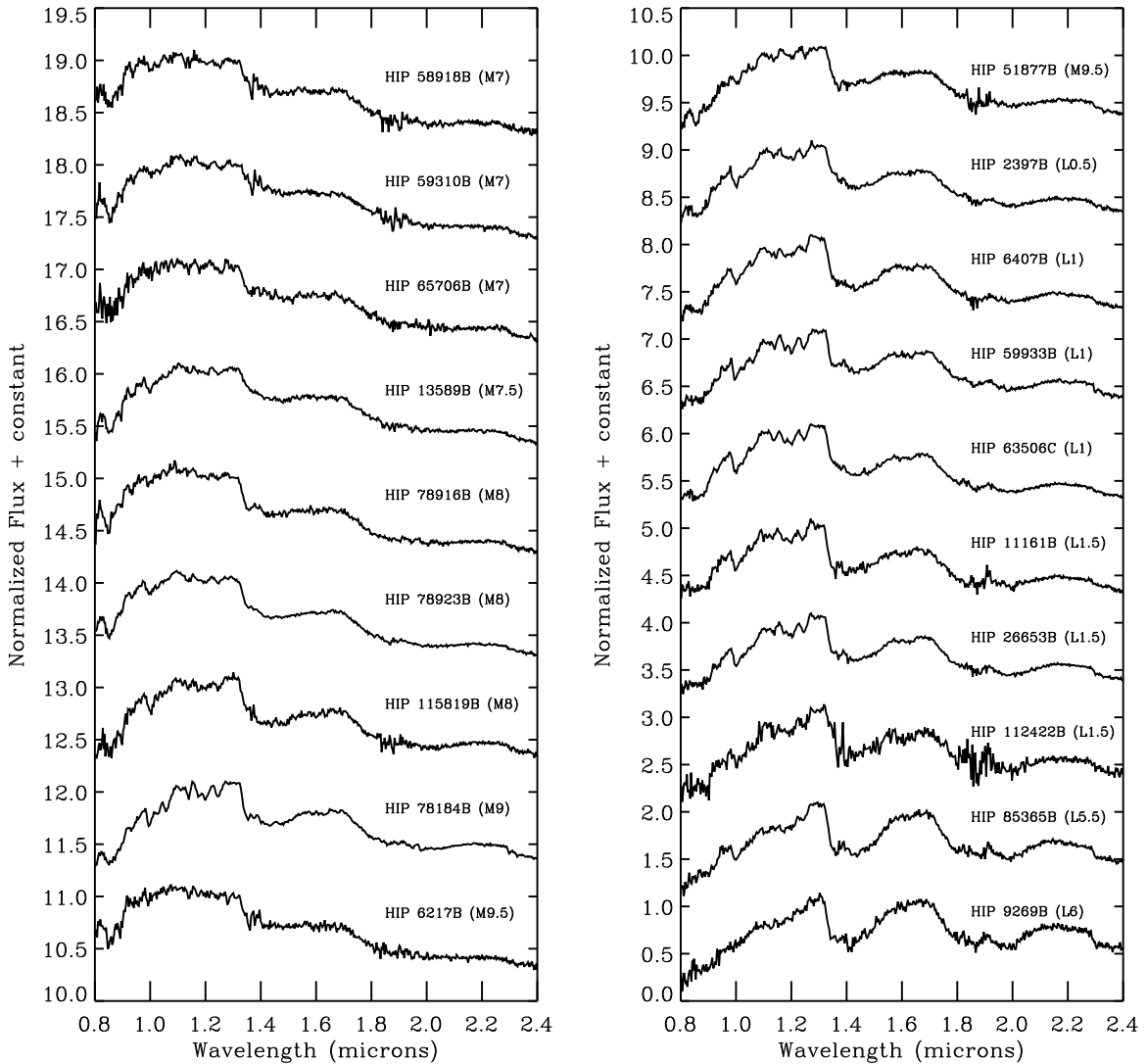


**Figure 3.** IRTF/SpeX spectra for our ultracool *Hipparcos* companions with spectral types of M7 or later. Spectra taken with SpeX SXD mode have been Gaussian smoothed to  $R = 200$ . Note that HIP 6407 B was resolved as being an L1+T3 binary itself. See Section 5.2.1 for details.

we aim to take the final results of our survey, model our selection biases, and determine the true separation distribution of the ultracool companion population.

In order to determine the stability of the population of systems containing a wide, ultracool companion, we estimated the total mass of each system. Where an object had a mass quoted in the literature, we used that value. For known L and T dwarfs with no quoted mass estimates and our new L and T companions, we used a value of  $0.075 M_{\odot}$ , in essence making our total mass estimates for these systems upper limits. For A–M stars with no mass in the literature, we converted their spectral type to mass using the relations of Kraus & Hillenbrand (2007).<sup>15</sup> The results are plotted in Figure 14 along with the maximum separation versus total mass relations suggested by Close et al. (2003) and Reid et al. (2001). It is clear that a substantial number of late-type companions lie outside both of these suggested maximum boundaries and are hence loosely bound. Dhital et al. (2010) used a simple model of interactions in the Galactic disk (based

on Weinberg et al. 1987) to calculate the typical maximum separation for a given system age and total mass. This is also plotted in Figure 14 for a number of different ages. It is clear that, though loosely bound, very few of the widest systems would be disrupted over the lifetime of the Galactic disk.

## 5.2. Interesting Individual Systems

### 5.2.1. HIP 6407Bab

We initially classified HIP 6407B as an L0 based on visual comparison to standards. However, the object has significantly stronger water absorption features suggestive of an object two or three subtypes later. As this may result from the contribution of an unresolved additional component, we observed this object on 2013 October 14 UT at the Keck II telescope using the facility near-infrared camera NIRC2 with laser guide star adaptive optics (LGS AO; Wizinowich et al. 2006; van Dam et al. 2006). We kept the LGS centered in NIRC2’s narrow field-of-view camera while we obtained dithered images of the target in the  $Y_{\text{NIRC2}}$ ,  $J_{\text{MKO}}$ ,  $H_{\text{MKO}}$ , and  $C\text{H}_4\text{s}$  bandpassess. The wavefront sensor recorded flux from the LGS equivalent to a  $V \approx 9.6\text{--}9.8$  mag star. The primary star HIP 6407 was used as the tip-tilt reference star, and the lower bandwidth sensor monitoring

<sup>15</sup> For the LSPM J1202+0742 ABC system (Smith et al. 2014), we estimated the spectral type of the brighter component based on their  $V - J$  color (M0, LSPM J1202+0742N) or 2MASS photometry (M1, LSPM J1202+0742S). We then used these to determine the total mass of the system.

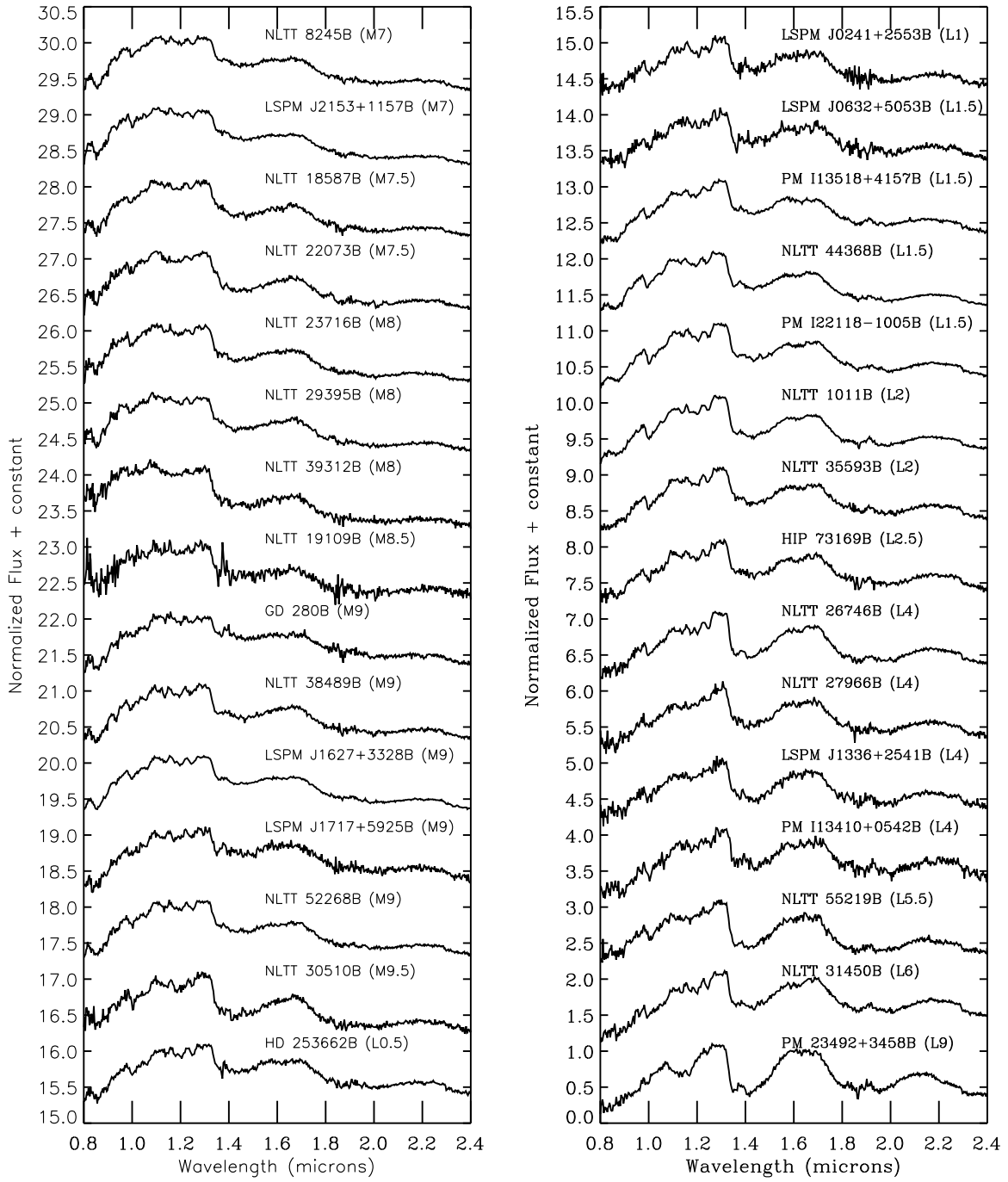


**Figure 4.** IRTF/SpeX spectra for our ultracool companions discovered serendipitously or by searching for wide companions to faint non-*Hipparcos* primaries.

this source recorded flux equivalent to a  $R \approx 7.6$  mag star. Our procedure for reducing and analyzing Keck LGS data is described in detail in our previous work (e.g., Liu et al. 2006; Dupuy et al. 2010). To summarize briefly, we measure binary parameters by fitting three-component Gaussians to determine the position and flux of each binary component, and we derive uncertainties by computing the scatter among individual dithered images. We used the NIRC2 astrometric calibration from Yelda et al. (2010), which includes a correction for the nonlinear distortion of the camera and has a pixel scale of  $9.952 \pm 0.002$  mas per pixel and an orientation for the detector's +y axis of  $+0^\circ 252 \pm 0^\circ 009$  east of north. We resolved HIP 6407B as a  $0''.131$  (7.4 AU) binary. Table 13 gives the

binary parameters we measured in each bandpass along with the weighted average of the separation ( $\rho$ ) and position angle (P.A.) values. Given the objects' separation and maximum total mass of  $0.16 M_\odot$  (as it consists of two substellar objects), the likely period of this system is  $>300$  yr, making it a poor mass–age benchmark.

We performed spectral decomposition analysis on HIP 6407B using the method described in Section 5.2 of Dupuy & Liu (2012). Briefly, we started with all possible pairs of the 178 IRTF/SpeX prism spectra from the library of Burgasser et al. (2010). For each template pairing, we determined the scale factors needed to minimize the rms deviation from our observed spectrum. We then computed the  $\chi^2$  of our Keck LGS AO

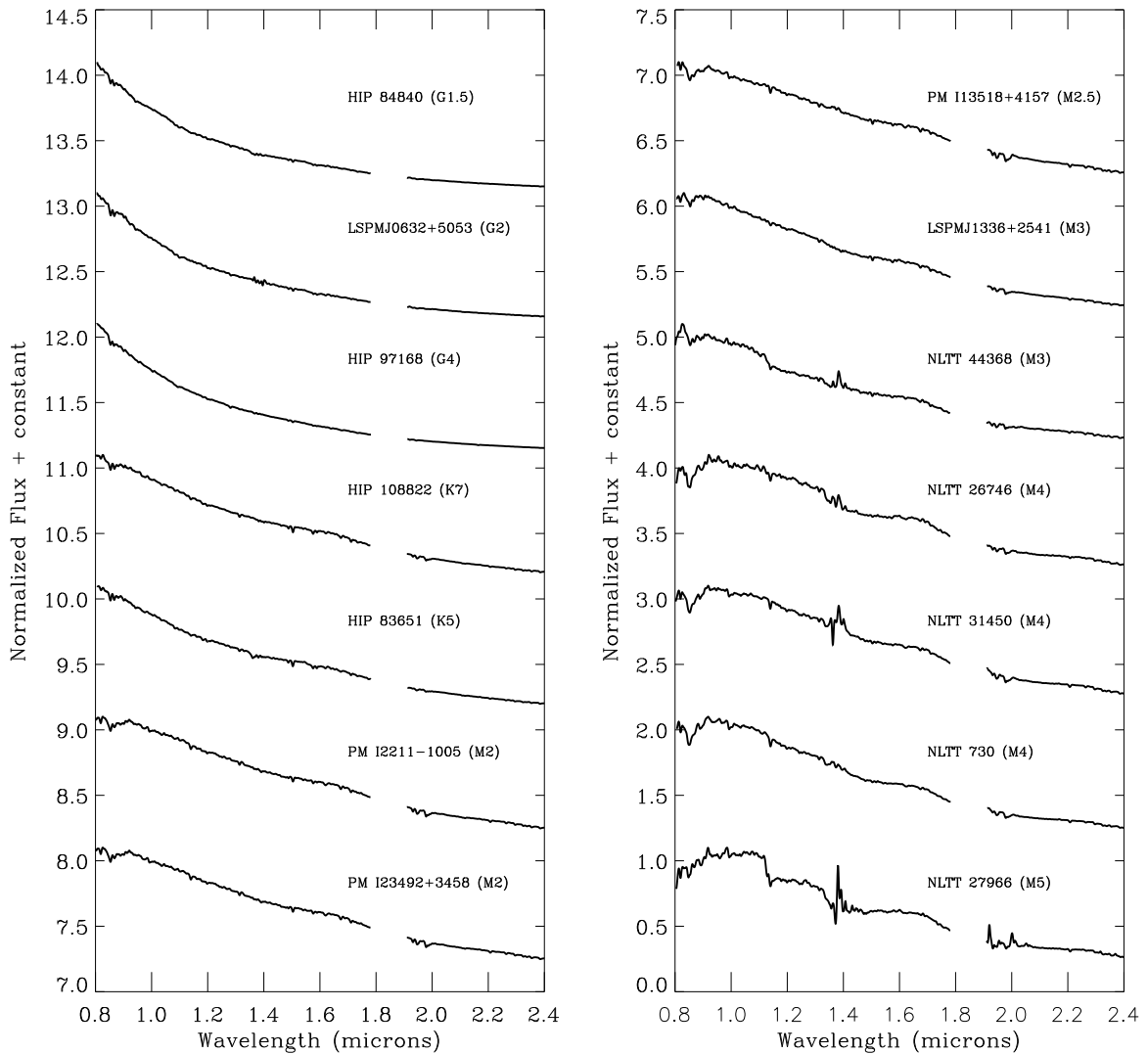


**Figure 5.** IRTF/SpeX spectra for the primaries of our companions that had no spectral type in the literature. These spectra were taken with SpeX SXD mode and have been Gaussian smoothed to  $R = 200$ .

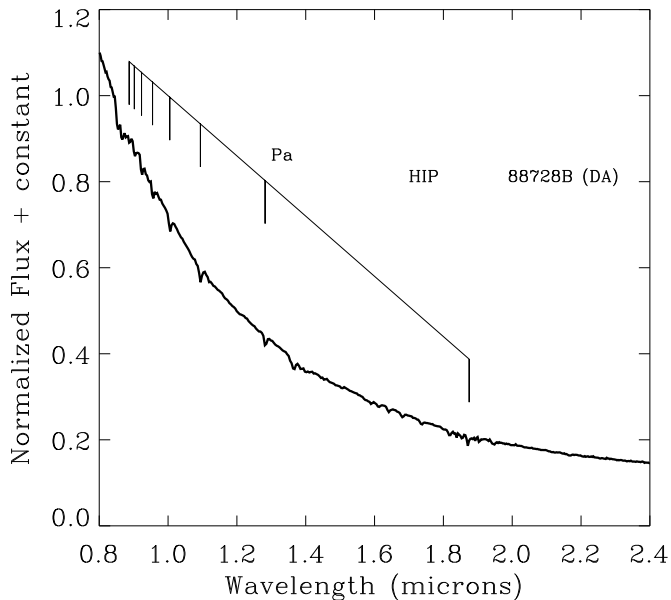


**Figure 6.** IRTF/SpeX spectra for our white dwarf *Hipparcos* companions. The wavelengths of the Paschen lines are also shown.

flux ratios in  $J$ ,  $H$ , and  $CH_4S$  bands compared to the flux ratios computed for each pairing. We excluded pairings that significantly disagreed with our measured flux ratios,  $p(\chi^2) < 0.05$ , and examined the remaining best pairings to determine the component spectral types. Our final spectral types of  $L1.0 \pm 0.5$  and  $T3 \pm 1$  account for the full range of spectral templates that gave equally good fits to our combined light spectrum. We estimated the flux ratio in the  $K$  band as well as flux ratios in the 2MASS photometric system by taking the mean and rms of each flux ratio among the ensemble of best-fit template pairings. Figure 15 shows the best match to our spectrum, which is provided by the templates.

The best match to our spectrum is provided by the templates DENIS-P J170548.3–051645 (L1; Burgasser et al. 2010; Allers & Liu 2013) and SDSS J120602.51+281328.7 (T3; Chiu et al. 2006; Burgasser et al. 2010) scaled to each other by the magnitudes shown in the lower panel of Figure 15, giving magnitude differences of  $d_J = 2.26 \pm 0.05$  mag and  $d_H = 2.51 \pm 0.05$  mag. We adopt spectral types of  $L1 \pm 1$  and  $T3 \pm 1$  for the components of HIP 6407B based on the typical uncertainty in infrared types for L dwarfs and the range of good matching templates for the secondary. Note that the template library from Burgasser et al. (2010) nominally only includes

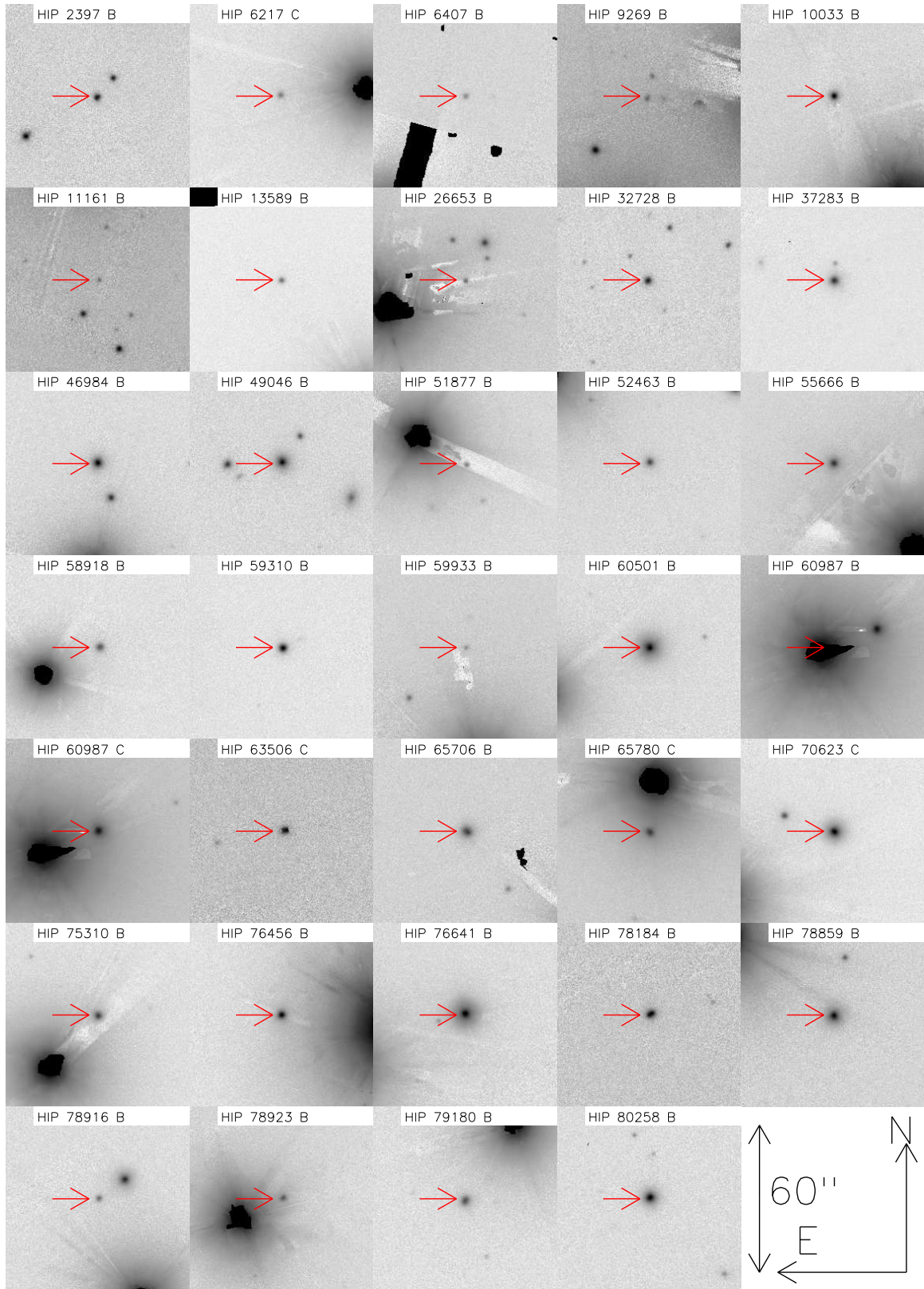


**Figure 7.**  $y_{P1}$  finder charts for our companions. Note that some regions are masked due to chip gaps and PS1 detector artifacts. Also note that some of the higher proper motion stars appear elongated due to these images being stacks of individual observations spread over the PS1 survey period.  
(A color version of this figure is available in the online journal.)

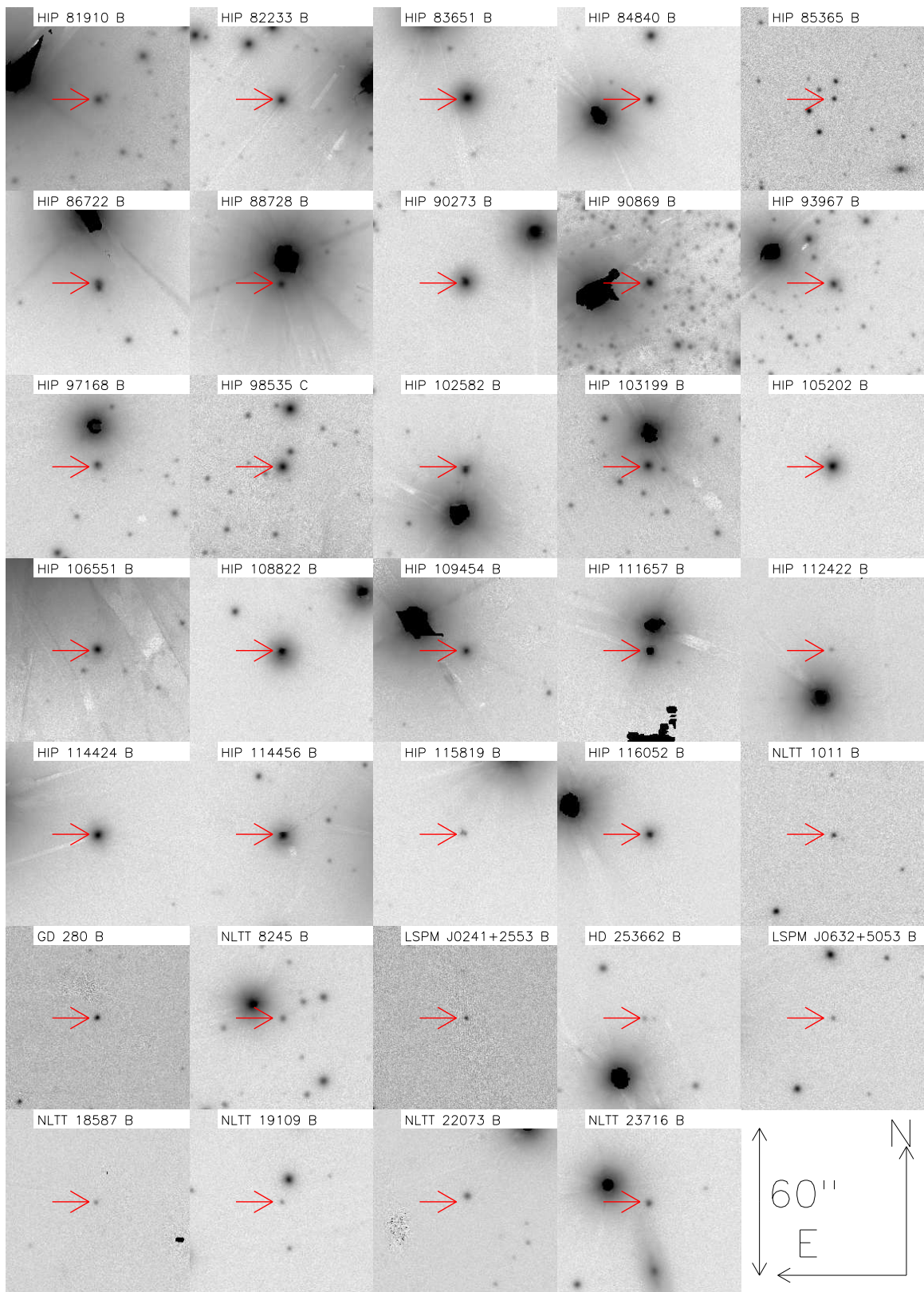


Figure 7. (Continued)

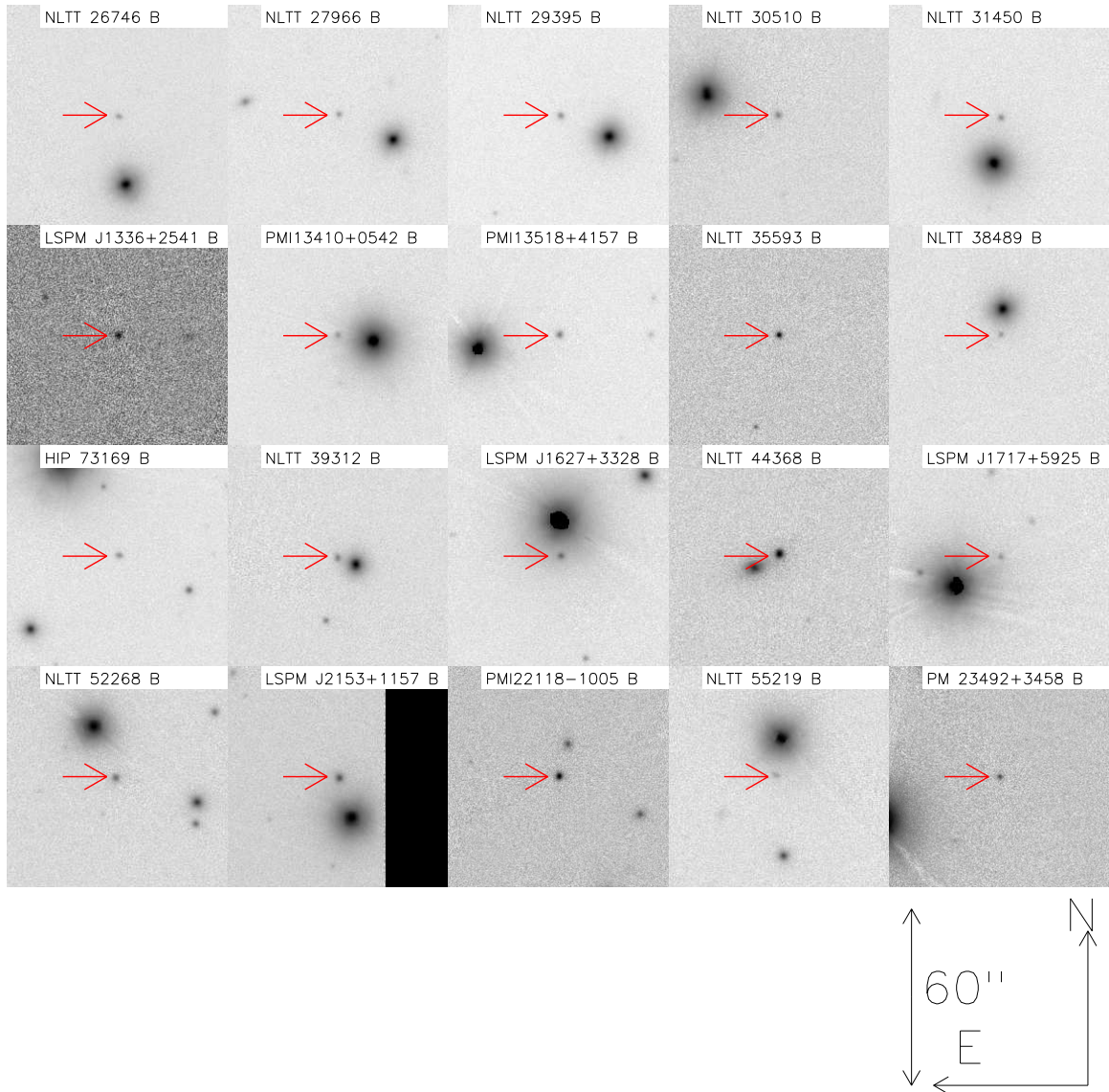


Figure 7. (Continued)

objects later than L0, which barely encompasses the spectral type of the proposed primary component. However, Figure 15 shows that the L1 template gives a very good match to the data, so the primary is not likely to be of much earlier type.

#### 5.2.2. HIP 70623 (HD 126614)

HIP 70623 (HD 126614) is a K0 star with an  $M \sin i = 0.38 M_{\text{Jup}}$  giant planet in a 3.41 yr orbit (Howard et al. 2010). There is also an additional M dwarf component in the system with a separation of 0''.5 (Howard et al. 2010) detected by adaptive optics imaging. The wide M5.5 companion we recover was identified by Gould & Chaname (2004) as a companion but has no previously published spectral type. Despite this object being identified as a companion before the Howard et al. (2010) identification of the closer companion, it has the designation HIP 70623/HD 126614 C.

#### 5.2.3. HIP 115819 (VZ Piscium)

VZ Piscium is a marginal-contact eclipsing binary with a period of 0.261 days (Hrivnak et al. 1995) classified as a

W-U Ma type variable. As angular momentum transfer to additional components can tighten an inner binary and lead to contact, Rucinski et al. (2007) observed VZ Piscium as part of an adaptive optics search for companions to contact binaries. We have identified an M8 companion at a separation of 30''. This fell outside the 36''  $\times$  36'' field of view of Rucinski et al. (2007). Note that Qian et al. (2004) suggest a closer companion to the binary may be causing a variation in the light curve with a period of  $\sim$ 25 yr. However, no close companion was identified by Rucinski et al. (2007), and our companion is too wide to introduce such a short period variation.

#### 5.2.4. HIP 103199 (HD 335289)

HIP 103199 (spectral type G5) is listed as runaway star by Tetzlaff et al. (2011). This is based on an estimated age of  $\sim 46 \pm 23$  Myr and the star's space motion. Fujii & Portegies Zwart (2011) hypothesize that such objects are the result of a three-body interaction that results in the formation of a runaway star and a close binary. HIP 103199 has a wide ( $\geq 646$  AU) binary companion found by Lépine & Bongiorno 2007, which we classify as M3.5. We converted our UKIRT photometry

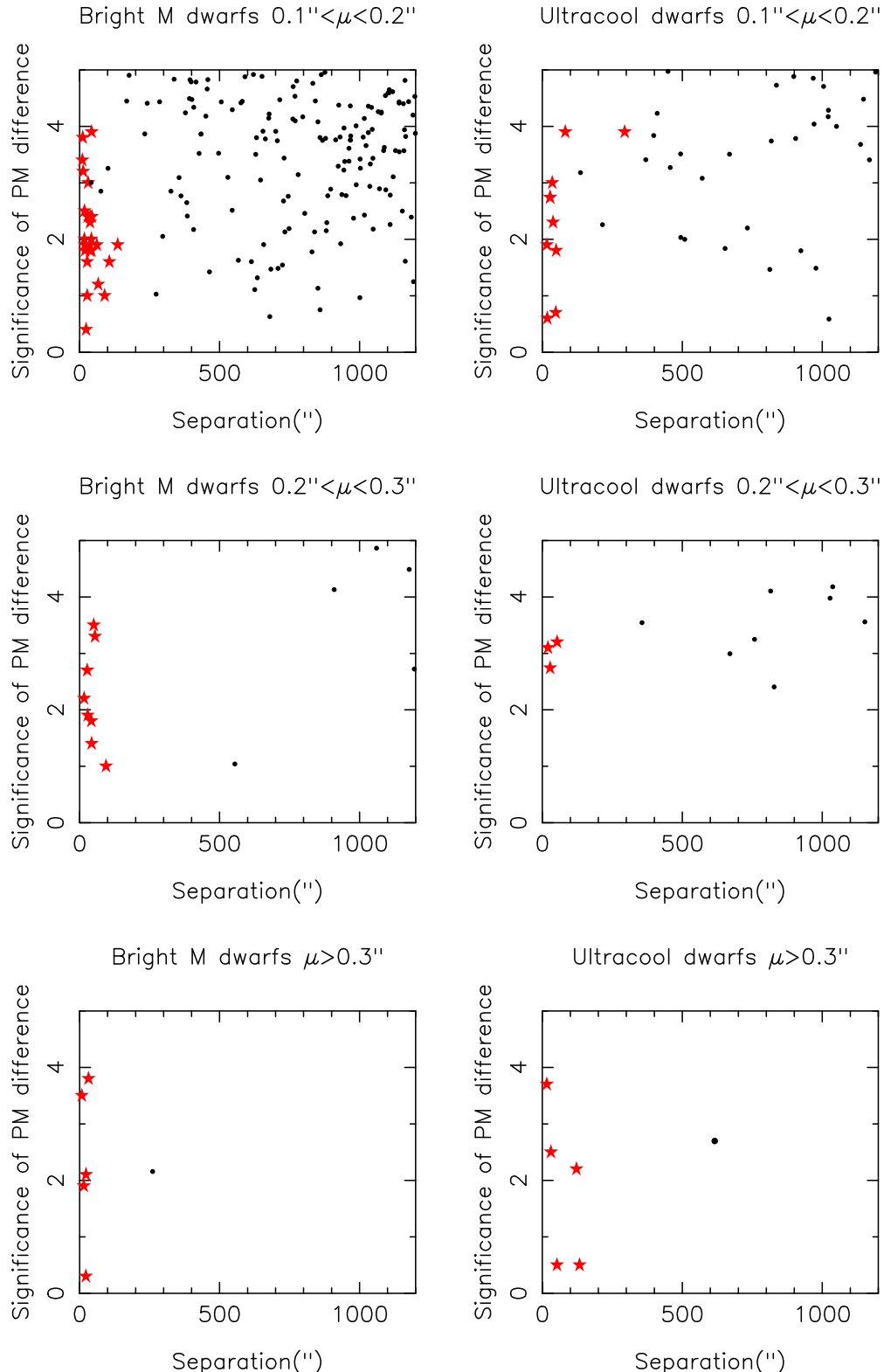


**Figure 8.** Our bright M (left column) and ultracool (right column) dwarf companions to *Hipparcos* stars (red stars) compared to a population of coincident objects (black dots). The coincident objects were generated using a method similar to that of Lépine & Bongiorno (2007) by offsetting the positions of primary stars in our input file and then searching for companions around these positions. The significance of the proper motion difference is the quadrature sum of the proper motion difference in each axis divided by the total proper motion error on that axis (see Equation (1)). Both of our samples lie in areas of the plot that are sparsely populated by coincident pairings.

(A color version of this figure is available in the online journal.)

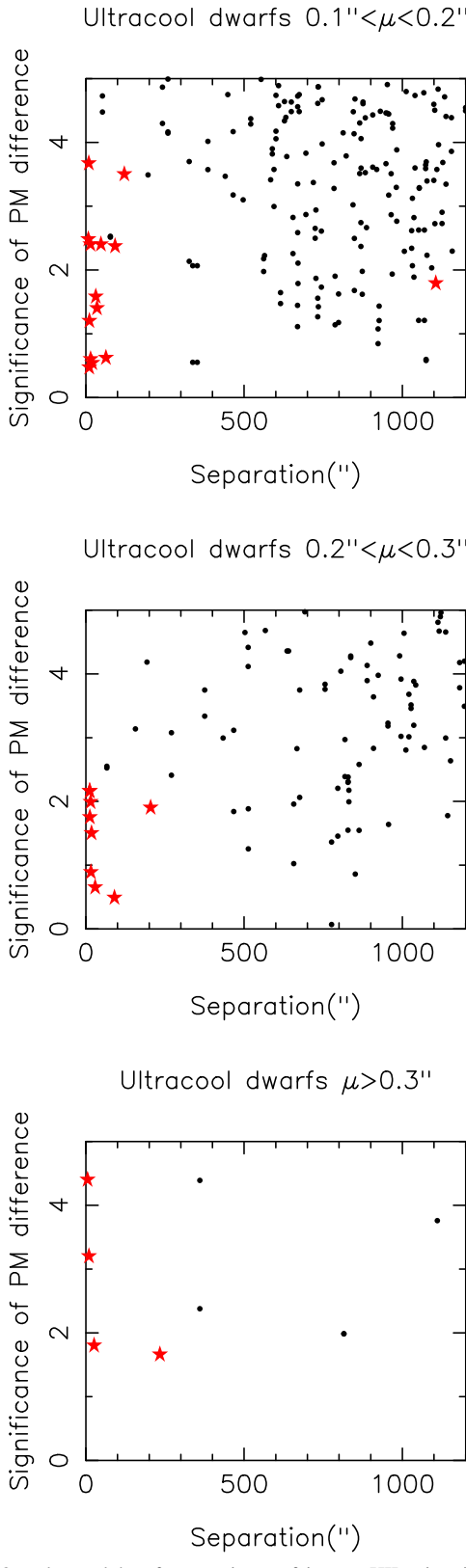


**Figure 9.** Our ultracool dwarf companions to faint non-HIP primaries (denoted by red stars) compared to a coincident population of objects (black dots). See Figure 8 caption for more details on the process. It appears one object, the apparent companion NLTT 35593 ( $\mu = 0.^{\circ}19 \text{ yr}^{-1}$ ), lies in a region inhabited by many coincident pairings. Hence, despite the pair's similar photometric distances, we consider this to be an unlikely companion, i.e., one which should be confirmed through other means.

(A color version of this figure is available in the online journal.)

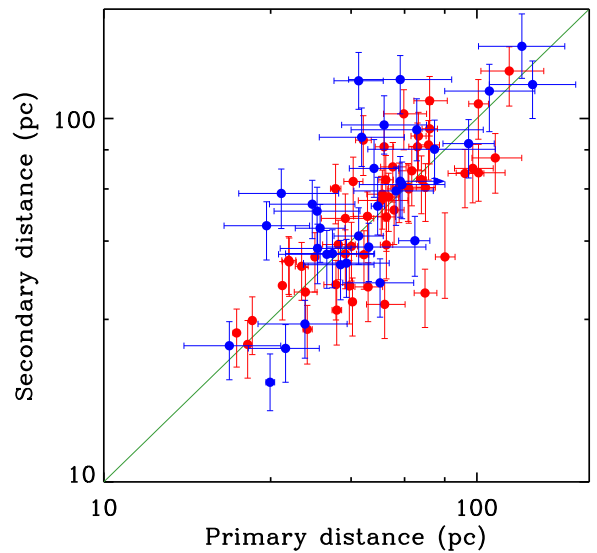


**Figure 10.** Plot of the photometric distances to our secondaries compared to the distances to the primaries. Points plotted in red have trigonometric parallaxes for their primaries, those in blue have photometric distance estimates. Note that one of our objects (HD 253662) is a known subgiant and hence our quoted photometric distance is a lower limit.

(A color version of this figure is available in the online journal.)

to the CIT system using the conversions of Carpenter (2001) in order to calculate the properties of the companion using evolutionary models. Using the *Hipparcos* distance to the primary of  $59.5^{+5.1}_{-4.3}$  pc, we derive an absolute *K*-band magnitude of  $7.42 \pm 0.18$  mag for the companion. Using the evolutionary models of Baraffe et al. (1998) and the spectral-type–effective temperature scale of Kenyon & Hartmann (1995), we derive *K*-band absolute magnitudes of  $6.18 \pm 0.25$  mag at 50 Myr and  $7.16 \pm 0.17$  mag at 300 Myr for an M3.5 where the quoted error is calculated from our half-subtype classification uncertainty. Based on this we suggest that the companion to HIP 103199 (HD 335289) is not overluminous due to youth, and it is likely that this system is not as young as suggested by Tetzlaff et al. (2011).

#### 5.2.5. HIP 60987 *B/C*

During the spectroscopic observations of our companion to HIP 60987 (spectral type M3, separation  $19''$ ), we identified that the primary itself was a visual double. A spectrum of this other companion (spectral type K7, separation  $\sim 5''$ ) was also obtained. As both companions had previous listings in the Washington Double Star catalog, we used the previously existing designations for the companions.

#### 5.2.6. NLTT 38489 *A/B*

The companion to NLTT 38489 stands out as having a photometric distance that is in particularly poor agreement with its primary. However, this object is only  $6.^{\circ}7$  away from its primary. Hence the photometry used to estimate the companion's photometric distance may be unreliable.

#### 5.2.7. LSPM J0241+2553 *A/B*

We do not have a spectrum for LSPM J0241+2553 *A*. To characterize this object we examined its reduced proper motion diagram placement compared to Figure 4 of Limoges et al. (2013) and concluded that this object was likely a white dwarf.

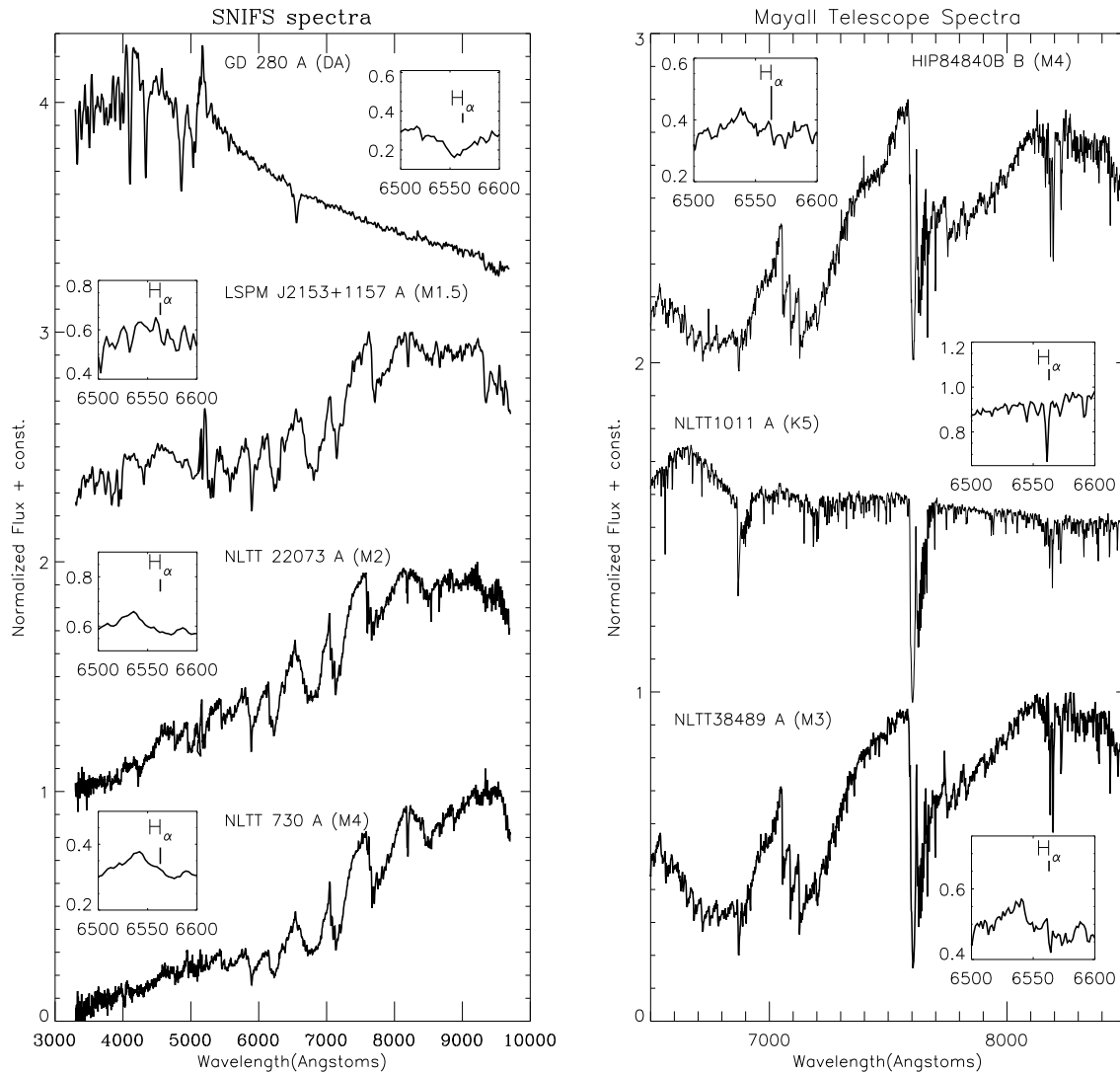


**Figure 11.** Optical spectroscopy of our primary stars and one companion. Left: spectra taken with SNIFS on the University of Hawaii 88 inch telescope on Mauna Kea. Right: spectra taken with the Ritchey–Chretien Spectrograph on the Mayall 4 m telescope on Kitt Peak. The spectra for GD 280 A and LSPM J2153+1157 A were both noisy and so have been Gaussian smoothed to  $R = 300$  to make their spectral features clearer. Note that the feature in the SNIFS spectra at 5200 Å is due to the boundary between the SNIFS red and blue channels. Note that the 7490–7700 Å region is strongly affected by tellurics.

### 5.2.8. HD 253662 A/B

HD 253662 A is listed in SIMBAD as a G8 subgiant. We estimated this object's photometric distance using the same mechanism as for other photometric distances using the G8 spectral type, the object's 2MASS magnitudes, and the absolute magnitudes quoted in Kraus & Hillenbrand (2007). As this object is a subgiant and hence more luminous than the dwarfs used to calibrate the Kraus & Hillenbrand (2007) absolute magnitudes, we quote our  $1\sigma$  lower error bound as a minimum distance.

### 5.2.9. The Possible Companion to NLTT 35593

The candidate companion to NLTT 35593 has a very similar photometric distance ( $65.8 \pm 12.8$  pc) to its primary ( $63.0 \pm 19.1$  pc). However, its wide separation ( $1106''$ ) puts it in a region similar to that in Figure 9 that is populated by chance alignments. Hence we consider it unlikely to be a bona-fide companion. Radial velocity or parallax measurements will be required to assess whether it is a true binary.

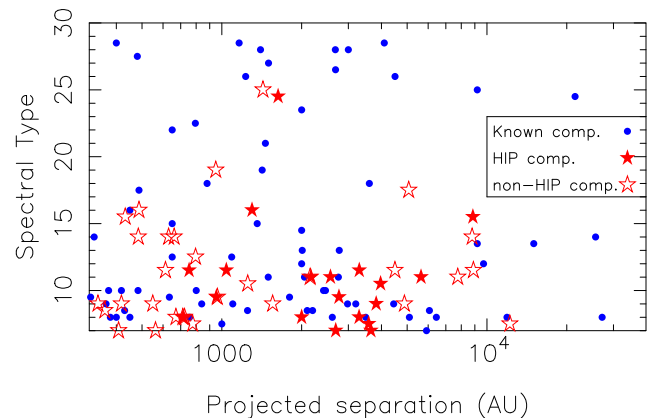


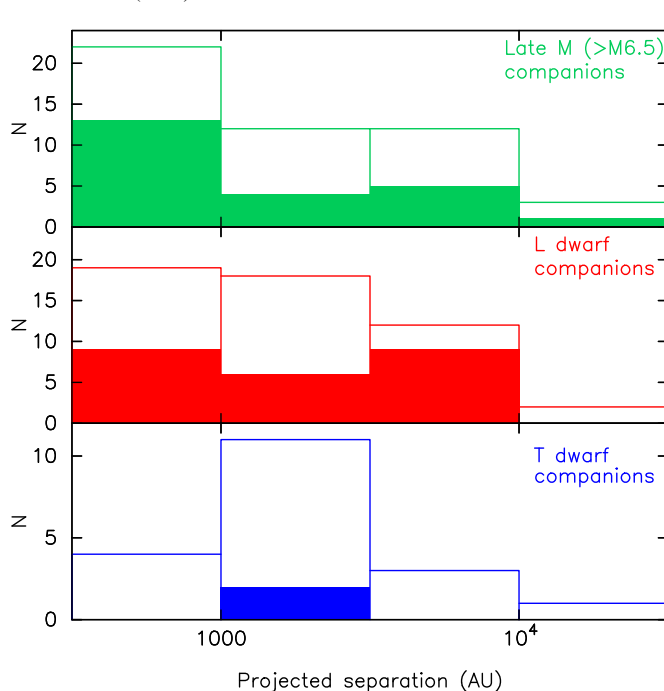
**Figure 12.** Field ultracool binary population (secondary component M7 or later). The y-axis shows the ultracool companion spectral type, which is 0 at M0, 10 at L0, and 20 at T0. The blue dots represent previously identified objects, solid red stars are companions from our *Hipparcos* search, and open red stars are our companions from other sources. Our two T dwarf discoveries from Deacon et al. (2012b) (a *Hipparcos* companion) and Deacon et al. (2012a) (a serendipitous companion discovery) are also plotted here.

(A color version of this figure is available in the online journal.)

**Table 10**  
Data on Our *Hipparcos* Stars

Object	SpT	RV (km s <sup>-1</sup> )	H <sub>p</sub> (mag)	B – V (mag)	[M/H] <sup>k</sup> (dex)	[Fe/H] <sup>e</sup> (dex)	Age (Gyr)	v <sub>tan</sub> (km s <sup>-1</sup> )	U (km s <sup>-1</sup> )	V (km s <sup>-1</sup> )	W (km s <sup>-1</sup> )
HIP 2397	K5 <sup>a</sup>	...	9.34	0.93	...	...	0.5~10 <sup>y</sup>	42.2	...	...	...
HIP 6217	K0 <sup>a</sup>	...	9.116	0.754	...	...	0.4~10 <sup>y*</sup>	58.5	...	...	...
HIP 6407	G5 <sup>a</sup>	...	8.74	0.64	...	-0.084 <sup>u</sup>	0.5~10 <sup>y</sup>	44.9	...	...	...
HIP 9269	G5 <sup>a</sup>	-35.3 ± 0.1 <sup>d</sup>	7.29	0.77	0.15	...	2.2~10.2 <sup>k</sup>	50.7	-10.9	15.8	-57.5
HIP 10033	F8 <sup>a</sup>	-12.9 <sup>f</sup>	7.24	0.5	...	-0.08	2.7~3.7 <sup>e</sup>	34.3	-35.8	6.4	-4.4
HIP 11161	F5 <sup>a</sup>	-41.7 <sup>f</sup>	8.03	0.42	...	-0.23	0.5~2.4 <sup>e</sup>	33.2	-45.1	-17.8	-22.2
HIP 13589	F8 <sup>a</sup>	...	8.8	0.66	...	...	0.4~10 <sup>y</sup>	61.0	...	...	...
HIP 26653	G5 <sup>q</sup>	12.51 ± 0.45 <sup>r</sup>	7.987	0.764	...	-0.07	1.1~9.3 <sup>*e</sup>	18.9	19.0	-9.1	-8.3
	...	...	...	...	-0.1	...	1.6~13.8 <sup>k</sup>				
HIP 32728	G0 <sup>a</sup>	...	9.09	0.66	...	...	0.3~10 <sup>y</sup>	52.3	...	...	...
HIP 37283	F5 <sup>a</sup>	7.0 <sup>f</sup>	7.0	0.47	...	-0.1	0.4~2.1 <sup>e</sup>	21.7	17.0	-6.6	-13.7
HIP 46984	F8 <sup>a</sup>	...	8.81	0.52	...	...	0.4~10 <sup>y</sup>	39.3	...	...	...
HIP 49046	M0 <sup>a</sup>	...	11.31	1.37	...	...	0.3~10 <sup>z</sup>	19.7	...	...	...
HIP 51877	G5 <sup>a</sup>	-46.68 ± 0.25 <sup>t</sup>	8.606	0.724	...	0.22 <sup>u</sup>	2.4~7.5 <sup>s</sup>	17.7	-17.0	-32.1	-45.9
HIP 52463	G4 <sup>a</sup>	12.9 ± 0.2 <sup>f</sup>	8.82	0.64	...	0.14	1.0~4.9 <sup>e</sup>	38.4	37.4	-2.1	15.4
HIP 55666	F5 <sup>a</sup>	-29.3 <sup>f</sup>	7.06	0.54	...	-0.08	3.6~5.1 <sup>e</sup>	29.8	5.9	-3.9	-41.2
HIP 58918	K1 <sup>a</sup>	...	10.79	1.02	...	...	0.1~10 <sup>y</sup>	78.7	...	...	...
HIP 59310	K5 <sup>a</sup>	...	10.19	1.1	...	...	0.2~10 <sup>y</sup>	34.1	...	...	...
HIP 59933	F8 <sup>a</sup>	-3.4 <sup>f</sup>	8.28	0.54	...	0.03	0.3~2.5 <sup>e</sup>	29.4	19.1	-20.7	-9.1
HIP 60501	M0 <sup>a</sup>	...	10.72	1.58	...	...	0.3~10 <sup>z</sup>	36.1	...	...	...
HIP 60987	F2 <sup>a</sup>	...	7.45	0.43	...	-0.12	1.3~2.4 <sup>e</sup>	37.4	...	...	...
HIP 63506	M0 <sup>a</sup>	...	11.37	1.58	...	...	0.3~10 <sup>z</sup>	79.9	...	...	...
HIP 65706	K7 <sup>b</sup>	...	11.22	1.58	...	...	0.3~10 <sup>z</sup>	63.6	...	...	...
HIP 65780	K0 <sup>a</sup>	8.64	0.82	...	...	...	0.5~10 <sup>y</sup>	80.0	...	...	...
HIP 70623	K0 <sup>l</sup>	...	8.96	0.81	0.46	...	3.3~6.0 <sup>k</sup>	73.0	...	...	...
HIP 75310	G5 <sup>a</sup>	17.3 ± 3.9 <sup>f</sup>	8.52	0.64	...	-0.22	6.3~9.3 <sup>e</sup>	49.5	-26.6	-43.2	-13.4
HIP 76456	F5 <sup>a</sup>	-15.7 <sup>f</sup>	6.56	0.433	...	-0.25	0.4~2.2 <sup>e</sup>	18.4	-21.3	11.0	3.0
HIP 76641	G5 <sup>a</sup>	...	8.78	0.658	...	...	0.4~10 <sup>y</sup>	42.1	...	...	...
HIP 78184	M0 <sup>a</sup>	...	10.42	1.27	...	...	0.3~10 <sup>z</sup>	53.3	...	...	...
HIP 78859	G0 <sup>a</sup>	...	8.16	0.57	...	...	0.7~10 <sup>y</sup>	70.3	...	...	...
HIP 78916	G0 <sup>a</sup>	...	8.86	0.599	...	...	0.4~10 <sup>y</sup>	59.1	...	...	...
HIP 78923	G5 <sup>a</sup>	1.2 ± 0.2 <sup>f</sup>	8.69	0.677	...	...	0.4~4.0 <sup>e</sup>	77.2	57.7	-20.5	46.9
HIP 79180	K7 <sup>a</sup>	-26.2 ± 0.5 <sup>h</sup>	9.38	0.74	...	...	0.3~10 <sup>z</sup>	97.0	-99.3	-12.8	-8.1
HIP 80258	K3 <sup>a</sup>	...	10.85	0.97	...	...	0.1~10 <sup>y</sup>	69.9	...	...	...
HIP 81910	G2 <sup>a</sup>	47.9 <sup>f</sup>	6.86	0.67	0.16	0.19	4.0~5.8 <sup>e</sup>	23.0	-46.7	-25.4	-0.5
	...	...	...	...	...	...	3.2~5.0 <sup>k</sup>				
HIP 82233	G2 <sup>a</sup>	57.4 <sup>f</sup>	7.55	0.57	...	-0.05	0.7~4.7 <sup>e</sup>	23.9	-62.0	-2.2	-4.0
	...	...	...	...	...	...	3.8~12.0 <sup>w</sup>				
HIP 83651	K5 <sup>m</sup>	...	10.6	1.21	...	...	0.1~10 <sup>y</sup>	47.5	...	...	...
HIP 84840	G1.5 <sup>m</sup>	...	10.0	0.80	...	...	0.1~10 <sup>y</sup>	20.3	...	...	...
HIP 85365	F3 <sup>a</sup>	0.4 <sup>f</sup>	4.62	0.38	...	-0.09	1.6~1.9 <sup>*</sup>	14.6	-1.9	-12.0	8.1
HIP 86722	K0 <sup>a</sup>	26.5 <sup>f</sup>	7.64	0.75	...	-0.33	3.0~11.8 <sup>e*</sup>	67.8	-68.1	-25.8	0.3
HIP 88728	F5 <sup>a</sup>	16.2 ± 0.5	7.08	0.51	...	-0.1 <sup>x</sup>	1.5~10 <sup>y</sup>	29.6	-29.7	-6.32	-14.8
HIP 90273	K7 <sup>b</sup>	...	11.87	1.51	...	...	0.3~10 <sup>z</sup>	67.5	...	...	...
HIP 90869	G2 <sup>a</sup>	31.0 <sup>f</sup>	8.07	0.58	...	-0.46	5.3~10.8 <sup>e</sup>	50.4	-38.9	-41.8	15.6
	...	...	...	...	...	...	1.9~5.7 <sup>k</sup>				
HIP 93967	F9 <sup>a</sup>	...	9.74	0.61	...	...	0.2~10 <sup>y</sup>	180.5	...	...	...
HIP 97168	G4 <sup>m</sup>	...	10.51	0.88	...	...	0.1~10 <sup>y</sup>	85.9	...	...	...
HIP 98535	F5 <sup>a</sup>	-4.9 <sup>f</sup>	8.16	0.77	...	-0.02	10.6~13.16 <sup>e</sup>	42.0	-38.5	-12.0	12.9
HIP 102582	K2 <sup>a</sup>	61.3 ± 9.8 <sup>o</sup>	9.86	1.032	...	...	0.2~10 <sup>y</sup>	88.9	-74.9	-4.1	-77.6
HIP 103199	G5 <sup>a</sup>	...	9.82	0.84	...	...	0.2~10 <sup>y</sup>	45.2	...	...	...
HIP 105202	F5 <sup>a</sup>	-1.1 <sup>f</sup>	7.38	0.49	...	-0.29	0.6~2.9 <sup>e</sup>	29.6	15.9	-6.6	-24.2
HIP 106551	K3III <sup>a</sup>	-68.1 ± 0.1 <sup>i</sup>	5.04	1.09	...	...	≤10 <sup>aa</sup>	50.3	-23.4	43.3	-39.9
HIP 108822	K7 <sup>m</sup>	...	12.11	0.0	...	...	0.3~10 <sup>z</sup>	74.8	...	...	...
HIP 109454	F5 <sup>a</sup>	6.6 <sup>f</sup>	8.05	0.41	...	-0.19	1.4~2.1 <sup>e</sup>	54.7	-52.9	-1.8	-15.4
HIP 111657	K7 <sup>c</sup>	...	10.69	1.27	...	...	0.3~10 <sup>z</sup>	61.6	...	...	...
HIP 112422	K2 <sup>a</sup>	...	10.33	0.94	...	...	0.1~10 <sup>y*</sup>	46.8	...	...	...
HIP 114424	G0 <sup>a</sup>	1.7 <sup>f</sup>	7.45	0.6	0.06	0.08	0.6~4.5 <sup>e</sup>	32.3	9.1	-25.3	-18.0
	...	...	...	...	...	...	3.7~11.7 <sup>k</sup>				
HIP 114456	K0 <sup>a</sup>	...	7.12	0.75	0.19	...	2.1~9.6 <sup>k</sup>	34.6	...	...	...
HIP 115819	K5 <sup>a</sup>	-4.3 ± 1.8 <sup>j</sup>	10.45	1.27	...	...	0.2~10 <sup>y</sup>	148.5	146.8	-7.8	-21.6
HIP 116052	G5 <sup>a</sup>	...	9.33	0.8	...	...	0.3~10 <sup>y</sup>	44.9	...	...	...

**Table 10**  
(Continued)

**Notes.**<sup>a</sup> SIMBAD.<sup>b</sup> Estimated from  $V - J$  color and the relations of Lépine & Gaidos (2011).<sup>c</sup> Estimated from 2MASS photometry and the SEDs of Kraus & Hillenbrand (2007).<sup>d</sup> Maldonado et al. (2010).<sup>e</sup> Casagrande et al. (2011), quoted age is the 16–84 percentile range.<sup>f</sup> Nordstrom et al. (2004).<sup>g</sup> Evans (1967).<sup>h</sup> Latham et al. (2002).<sup>i</sup> Massarotti et al. (2008).<sup>j</sup> Bilir et al. (2005).<sup>k</sup> Valenti & Fischer (2005).<sup>l</sup> Howard et al. (2010).<sup>m</sup> This work.<sup>n</sup> Latham (2004).<sup>o</sup> Dawson & De Robertis (2005).<sup>p</sup> Wielen et al. (2000).<sup>q</sup> Montes et al. (2001).<sup>r</sup> White et al. (2007).<sup>s</sup> Isaacson & Fischer (2010); note the age quoted in the source does not give a range of values. We obtained a range of values by taking the quoted age and applying the 0.25 dex scatter to the age–activity relation found by Mamajek & Hillenbrand (2008).<sup>t</sup> Chubak & Marcy (2011).<sup>u</sup> Robinson et al. (2007).<sup>v</sup> Ramírez et al. (2009).<sup>w</sup> Calculated from the Mamajek & Hillenbrand (2008) Ca H&K activity to age relation using the activity measurement of Arriagada (2011).<sup>x</sup> Metallicity from Lee et al. (2011).<sup>y</sup> This work; minimum age calculated from limiting X-ray flux and the relations of Mamajek & Hillenbrand (2008); approximate maximum age from disk-like kinematics.<sup>z</sup> This work; minimum age is that from Shkolnik et al. (2009) for objects with no X-ray emission; approximate maximum age from disk-like kinematics.<sup>aa</sup> This work; approximate maximum age from disk-like kinematics.<sup>bb</sup> Gontcharov (2006).

**Figure 13.** Histograms showing the projected separations of the wide ( $>100$  AU) companion population. The top panel shows M7, M8, and M9 dwarfs; the middle panel L dwarfs; and the lower panel T dwarfs. For each spectral bin, the open histogram is the total population and the solid histogram is the contribution from our PS1-based efforts (this paper; Deacon et al. 2012a, 2012b).

(A color version of this figure is available in the online journal.)

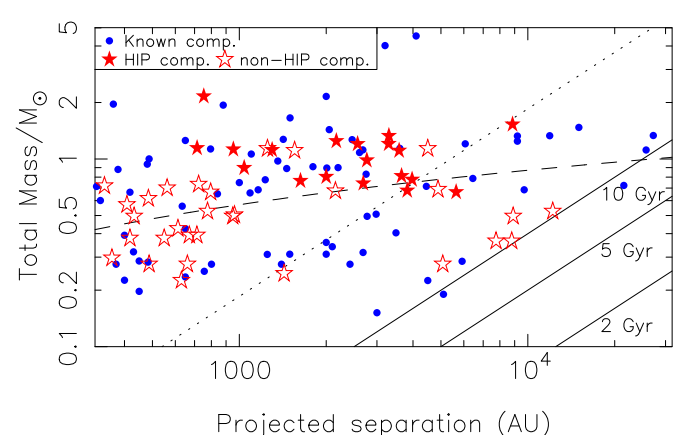


**Figure 14.** Total mass vs. separation for binary systems with at least one ultracool dwarf component from the literature and from our discoveries. The plot symbols are the same as Figure 12. In cases where we did not have an estimated mass for a substellar companion, we used a mass of  $0.075 M_{\odot}$ . Hence these are upper limits on the total mass. All other masses are derived from the literature or from the spectral type to mass relation from Kraus & Hillenbrand (2007). The dotted line represents the approximate maximum separation (equivalent to  $v_{\text{esc}} = 0.57 \text{ km s}^{-1}$ ) suggested by Close et al. (2003) while the dashed line is the suggested log-normal maximum separation suggested by Reid et al. (2001). The three solid lines are the typical separations beyond which a binary is expected to be broken up by interactions in the Galactic disk over the course of 2, 5, and 10 Gyr (Dhital et al. 2010).

(A color version of this figure is available in the online journal.)

**Table 11**  
Data on Our other Primary Stars

Object	SpT	V (mag.)	V – J (mag.)	Distance (pc.)	$\mu_\alpha \cos \delta$ (as yr $^{-1}$ )	$\mu_\delta$ (as yr $^{-1}$ )	Age (Gyr)	[M/H] (dex)	$v_{\tan}$ (km s $^{-1}$ )
Other Companion Discoveries									
NLTT 1011	K5 <sup>b</sup>	11.13	2.0	68.2 $^{+6.6}_{-6.5}$	-0.076	-0.192	0.3– $\sim 10^i$	...	66.8
GD 280	DA <sup>b</sup>	16.69	0.02	77 $^{+35}_{-26}$	0.169	-0.055	<10 <sup>k</sup>	...	
NLTT 8245	M0 <sup>c</sup>	12.63	2.98	53.0 $^{+8.7}_{-7.5}$	-0.093	-0.164	0.3– $\sim 10^i$	...	47.4
LSPM J0241+2553	WD <sup>l</sup>	18.19	1.19	69 $^{+35}_{-23}$	-0.037	-0.153	<10 <sup>k</sup>	...	
HD 253662	G8IV <sup>d</sup>	9.92	1.36	>62.3	-0.013	-0.164	0.3–<10 <sup>k</sup>	...	
LSPM J0632+5053	G2 <sup>b</sup>	9.87	1.26	95.0 $^{+16.3}_{-13.9}$	0.035	-0.154	0.2– $\sim 10^g$	...	71.1
NLTT 18587	M2 <sup>c</sup>	16.07	3.56	132 $^{+40}_{-31}$	0.177	-0.109	0.3– $\sim 10^i$	...	130
NLTT 19109	M4 <sup>c</sup>	17.8	4.33	132 $^{+49}_{-36}$	0.035	-0.165	0.3– $\sim 10^i$	...	106
NLTT 22073	M2 <sup>b</sup>	12.51	3.43	29.9 $^{+12.7}_{-6.9}$	-0.315	0.16	0.4– $\sim 10^h$	0.06 <sup>b</sup>	50.1
NLTT 23716	K7 <sup>c</sup>	11.84	2.70	48.2 $^{+7.9}_{-6.8}$	0.060	-0.277	0.3– $\sim 10^i$	...	64.8
NLTT 26746	M4 <sup>b</sup>	15.68	4.55	41.0 $^{+12.2}_{-10.3}$	-0.251	-0.147	0.3– $\sim 10^i$	...	56.5
NLTT 29395	M3 <sup>c</sup>	15.00	3.87	56.4 $^{+16.9}_{-13.0}$	0.165	-0.112	0.3– $\sim 10^i$	...	53.3
NLTT 30510	M2 <sup>c</sup>	14.17	3.66	49.1 $^{+14.8}_{-11.3}$	0.218	-0.390	0.3– $\sim 10^i$	...	104
NLTT 31450	M4 <sup>b</sup>	14.93	4.15	34.6 $^{+10.3}_{-8.7}$	-0.034	-0.202	0.3– $\sim 10^i$	...	33.6
PMI 13410+0542	M1 <sup>c</sup>	13.13	3.21	51.3 $^{+21.7}_{-11.8}$	0.047	-0.014	0.3– $\sim 10^i$	...	11.9
PMI 13518+4157	M2.5 <sup>b</sup>	13.93	4.04	43.1 $^{+9.9}_{-8.8}$	-0.059	-0.058	0.3– $\sim 10^i$	...	16.9
NLTT 38489	M3 <sup>b</sup>	16.05	4.22	62.3 $^{+23.3}_{-17.0}$	-0.147	0.183	1.2– $\sim 10^h$	...	69.3
NLTT 39312	M2 <sup>c</sup>	16.37	3.63	141 $^{+43}_{-33}$	-0.025	-0.347	0.3– $\sim 10^i$	...	232.4
LSPM J1627+3328	K7 <sup>d</sup>	11.55	2.73	38.0 $^{+6.3}_{-5.4}$	-0.171	-0.014	0.3– $\sim 10^i$	...	30.9
NLTT 44368	M3 <sup>b</sup>	13.17	2.78	55.0 $^{+12.7}_{-11.2}$	-0.056	0.215	0.3– $\sim 10^i$	...	57.9
LSPM J1717+5925	G6 <sup>f</sup>	10.52	1.36	108 $^{+35}_{-26}$	-0.090	-0.15	0.2– $\sim 10^g$	...	89.5
NLTT 52268	M3 <sup>c</sup>	14.36	3.97	37.3 $^{+11.3}_{-8.7}$	0.16	-0.089	0.3– $\sim 10^i$	...	32.4
LSPM J2153+1157	M1.5 <sup>b</sup>	13.9	3.82	36.2 $^{+10.9}_{-8.4}$	-0.093	-0.128	0.3– $\sim 10^i$	0.26 <sup>b</sup>	27.1
PM I22118–1005	M2 <sup>b</sup>	12.87	3.25	37.4 $^{+8.6}_{-7.7}$	0.028	-0.25	0.3– $\sim 10^i$	...	44.6
NLTT 55219	M2 <sup>c</sup>	13.93	3.65	44.7 $^{+13.5}_{-10.4}$	0.324	0.16	0.3– $\sim 10^i$	...	76.6
Serendipitous Companion Discoveries									
NLTT 730	M4 <sup>b</sup>	15.46	4.37	21.7 $^{+8.1}_{-5.3}$	0.375	-0.234	3– $\sim 10^i$	-0.15 <sup>b</sup>	84.2
NLTT 27966	M5 <sup>b</sup>	16.53	4.51	39.6 $^{+13.3}_{-10.2}$	-0.153	0.182	0.3– $\sim 10^i$	...	31.7
LSPM J1336+2541	M3 <sup>b</sup>	14.73	3.55	60.7 $^{+15.7}_{-13.9}$	-0.157	0.057	0.3– $\sim 10^i$	...	48.1
HIP 73169	M0 <sup>e</sup>	11.96	3.01	27.3 $^{+8.3}_{-6.3}$	-0.267	-0.076	0.3– $\sim 10^i$	...	36.0
PM I23492+3458	M2 <sup>b</sup>	12.73	3.6	30.7 $^{+7.1}_{-6.3}$	-0.011	-0.108	0.3– $\sim 10^i$	...	15.8
Unlikely Companions									
NLTT 35593	M2 <sup>c</sup>	14.57	3.6	63.0 $^{+19.1}_{-14.6}$	-0.1837	-0.0548	0.3– $\sim 10^i$	...	57.3

**Notes.**

- <sup>a</sup> Approximate spectral type based on 2MASS photometry and the SEDs from Kraus & Hillenbrand (2007).
- <sup>b</sup> This work.
- <sup>c</sup> Based on V – J color and the relations presented in Lépine & Gaidos (2011).
- <sup>d</sup> SIMBAD.
- <sup>e</sup> Gray et al. (2006).
- <sup>f</sup> Hovhannisyan et al. (2009).
- <sup>g</sup> This work; minimum age calculated from limiting X-ray flux and the relations of Mamajek & Hillenbrand (2008); approximate maximum age from disk-like kinematics.
- <sup>h</sup> This work; minimum age calculated from lack of activity and the activity lifetimes of West et al. (2008); approximate maximum age from disk-like kinematics.
- <sup>i</sup> This work; minimum age is that from Shkolnik et al. (2009) for objects with no X-ray emission; approximate maximum age from disk-like kinematics.
- <sup>j</sup> No 2MASS photometry; approximate V – J calculated from optical photometry by Lépine & Shara (2005).
- <sup>k</sup> This work; approximate maximum age from disk-like kinematics.
- <sup>l</sup> This work; based on reduced proper motion diagram placement.

**Table 12**  
Known Companions with Spectral Type M7 or Later that have Projected Separations of 100 AU or More

Object	Position (J2000)	Separation		SpT Companion	SpT Primary	Companion Mass ( $M_{\odot}$ )	Age (Gyr)	References
		(AU)	(")					
2MASS J1258+4013 B	12 58 37.98 +40 14 01.7	6700	63	M7	M6	0.086–0.105	1–5	1
GG Tau Bb	04 32 30.31 +17 31 29.9 <sup>o</sup>	210	1.5	M7	K7+M0.5+M5	0.038–0.05	0.01–0.02	2
HD 65216 B	07 53 42.55 –63 38 51.5 <sup>p</sup>	253	7.0	M7	G5	0.09	3–6	3
C				L2		0.078		
$\eta$ Tel B	19 22 51.26 –54 25 30.7	190	4.2	M7/8	A0V	<0.04	0.0017–0.025 <sup>a</sup>	4
G121–42 B	12 00 32.92 +20 48 51.3 <sup>q</sup>	5916	204.0	M7	M4	<0.085	4.0–5.0	5
USco 1602–2401	16 02 51.17 –24 01 50.5	1000	7.0	M7.5	K4	0.029–0.067	0.010–0.013 <sup>k</sup>	65
TWA 5 B	11 31 55.4 –34 36 29	100	2.0	M8	M1.5	~0.02	0.01–0.3	6
LP 213–68 Ba	10 47 12.65 +40 26 43.7 <sup>r</sup>	230	14	M8	M6.5	0.080–0.101	...	7, 8
Bb				L1		0.068–0.090		
HII 1348 B	03 47 18.04 +24 23 25.73 <sup>t</sup>	132	1.1	M8	K5*	0.053–0.055	0.100–0.125	73
BD+13 1727 B	07 39 43.86 +13 05 07.1	380	10.5	M8+L0.5	K5	...	...	9
V1428 Aql B	19 16 57.62 +05 09 02.2 <sup>r</sup>	400	75	M8	M3	...	...	10
LP 655–23 B	04 30 51.58 –08 49 00.8	450	20	M8	M4	0.082–0.090	1–8	11, 12
2MASS J0126–5022 B	01 27 02.83 –50 23 21.1	5100	82.0	M8	M6.5	0.062–0.100 <sup>b</sup>	>0.2 <sup>b</sup>	13, 14
HD 221356 B	23 31 01.616 –04 06 19.39	11900	452	M8	F8	0.088	5.5–8	11
C				L3		0.072		
HD 221356 D	23 31 30.95 –04 05 23.4	2050	12.13	L1	F8+M8+L3	0.073–0.085	2.5–7.9	29
G 266–33 B	00 03 42.27 –28 22 41.0	2610	66.0	M8	G8	0.1–0.103	0.9–1.4	5
G 63–23 B	13 20 41.59 +09 57 50.6	6445	169.0	M8	K5	0.083–0.093	0.5–3.0	5
NLTT 29131 B	11 58 24.04 –01 22 45.5	3490	26.8	M8 <sup>v</sup>	M4	...	...	77
LSPM J1202+0742 C <sup>x</sup>	12 01 59.65 +07 35 53.6	27200	446	M8 <sup>v</sup>	M0 <sup>y</sup> +M1 <sup>y</sup>	...	...	77
SDSS J163126.17+294847.1 B	16 31 26.17 +29 48 36.9 <sup>r</sup>	756	10.1	M8	M5.5	...	...	15
ULAS J132835.49+080819.5 B	13 28 34.69 +08 08 18.9	1250	11.9	M6	M8.5 <sup>w</sup>	...	...	77
LSPM J2010+0632 B	20 10 35.39 +06 34 36.7	2100	143	M8.5	M3.5	...	...	16
HD 212168 C	22 26 44.3 –75 03 42	6070	265	M8.5	G0	0.09–0.1	...	17
APMMP J2354–3316 C	23 54 09.29 –33 16 26.6 <sup>r</sup>	2200	8.0	M8.5	DA+M4	0.10	~1.8	18
USco 1612–1800	16 12 48.97 –18 00 49.6	430	3.0	M8.5	M3	0.019–0.042	0.010–0.013 <sup>k</sup>	65
2MASS J00301179–3740483 B	00 30 06.26 –37 39 48.3 <sup>r</sup>	89	4450	DA	M9	0.07–0.08	>1.9	75
USco 1610–1913 B	16 10 32.33 –19 13 08.67	840	5.8	M9	K7	0.017–0.027	0.010–0.013 <sup>k</sup>	65
HIP 77900 B	15 54 30.47 –27 19 57.51	3200	21.8	M9	B6	0.017–0.027	0.010–0.013 <sup>k</sup>	65
GSC 08047–00232 C	01 52 14.63 –52 19 30.0 <sup>o</sup>	200	3.2	M9	M0.5+K3	0.015–0.035 <sup>c</sup>	0.01–0.04	19
NLTT 22980 B	09 56 13.13 +01 45 14.3 <sup>r</sup>	2980	30.4	M9	M2	...	...	15
HR 6037 B	16 17 04.35 –67 56 26.3	366.0	6.7	M9	A6	0.42–0.82	0.2–0.4	20
SR 12 C	16 27 19.51 –24 41 40.4 <sup>u</sup>	1100	8	M9 <sup>m</sup>	K4+M2.5	0.012–0.015	~0.002	70
GSC 06214–210 B	16 21 54.67 –20 43 11.3 <sup>r</sup>	320	12.9	M9.5 <sup>n</sup>	K5	0.012–0.016	~0.005	69
G216–7 C	22 37 32.556 +39 22 39.81	634	33.6	M9.5	M3.5+M3.5	0.06–0.08	1–10	21
LEHPM 494 B	00 21 05.90 –42 44 43.3 <sup>r</sup>	1800	78	M9.5	M6	0.075–0.083	2–10	11
DENIS J0551–4434 B	05 51 46.05 –44 34 11.0 <sup>o</sup>	220	2.2	L0	M8.5	~0.06 <sup>o</sup>	0.1–10	22
Denis-P J1347–7610 B	13 47 59.11 –76 10 05.4 <sup>r</sup>	418	16.8	L0	M0	...	0.2–1.4	23
HD 89744 B	10 22 14.89 +41 14 26.7 <sup>r</sup>	2460	63	L0	F7	0.077–0.080	1.5–3	24
NLTT 2274 B	00 41 54.54 +13 41 35.5	483.0	23.0	L0	M4	0.081–0.083	4.5–10.0	5
LP 312–49 B	08 58 36.97 +27 10 50.8	801	15.4	L0	M4	...	...	15
SDSS J130432.93+090713.7 B	13 04 33.16 +09 07 06.9	374	7.6	L0	M4.5	...	...	15
SDSS J163814.32+321133.5 B	16 38 17.31 +32 11 44.1	2420	46.0	L0	M4	...	...	15
1RXS J235133.3+312720 B	23 51 33.48 +31 27 22.9 <sup>r</sup>	120	2.4	L0	M2	0.026–0.038	0.05–0.15	71
GJ 1048 B	02 35 59.93 –23 31 20.5 <sup>r</sup>	250	11.9	L1	K2	0.055–0.075	0.6–2	25
AB Pic B	06 19 12.94 –58 03 20.9 <sup>s</sup>	275	5.5	L1	K2	~0.01	~0.03 <sup>e</sup>	26
G124–62 Ba	14 41 37.167 –09 45 59.0 <sup>r</sup>	1496	44.0	L1	dM4.5e	0.054–0.082	0.5–0.8	27
Bb				L1 <sup>f</sup>		0.054–0.082		
GQ Lup B	15 49 12.09 –35 39 03.9 <sup>o</sup>	103	0.7	L1	K7	0.010–0.020 <sup>g</sup>	< 0.002	28
ROX 42B b	16 10 31.98 –19 13 04.4 <sup>r</sup>	140	1.8	L1 <sup>m</sup>	M1	0.006–0.014	0.0015–0.003	68, 79
G 255–24 B	13 32 45.31 +74 59 44.2	9710	38.3	L2	K8	...	0.2–10.0	30
2MASS J05254550–7425263 B	05 25 38.76 –74 26 00.8	2000	44	L2	M3	0.06–0.075	1.0–10.0	31
G196–3 B	10 04 20.67 +50 22 59.6 <sup>r</sup>	300	16.2	L2	M2.5	0.015–0.04	0.06–0.3	32
Gl 618.1 B	16 20 26.147 –04 16 31.55	1090	35	L2.5	M0	0.06–0.079	0.5–12	24
HD 106906 b	12 17 52.53 –55 58 27.3 <sup>r</sup>	650	7.1	L2.5	F5	0.003–0.007	0.013–0.015 <sup>k</sup>	66
G 63–33 B	13 20 44.27 +04 09 04.5	2010	66	L3	K2	0.079–0.081	3.3–5.1	5
G 73–26 B	02 07 35.60 +13 55 56.3	2774	73	L3	M2	0.079–0.081	3.0–4.0	5/15
eta Cancri B	08 32 31.87 +20 27 00.0	15020	164	L3.5	K3III	0.063–0.082	2.2–6.1	15
G 171–58 B	00 25 03.65 +47 59 19.1	9200	218	L4	F8	0.045–0.083	1.8–3.5	5
G 200–28 B	14 16 59.78 +50 06 26.4	25700	570	L4	G5	0.077–0.078	7.0–12.0	5
LHS 5166 B	10 18 18.74 +59 09 53.7 <sup>r</sup>	160	8.43	L4	M4.5	0.055–0.075	2.6–8	27
1RXS J1609–2105 b	16 09 30.37 –21 04 56.9 <sup>r</sup>	330	2.2	L4 <sup>l</sup>	M0	0.009–0.016	0.010–0.013 <sup>k</sup>	67
GJ 1001 B	00 04 34.85 –40 44 05.9	180	18.6	L4.5	M4	0.060–0.075	1–10	33, 34, 35

**Table 12**  
(Continued)

Object	Position (J2000)	Separation		SpT Companion	SpT Primary	Companion Mass ( $M_{\odot}$ )	Age (Gyr)	References
		(AU)	( $''$ )					
C				L4.5		0.060–0.075		
Gl 417 Bab	11 12 25.674 +35 48 13.17 <sup>r</sup>	2000	90.0	L4.5+L6 <sup>g</sup>	G0+G0	0.02–0.05 <sup>‡</sup>	0.08–0.3	34, 36
G203–50 B	17 11 45.59 +40 28 57.8 <sup>r</sup>	135	6.4	L5.0	M4.5	0.051–0.074	1–5	37
GJ 499 B	13 05 41.07 +20 46 39.4	1360	516	L5	K5+M4	...	3.5–10.0	30
G 259–20 B	17 43 08.60 +85 26 59.4	650	30	L5	M2.5	...	...	16
LP 261–75 B	09 51 05.49 +35 58 02.1 <sup>r</sup>	450	13.0	L6	M4.5	0.019–0.025	0.1–0.2	38
2MASS J01303563–4445411 B	01 30 35.80 –44 45 41.4	130	3.28	L6	M9	0.032–0.076	0.25–0.8	39
HD 203030 B	21 18 58.97 +26 13 46.1 <sup>s</sup>	487	11.0	L7.5	G8	0.012–0.031	0.13–0.4	42
Gl 337 CD	09 12 14.69 +14 59 39.6 <sup>r</sup>	43	L8+ $\geq$ L8	G8+K1	0.04–0.074 <sup>‡</sup>	0.6–3.4	24, 43	
Gl 584 C	15 23 22.63 +30 14 56.2 <sup>r</sup>	3600	194	L8	G1	0.045–0.075	1–2.5	44
HD 46588 B	06 46 27.56 +79 35 04.5 <sup>r</sup>	1420	79.2	L9	F7	0.045–0.072	1.3–4.3	45
$\epsilon$ Indi Ba	22 04 10.52 –56 46 57. <sup>r</sup>	1460	402.0	T1	K5	0.060–0.073 <sup>i</sup>	$\sim$ 5 <sup>h</sup>	46, 47
Bb				T6		0.047–0.060 <sup>h</sup>	0.5–7.0 <sup>z</sup>	
2MASS J111806.99–064007.8 B	11 18 07.130 –06 40 15.82	650	7.7	T2	M4.5	0.06–0.07–6.0	...	48
HN Peg B	21 44 28.47 +14 46 07.8 <sup>r</sup>	795	43	T2.5	G0	0.012–0.030	0.1–0.5	49
GU Psc B	01 12 36.48 +17 04 31.8	2000	41.97	T3.5	M3	0.07–0.13	0.009–0.013	76
HIP 38939 B	07 58 01.61 –25 39 01.4	1630	88	T4.5	K4	0.018–0.058	0.3–2.8	50
LSPM J1459+0851 B	14 59 35.30 +08 57 51.6	21500	365	T4.5	DA	0.064–0.075	4–10	74
LHS 2803 B	13 48 02.90 –13 44 07.1	1400	67.6	T5	M4.5	0.068–0.081	3.5–10	51, 31
HD 118865 B	13 39 43.79 +01 04 36.4	9200	148	T5	F5	...	1.5–4.9	52
HIP 73786 B	15 04 57.66 +05 38 00.8	1230	63.8	T6	K5	...	>1.6	53, 54
LHS 302 B	11 22 54.73 +25 50 21.5	4500	265	T6	M5	...	...	55
G 204–39 B	17 58 05.46 +46 33 09. <sup>r</sup>	2685	198	T6.5	M3	0.02–0.035	0.5–3.0	5
Gl 570 D	14 57 14.96 –21 21 47.8 <sup>r</sup>	1500	258	T7	K4+M1.5+M3	0.03–0.07	2–5	56
HD 3651 B	00 39 18.91 +21 15 16.8 <sup>r</sup>	480	43	T7.5	K0	0.018–0.058 <sup>j</sup>	0.7–4.7	49, 57
SDSS J1416+30 B	14 16 23.94 +13 48 36.3	45–135	9.0	T7.5	L6p	0.03–0.04	$\sim$ 10	58, 59, 60
LHS 2907 B	14 23 20.86 +01 16 38.1	2680	156	T8	G1	0.019–0.047	2.3–14.4	16, 61
LHS 6176 B	09 50 47.28 +01 17 34.3	1400	52	T8	M4	...	>3.5	16, 52
Wolf 1130 B	20 05 20.38 +54 24 33.9	3000	188.5	T8	sd M1.5+DA	0.020–0.050	>2	72
Ross 458 C	13 00 41.73 +12 21 14.7	1162	102	T8.5	M0.5+M7	0.005–0.0014	<1.0	62
$\xi$ UMa E	11 18 38.70 +31 25 37.9	4100	510	T8.5	F9+G0 <sup>†</sup>	0.014–0.038	4.0–8.0	63
Wolf 940 B	21 46 38.83 –00 10 38.7	400	32	T8.5	M4	0.02–0.032	3.5–6	64
WD 0806–661	08 07 14.68 –66 18 48.7	2500	130	>Y0	DQ	0.03–0.10	1.2–2	78

**Notes.** Based on Table 1 from Faherty et al. (2010). This only contains objects that are spectrally confirmed companions. We do not include untyped candidate companions but make an exception for the Y dwarf companion to WD 0806–661 (Luhman et al. 2011), which is too faint in the near-infrared for spectral confirmation.

<sup>a</sup> Binks & Jeffries (2014).

<sup>b</sup> Artigau et al. (2009).

<sup>c</sup> Chauvin et al. (2005b).

<sup>e</sup> Mass calculated by Faherty et al. (2010), Faherty private communication.

<sup>e</sup> Song et al. (2003).

<sup>f</sup> Reid et al. (2008).

<sup>g</sup> Burgasser et al. (2005).

<sup>h</sup> Marois et al. (2007).

<sup>i</sup> King et al. (2010).

<sup>j</sup> Liu et al. (2007).

<sup>k</sup> Pecaut et al. (2012).

<sup>l</sup> Lafrenière et al. (2010).

<sup>m</sup> Bowler et al. (2014).

<sup>n</sup> Bowler et al. (2011).

<sup>o</sup> Position from SIMBAD.

<sup>p</sup> Position from Washington Double Star Catalogue.

<sup>q</sup> Position from Webb et al. (1999).

<sup>r</sup> Position from 2MASS.

<sup>s</sup> Position from Faherty et al. (2009).

<sup>t</sup> Position calculated using the position of the primary and the separation and position angle quoted in the discovery paper.

<sup>u</sup> Position of primary; discovery paper does not quote a position angle so calculation of the secondary's position is not possible.

<sup>v</sup> West et al. (2008).

<sup>w</sup> Zhang et al. (2010).

<sup>x</sup> This object is listed in Smith et al. (2014) as a companion to both components of the LSPM J1202+0742 system (the N and S components). We call it LSPM J1202+0742 C.

<sup>y</sup> Spectral type estimated from 2MASS photometry and empirical SEDs for Kraus & Hillenbrand (2007).

<sup>z</sup> Liu et al. (2010).

<sup>†</sup> Both of these components of  $\xi$  UMa are themselves spectroscopic binaries.

<sup>\*</sup> The primary star is a spectroscopic binary.

<sup>‡</sup> This mass estimate was based on the spectrophotometric properties of the object before it was determined to be an unresolved binary.

**Table 12**  
(Continued)

**References.** (1) Radigan et al. (2009); (2) White et al. (1999); (3) Mugrauer et al. (2007); (4) Lowrance et al. (2000); (5) Faherty et al. (2010); (6) Lowrance et al. (1999); (7) Gizis et al. (2000); (8) Close et al. (2003); (9) Cruz et al. (2007); (10) van Biesbroeck (1944); (11) Caballero (2007); (12) Cruz et al. (2003); (13) Artigau et al. (2007); (14) Deacon & Hambly (2007); (15) Zhang et al. (2010); (16) Luhman et al. (2012); (17) Caballero & Montes (2012); (18) Scholz et al. (2004); (19) Neuhaeuser & Guenther (2004); (20) Huélamo et al. (2010); (21) Kirkpatrick et al. (2001); (22) Billères et al. (2005); (23) Phan-Bao et al. (2008); (24) Wilson et al. (2001); (25) Gizis et al. (2001); (26) Chauvin et al. (2005a); (27) Seifahrt et al. (2005); (28) Neuhaeuser et al. (2005); (29) Gauza et al. (2012); (30) Gomes et al. (2013); (31) Mužić et al. (2012); (32) Rebolo (1998); (33) Golimowski et al. (2004); (34) Kirkpatrick et al. (1999); (35) Martín (1999); (36) Bouy et al. (2003); (37) Radigan et al. (2008); (38) Reid & Walkowicz (2006); (39) Dhital et al. (2011); (40) Faherty et al. (2011); (41) Dupuy & Liu (2012); (42) Metchev & Hillenbrand (2006); (43) Burgasser et al. (2005); (44) Kirkpatrick et al. (2000); (45) Loutrel et al. (2011); (46) Scholz et al. (2003); (47) McCaughrean et al. (2004); (48) Reylí et al. (2013); (49) Luhman et al. (2007); (50) Deacon et al. (2012b); (51) Deacon et al. (2012a); (52) Burningham et al. (2013); (53) Scholz (2010a); (54) Murray et al. (2011); (55) Kirkpatrick et al. (2011); (56) Burgasser et al. (2000); (57) Mugrauer et al. (2006); (58) Scholz (2010b); (59) Burningham et al. (2010); (60) Bowler et al. (2009); (61) Pinfield et al. (2012); (62) Goldman et al. (2010); (63) Burningham et al. (2013); (64) Burningham et al. (2009); (65) Aller et al. (2013); (66) Bailey et al. (2014); (67) Lafrenière et al. (2008); (68) Kraus et al. (2014); (69) Ireland et al. (2011); (70) Kuzuhara et al. (2011); (71) Bowler et al. (2012); (72) Mace et al. (2013); (73) Geissler et al. (2012); (74) Day-Jones et al. (2011); (75) Day-Jones et al. (2008); (76) Naud et al. (2014); (77) Smith et al. (2014); (78) (Luhman et al. 2011); (79) (Currie et al. 2014).

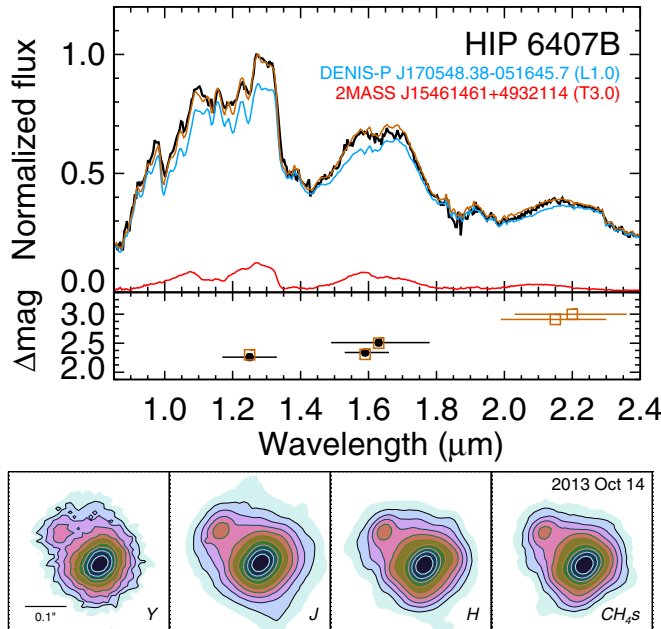


**Figure 15.** Upper panel: the spectral decomposition of HIP 6407B. The best match was the combination of the L1 dwarf DENIS-P J170548.3–051645 (Burgasser et al. 2010; Allers & Liu 2013) and the T3 dwarf SDSS J120602.51+281328.7 (Chiu et al. 2006; Burgasser et al. 2010). Middle panel: the resulting flux ratios between the two objects. Lower panel: Keck LGS AO images from which we derive astrometry and flux ratios with contours drawn at logarithmic intervals. Images have been rotated such that north is up.

(A color version of this figure is available in the online journal.)

**Table 13**  
Keck LGS AO Observations of HIP 6407Bab on 2013 October 13 UT

Filter	$\rho$ (mas)	P.A. (°)	$\Delta m$ (mag)
$Y_{\text{NIRC2}}$	$129.7 \pm 2.7$	$48.4 \pm 1.2$	$2.13 \pm 0.06$
$J_{\text{MKO}}$	$125.1 \pm 1.6$	$51.1 \pm 1.4$	$2.26 \pm 0.05$
$H_{\text{MKO}}$	$125.9 \pm 1.0$	$51.3 \pm 0.4$	$2.51 \pm 0.05$
$CH_4s$	$122.4 \pm 2.9$	$50.3 \pm 1.3$	$2.34 \pm 0.05$
weighted mean	$125.8 \pm 0.8$	$51.0 \pm 0.4$	...

## 6. CONCLUSIONS

We have presented 57 newly discovered companions to known nearby stars, with 24 of these being previously unknown L dwarf companions. With the addition of spectral classification of previously known objects, we have characterized a total of 88 wide, common proper motion companions to nearby stars. We

have increased the sample of late M companions with projected separations greater than  $\sim 300$  AU by 88% and increased the number of L dwarf companions in the same separation range by 82%. Examination of our discoveries and the previously known wide ultracool companion population indicates that although many of the systems are loosely bound, they are unlikely to be disrupted over several Gyr. This paper provides a large sample of wide ultracool companions to stars, which are excellent laboratories for testing models of substellar evolution and atmospheres. Additionally our late-type companions provide an opportunity to extend metallicity determinations for M dwarfs to cooler temperatures (Mann et al. 2014).

The Pan-STARRS1 Surveys (PS1) have been made possible through contributions of the Institute for Astronomy, the University of Hawaii, the Pan-STARRS Project Office, the Max-Planck Society and its participating institutes, the Max Planck Institute for Astronomy, Heidelberg and the Max Planck Institute for Extraterrestrial Physics, Garching, The Johns Hopkins University, Durham University, the University of Edinburgh, Queen’s University Belfast, the Harvard-Smithsonian Center for Astrophysics, the Las Cumbres Observatory Global Telescope Network Incorporated, the National Central University of Taiwan, the Space Telescope Science Institute, the National Aeronautics and Space Administration under grant No. NNX08AR22G issued through the Planetary Science Division of the NASA Science Mission Directorate, the National Science Foundation under grant No. AST-1238877, the University of Maryland, and Eotvos Lorand University (ELTE). The authors thank Bill Golisch, Dave Griep, and Eric Volquardsen for assisting with the IRTF observations. This research has benefited from the SpeX Prism Spectral Libraries, maintained by Adam Burgasser, at <http://www.brown dwarfs.org/spepxprism>. This publication makes use of data products from the Two Micron All Sky Survey, which is a joint project of the University of Massachusetts and the Infrared Processing and Analysis Center/California Institute of Technology, funded by the National Aeronautics and Space Administration and the National Science Foundation. This research has benefited from the M, L, and T dwarf compendium housed at DwarfArchives.org and maintained by Chris Gelino, Davy Kirkpatrick, and Adam Burgasser. M.C.L. and E.A.M. were supported by NSF grants AST09-09222 (awarded to M.C.L.) and AST-0709460 (awarded to E.A.M.). E.A.M. was also supported by AFRL Cooperative Agreement FA9451-06-2-0338. This publication makes use of data products from the Wide-field Infrared Survey Explorer, which is a joint project of the University of California,

Los Angeles, and the Jet Propulsion Laboratory/California Institute of Technology, funded by the National Aeronautics and Space Administration. The United Kingdom Infrared Telescope is operated by the Joint Astronomy Centre on behalf of the Science and Technology Facilities Council of the U.K. This paper makes use of observations processed by the Cambridge Astronomy Survey Unit (CASU) at the Institute of Astronomy, University of Cambridge. The authors thank Mike Irwin and the team at CASU for making the reduced WFCAM data available promptly and Tim Carroll, Thor Wold, Jack Ehle and Watson Varricatt for assisting with UKIRT observations. This research has made use of the SIMBAD database, operated at CDS, Strasbourg, France. The VISTA Data Flow System pipeline processing and science archive are described in Irwin et al. (2004) and Hambly et al. (2008). We have used data from the first data release. This paper makes use of the Topcat software package (Taylor 2005). This research has made use of the Washington Double Star Catalog maintained at the U.S. Naval Observatory. We thank Luca Casagrande, Jackie Faherty, Adam Kraus, Eddie Schlafly, and Josh Schlieder for helpful discussions and our referee Sébastien Lépine for many helpful comments which improved the manuscript. Finally, the authors wish to recognize and acknowledge the very significant cultural role and reverence that the summit of Mauna Kea has always had within the indigenous Hawaiian community. We are most fortunate to have the opportunity to conduct observations from this mountain.

**Facilities:** IRTF (SpeX), PS1, UKIRT (WFCAM), UH:2.2m (SNIFS)

## REFERENCES

- Ahn, C. P., Alexandroff, R., Allende Prieto, C., et al. 2012, *ApJS*, **203**, 21
- Aldering, G., Adam, G., Antilogus, P., et al. 2002, *Proc. SPIE*, **4836**, 61
- Allen, P. R., Burgasser, A. J., Faherty, J. K., & Kirkpatrick, J. D. 2012, *AJ*, **144**, 62
- Aller, K. M., Kraus, A. L., Liu, M. C., et al. 2013, *ApJ*, **773**, 63
- Allers, K. N., & Liu, M. C. 2013, *ApJ*, **772**, 79
- Arriagada, P. 2011, *ApJ*, **734**, 70
- Artigau, E., Lafrenière, D., Albert, L., & Doyon, R. 2009, *ApJ*, **692**, 149
- Artigau, E., Lafrenière, D., Doyon, R., et al. 2007, *ApJL*, **659**, L49
- Bacon, R., Copin, Y., Monnet, G., et al. 2001, *MNRAS*, **326**, 23
- Bailey, V., Meshkat, T., Reiter, M., et al. 2014, *ApJL*, **780**, L4
- Baraffe, I., Chabrier, G., Allard, F., & Hauschildt, P. H. 1998, *A&A*, **412**, 403
- Best, W. M. J., Liu, M. C., Magnier, E. A., et al. 2013, *ApJ*, **777**, 84
- Bilir, S., Karata, Y., Demircan, O., & Eker, Z. 2005, *MNRAS*, **357**, 497
- Billères, M., Delfosse, X., Beuzit, J.-L., et al. 2005, *A&A*, **440**, L55
- Binks, A. S., & Jeffries, R. D. 2014, *MNRAS*, **438**, 11
- Bochanski, J. J., West, A. A., Hawley, S. L., & Covey, K. R. 2007, *AJ*, **133**, 531
- Bouy, H., Brandner, W., Martin, E. L., et al. 2003, *AJ*, **126**, 1526
- Bowler, B. P., Liu, M. C., & Cushing, M. C. 2009, *ApJ*, **706**, 1114
- Bowler, B. P., Liu, M. C., Kraus, A. L., & Mann, A. W. 2014, *ApJ*, **784**, 65
- Bowler, B. P., Liu, M. C., Kraus, A. L., Mann, A. W., & Ireland, M. J. 2011, *ApJ*, **743**, 148
- Bowler, B. P., Liu, M. C., Shkolnik, E. L., et al. 2012, *ApJ*, **753**, 142
- Burgasser, A. J. 2007, *ApJ*, **659**, 655
- Burgasser, A. J., Cruz, K. L., Cushing, M., et al. 2010, *ApJ*, **710**, 1142
- Burgasser, A. J., Geballe, T. R., Leggett, S. K., Kirkpatrick, J. D., & Goliowski, D. A. 2006, *ApJ*, **637**, 1067
- Burgasser, A. J., Kirkpatrick, J. D., Cutri, R. M., et al. 2000, *ApJL*, **531**, L57
- Burgasser, A. J., Kirkpatrick, J. D., & Lowrance, P. J. 2005, *AJ*, **129**, 2849
- Burgasser, A. J., McElwain, M. W., Kirkpatrick, J. D., et al. 2004, *AJ*, **127**, 2856
- Burningham, B., Cardoso, C. V., Smith, L., et al. 2013, *MNRAS*, **433**, 457
- Burningham, B., Pinfield, D. J., Leggett, S. K., et al. 2009, *MNRAS*, **395**, 1237
- Burningham, B., Pinfield, D. J., Lucas, P. W., et al. 2010, *MNRAS*, **406**, 1885
- Caballero, J. A. 2007, *ApJ*, **667**, 520
- Caballero, J. A., & Montes, D. 2012, *Obs*, **132**, 176
- Carpenter, J. M. 2001, *AJ*, **121**, 2851
- Casagrande, L., Schönrich, R., Asplund, M., et al. 2011, *A&A*, **530**, A138
- Casali, M., Adamson, A., Oliveira, C. A. D., et al. 2007, *A&A*, **467**, 777
- Chauvin, G., Lagrange, A.-M., Lacombe, F., et al. 2005a, *A&A*, **430**, 1027
- Chauvin, G., Lagrange, A.-M., Zuckerman, B., et al. 2005b, *A&A*, **438**, L29
- Chiu, K., Fan, X., Leggett, S. K., et al. 2006, *AJ*, **131**, 2722
- Chubak, C., & Marcy, G. 2011, *BAAS*, **43**, 434.12
- Close, L. M., Siegler, N., Freed, M., & Biller, B. 2003, *ApJ*, **587**, 407
- Covey, K. R., Ivezić, V., Schlegel, D., et al. 2007, *AJ*, **134**, 2398
- Cruz, K. L., & Reid, I. N. 2002, *AJ*, **123**, 34
- Cruz, K. L., Reid, I. N., Kirkpatrick, J. D., et al. 2007, *AJ*, **133**, 439
- Cruz, K. L., Reid, I. N., Liebert, J., Kirkpatrick, J. D., & Lowrance, P. J. 2003, *AJ*, **126**, 2421
- Currie, T., Daemgea, S., Debes, J., et al. 2014, *ApJL*, **780**, L30
- Cushing, M. C., Rayner, J. T., & Vacca, W. D. 2005, *ApJ*, **623**, 1115
- Cushing, M. C., Vacca, W. D., & Rayner, J. T. 2004, *PASP*, **116**, 362
- Cutri, R. M., Wright, E. L., Conrow, T., et al. 2012, supplement to the WISE All-Sky Data Release Products (available online at <http://wise2.ipac.caltech.edu/docs/release/allsky/expsup/index.html>)
- Dawson, P. C., & De Robertis, M. M. 2005, *PASP*, **117**, 1
- Day-Jones, A. C., Pinfield, D. J., Napiwotzki, R., et al. 2008, *MNRAS*, **388**, 838
- Day-Jones, A. C., Pinfield, D. J., Ruiz, M. T., et al. 2011, *MNRAS*, **410**, 705
- Deacon, N. R., & Hambly, N. C. 2007, *A&A*, **468**, 163
- Deacon, N. R., Hambly, N. C., King, R. R., & McCaughean, M. J. 2009, *MNRAS*, **394**, 857
- Deacon, N. R., Liu, M. C., Magnier, E. A., et al. 2011, *AJ*, **142**, 77
- Deacon, N. R., Liu, M. C., Magnier, E. A., et al. 2012a, *ApJ*, **757**, 100
- Deacon, N. R., Liu, M. C., Magnier, E. A., et al. 2012b, *ApJ*, **755**, 94
- Delgado-Donate, E. J., Clarke, C. J., Bate, M. R., & Hodgkin, S. T. 2004, *MNRAS*, **351**, 617
- Dhital, S., Burgasser, A. J., Looper, D. L., & Stassun, K. G. 2011, *AJ*, **141**, 7
- Dhital, S., West, A. A., Stassun, K. G., & Bochanski, J. J. 2010, *AJ*, **139**, 2566
- Dupuy, T. J., & Liu, M. C. 2012, *ApJS*, **201**, 19
- Dupuy, T. J., Liu, M. C., Bowler, B. P., et al. 2010, *ApJ*, **721**, 1725
- Dupuy, T. J., Liu, M. C., & Ireland, M. J. 2009, *ApJ*, **692**, 729
- Emerson, J., & Sutherland, W. 2010, *Msngr*, **139**, 2
- Evans, D. S. 1967, in IAU Symp. 30, Determination of Radial Velocities and their Applications, ed. A. H. Batten & J. F. Heard (Toronto: Academic Press), 57
- Faherty, J. K., Burgasser, A. J., Bochanski, J. J., et al. 2011, *AJ*, **141**, 71
- Faherty, J. K., Burgasser, A. J., Cruz, K. L., et al. 2009, *AJ*, **137**, 1
- Faherty, J. K., Burgasser, A. J., West, A. A., et al. 2010, *AJ*, **139**, 176
- Fujii, M. S., & Portegies Zwart, S. 2011, *Sci*, **334**, 1380
- Gauza, B., Béjar, V. J. S., Rebolo, R., et al. 2012, *MNRAS*, **427**, 2457
- Geissler, K., Metchev, S. A., Pham, A., et al. 2012, *ApJ*, **746**, 44
- Giclas, H. L., Burnham, R., & Thomas, N. G. 1967, *LowOB*, **141**, 49
- Gizis, J. E., Kirkpatrick, J. D., & Wilson, J. C. 2001, *AJ*, **121**, 2185
- Gizis, J. E., Monet, D. G., Reid, I. N., Kirkpatrick, J. D., & Burgasser, A. J. 2000, *MNRAS*, **311**, 385
- Goldman, B., Marsat, S., Henning, T., Clemens, C., & Greiner, J. 2010, *MNRAS*, **405**, 1140
- Golimowski, D. A., Leggett, S. K., Marley, M. S., et al. 2004, *AJ*, **127**, 3516
- Gomes, J. I., Pinfield, D. J., Marocco, F., et al. 2013, *MNRAS*, **431**, 2745
- Gontcharov, G. A. 2006, *AstL*, **32**, 759
- Gould, A., & Chaname, J. 2004, *ApJS*, **150**, 455
- Gray, R. O., Corbally, C. J., Garrison, R. F., et al. 2006, *AJ*, **132**, 161
- Hambly, N. C., Collins, R. S., Cross, N. J. G., et al. 2008, *MNRAS*, **384**, 637
- Hamuy, M., Walker, A. R., Suntzeff, N. B., et al. 1992, *PASP*, **104**, 533
- Hodgkin, S. T., Irwin, M. J., Hewett, P. C., & Warren, S. J. 2009, *MNRAS*, **394**, 675
- Hog, E., Fabricius, C., Makarov, V. V., et al. 2000, *A&A*, **30**, 27
- Hovhannyan, L. R., Mickaelian, A. M., Weedman, D. W., et al. 2009, *AJ*, **138**, 251
- Howard, A. W., Johnson, J. A., W. Marcy, G., et al. 2010, *ApJ*, **721**, 1467
- Hrívňák, B. J., Guinan, E. F., & Lu, W. 1995, *ApJ*, **455**, 300
- Huelamo, N., Nürnberger, D. E. A., Ivanov, V. D., et al. 2010, *A&A*, **521**, L54
- Innes, R. T. A. 1915, *CiUO*, 30
- Ireland, M. J., Kraus, A., Martinache, F., Law, N., & Hillenbrand, L. A. 2011, *ApJ*, **726**, 113
- Irwin, M. J., Lewis, J., Hodgkin, S., et al. 2004, *Proc. SPIE*, **5493**, 411
- Isaacson, H., & Fischer, D. 2010, *ApJ*, **725**, 875
- Kendall, T., Tamura, M., Tinney, C. G., et al. 2007, *A&A*, **466**, 1059
- Kenyon, S. J., & Hartmann, L. 1995, *ApJS*, **101**, 117
- King, R. R., McCaughean, M. J., Homeier, D., et al. 2010, *A&A*, **510**, A99
- Kirkpatrick, J. D., Cushing, M. C., Gelino, C. R., et al. 2011, *ApJS*, **197**, 19
- Kirkpatrick, J. D., Dahn, C. C., Monet, D. G., et al. 2001, *AJ*, **121**, 3235
- Kirkpatrick, J. D., Looper, D. L., Burgasser, A. J., et al. 2010, *ApJS*, **190**, 100
- Kirkpatrick, J. D., Reid, I. N., Liebert, J., et al. 1999, *ApJ*, **519**, 802
- Kirkpatrick, J. D., Reid, I. N., Liebert, J., et al. 2000, *AJ*, **120**, 447

- Kouwenhoven, M. B. N., Goodwin, S. P., Parker, R. J., et al. 2010, *MNRAS*, **404**, 1835
- Kraus, A. L., & Hillenbrand, L. A. 2007, *AJ*, **136**, 2340
- Kraus, A. L., Ireland, M. J., Cieza, L. A., et al. 2014, *ApJ*, **781**, 20
- Kuzuhara, M., Tamura, M., Ishii, M., et al. 2011, *AJ*, **141**, 119
- Lafrenière, D., Jayawardhana, R., & van Kerkwijk, M. H. 2008, *ApJL*, **689**, L153
- Lafrenière, D., Jayawardhana, R., & van Kerkwijk, M. H. 2010, *ApJ*, **719**, 497
- Lantz, B. 2004, *Proc. SPIE*, **5249**, 146
- Latham, D. W. 2004, in Spectroscopically and Spatially Resolving the Components of the Close Binary Stars, Vol. 318, ed. R. W. Hilditch, H. Hensberge, & K. Pavlovsk (San Francisco, CA: ASP), 276
- Latham, D. W., Stefanik, R. P., Torres, G., et al. 2002, *AJ*, **124**, 1144
- Law, N. M., Dhital, S., Kraus, A., Stassun, K. G., & West, A. A. 2010, *ApJ*, **720**, 1727
- Lawrence, A., Warren, S. J., Almaini, O., et al. 2007, *MNRAS*, **379**, 1599
- Lee, Y. S., Beers, T. C., Prieto, C. A., et al. 2011, *AJ*, **141**, 90
- Lépine, S. 2005, *AJ*, **130**, 1680
- Lépine, S., & Bongiorno, B. 2007, *AJ*, **133**, 889
- Lépine, S., & Gaidos, E. 2011, *AJ*, **142**, 138
- Lépine, S., Hilton, E. J., Mann, A. W., et al. 2013, *AJ*, **145**, 102
- Lépine, S., & Shara, M. M. 2005, *AJ*, **129**, 1483
- Limoges, M.-M., Lépine, S., & Bergeron, P. 2013, *AJ*, **145**, 136
- Liu, M. C., Deacon, N. R., Magnier, E. A., et al. 2011, *ApJL*, **740**, L32
- Liu, M. C., Dupuy, T. J., & Ireland, M. J. 2008, *ApJ*, **689**, 436
- Liu, M. C., Dupuy, T. J., & Leggett, S. K. 2010, *ApJ*, **722**, 311
- Liu, M. C., Leggett, S. K., & Chiu, K. 2007, *ApJ*, **660**, 1507
- Liu, M. C., Leggett, S. K., Golimowski, D. A., et al. 2006, *ApJ*, **647**, 1393
- Loutrel, N. P., Luhman, K. L., Lowrance, P. J., & Bochanski, J. J. 2011, *ApJ*, **739**, 81
- Lowrance, P. J., McCarthy, C., Becklin, E. E., et al. 1999, *ApJL*, **512**, L69
- Lowrance, P. J., Schneider, G., Kirkpatrick, J. D., et al. 2000, *ApJ*, **541**, 390
- Luhman, K. L., Burgasser, A. J., & Bochanski, J. J. 2011, *ApJL*, **730**, L9
- Luhman, K. L., Loutrel, N. P., McCurdy, N. S., et al. 2012, *ApJ*, **760**, 152
- Luhman, K. L., Patten, B. M., Marengo, M., et al. 2007, *ApJ*, **654**, 570
- Mace, G. N., Kirkpatrick, J. D., Cushing, M. C., et al. 2013, *ApJ*, **777**, 36
- Magnier, E. A., Liu, M., Monet, D. G., & Chambers, K. C. 2008, IAU Symp. 248, A Giant Step: from Milli- to Micro-arcsecond Astrometry (Cambridge: Cambridge Univ. Press), 553
- Maldonado, J., Martínez-Arnáiz, R. M., Eiroa, C., Montes, D., & Montesinos, B. 2010, *A&A*, **521**, A12
- Mamajek, E. E., & Hillenbrand, L. A. 2008, *ApJ*, **687**, 1264
- Mamajek, E. E., Meyer, M. R., & Liebert, J. 2002, *AJ*, **124**, 1670
- Mann, A. W., Brewer, J. M., Gaidos, E., Lépine, S., & Hilton, E. J. 2013a, *AJ*, **145**, 52
- Mann, A. W., Deacon, N. R., Gaidos, E., et al. 2014, *AJ*, **147**, 160
- Mann, A. W., Gaidos, E., & Ansdel, M. 2013b, *ApJ*, **779**, 188
- Marois, C., Macintosh, B., & Barman, T. 2007, *ApJL*, **654**, L151
- Martín, E. L. 1999, *Sci*, **283**, 1718
- Massarotti, A., Latham, D. W., Stefanik, R. P., & Fogel, J. 2008, *AJ*, **135**, 209
- McCaughrean, M. J., Close, L. M., Scholz, R.-D., et al. 2004, *A&A*, **413**, 1029
- Metchev, S. A., & Hillenbrand, L. A. 2006, *ApJ*, **651**, 1166
- Montes, D., López-Santiago, J., Gálvez, M., et al. 2001, *MNRAS*, **328**, 45
- Mugrauer, M., Seifahrt, A., & Neuhauser, R. 2007, *MNRAS*, **378**, 1328
- Mugrauer, M., Seifahrt, A., Neuhauser, R., & Mazeh, T. 2006, *MNRAS*, **373**, L31
- Murray, D. N., Burningham, B., Jones, H. R. A., et al. 2011, *MNRAS*, **414**, 575
- Mužić, K., Radigan, J., Jayawardhana, R., et al. 2012, *AJ*, **144**, 180
- Naud, M.-E., Artigau, E., Malo, L., et al. 2014, *ApJ*, **787**, 5
- Neuhäuser, R., & Guenther, E. W. 2004, *A&A*, **420**, 647
- Neuhäuser, R., Guenther, E. W., Wuchterl, G., et al. 2005, *A&A*, **435**, L13
- Nordstrom, B., Mayor, M., Andersen, J., et al. 2004, *A&A*, **418**, 989
- Pecaut, M. J., & Mamajek, E. E. 2013, *ApJS*, **208**, 9
- Pecaut, M. J., Mamajek, E. E., & Bubar, E. J. 2012, *ApJ*, **746**, 154
- Phan-Bao, N., Bessell, M. S., Martín, E. L., et al. 2008, *MNRAS*, **383**, 831
- Pinfield, D. J., Burningham, B., Lodieu, N., et al. 2012, *MNRAS*, **422**, 1922
- Pinfield, D. J., Jones, H. R. A., Lucas, P. W., et al. 2006, *MNRAS*, **368**, 1281
- Qian, S. B., Soonthornthum, B., Xiang, F. Y., Zhu, L. Y., & He, J. J. 2004, *AN*, **325**, 714
- Radigan, J., Lafrenière, D., Jayawardhana, R., & Doyon, R. 2008, *ApJ*, **689**, 471
- Radigan, J., Lafrenière, D., Jayawardhana, R., & Doyon, R. 2009, *ApJ*, **698**, 405
- Raghavan, D., McAlister, H. A., Henry, T. J., et al. 2010, *ApJS*, **190**, 1
- Ramírez, I., Meléndez, J., & Asplund, M. 2009, *A&A*, **508**, L17
- Rayner, J. T., Cushing, M. C., & Vacca, W. D. 2009, *ApJS*, **185**, 289
- Rayner, J. T., Toomey, D. W., Onaka, P. M., et al. 2003, *PASP*, **115**, 362
- Rebolo, R. 1998, *Sci*, **282**, 1309
- Reid, I. N., Cruz, K. L., Kirkpatrick, J. D., et al. 2008, *AJ*, **136**, 1290
- Reid, I. N., Gizis, J. E., Kirkpatrick, J. D., & Koerner, D. W. 2001, *AJ*, **121**, 489
- Reid, I. N., Hawley, S. L., & Gizis, J. E. 1995, *AJ*, **110**, 1838
- Reid, I. N., & Walkowicz, L. M. 2006, *PASP*, **118**, 671
- Reipurth, B., & Mikkola, S. 2012, *Natur*, **492**, 221
- Reylé, C., Delorme, P., Artigau, E., et al. 2013, *A&A*, **561**, A66, 8
- Robinson, S. E., Ammons, S. M., Kretke, K. A., et al. 2007, *ApJS*, **169**, 430
- Rojas-Ayala, B., Covey, K. R., Muirhead, P. S., & Lloyd, J. P. 2010, *ApJL*, **720**, L113
- Rucinski, S. M., Pribulla, T., & van Kerkwijk, M. H. 2007, *AJ*, **134**, 2353
- Salim, S., & Gould, A. 2003, *ApJ*, **582**, 1011
- Saumon, D., Marley, M. S., Leggett, S. K., et al. 2007, *ApJ*, **656**, 1136
- Schmitt, J. H. M. M., Fleming, T. A., & Giampapa, M. S. 1995, *ApJ*, **450**, 392
- Scholz, R.-D. 2010a, *A&A*, **515**, A92
- Scholz, R.-D. 2010b, *A&A*, **510**, L8
- Scholz, R.-D., Lodieu, N., Ibata, R., et al. 2004, *MNRAS*, **347**, 685
- Scholz, R.-D., McCaughrean, M. J., Lodieu, N., & Kuhlbrodt, B. 2003, *A&A*, **398**, L29
- Seifahrt, A., Guenther, E., & Neuhäuser, R. 2005, *A&A*, **440**, 967
- Shkolnik, E., Liu, M. C., & Reid, I. N. 2009, *ApJ*, **699**, 649
- Skrutskie, M. F., Cutri, R. M., Stiening, R., et al. 2006, *AJ*, **131**, 1163
- Smith, L., Lucas, P. W., Burningham, B., et al. 2014, *MNRAS*, **437**, 3603
- Song, I., Zuckerman, B., & Bessell, M. S. 2003, *ApJ*, **599**, 342
- Taylor, M. 2005, in ASP Conf. Ser. 347, Astronomical Data Analysis Software and Systems XIV, ed. P. Shopbell, M. Britton, & R. Ebert (San Francisco, CA: ASP), 29
- Tetzlaff, N., Neuhäuser, R., & Hohle, M. M. 2011, *MNRAS*, **410**, 190
- Tokovinin, A., & Lépine, S. 2012, *AJ*, **144**, 102
- Tonry, J. L., Stubbs, C. W., Lykke, K. R., et al. 2012, *ApJ*, **750**, 99
- Umbreit, S., Burkert, A., Henning, T., Mikkola, S., & Spurzem, R. 2005, *ApJ*, **623**, 940
- Vacca, W. D., Cushing, M. C., & Rayner, J. T. 2003, *PASP*, **115**, 389
- Valenti, J. A., & Fischer, D. A. 2005, *ApJS*, **159**, 141
- van Biesbroeck, G. 1944, *AJ*, **51**, 61
- van Dam, M. A., Bouchez, A. H., Le Mignant, D., et al. 2006, *PASP*, **118**, 310
- van Leeuwen, F. 2007, *A&A*, **474**, 653
- Voges, W., Aschenbach, B., Boller, T., et al. 2000, IAUC, **7432**, 3
- Webb, R. A., Zuckerman, B., Platais, I., et al. 1999, *ApJL*, **512**, L63
- Weinberg, M. D., Shapiro, S. L., & Wasserman, I. 1987, *ApJ*, **312**, 367
- West, A. A., Hawley, S. L., Bochanski, J. J., et al. 2008, *AJ*, **135**, 785
- White, R. J., Gabor, J. M., & Hillenbrand, L. A. 2007, *AJ*, **133**, 2524
- White, R. J., Ghez, A. M., Reid, I. N., & Schultz, G. 1999, *ApJ*, **520**, 811
- Wielen, R., Schwan, H., Dettbarn, C., et al. 2000, Sixth Catalogue of Fundamental Stars (Karlsruhe: Verlag G. Braun)
- Wilson, J. C., Kirkpatrick, J. D., Gizis, J. E., et al. 2001, *AJ*, **122**, 1989
- Wizinowich, P. L., Le Mignant, D., Bouchez, A. H., et al. 2006, *PASP*, **118**, 297
- Wright, E. L., Eisenhardt, P. R. M., Mainzer, A. K., et al. 2010, *AJ*, **140**, 1868
- Wright, E. L., Skrutskie, M. F., Kirkpatrick, J. D., et al. 2013, *AJ*, **145**, 84
- Yelda, S., Lu, J. R., Ghez, A. M., et al. 2010, *ApJ*, **725**, 331
- Zhang, Z. H., Pinfield, D. J., Day-Jones, A. C., et al. 2010, *MNRAS*, **1834**, 1817